PULSED NEUTRON MEASUREMENTS IN TWO ADJACENT FINITE MEDIA

Thesis by

Georges P. Giraudbit

In Partial Fulfillment of the Requirements

For the Degree of

Mechanical Engineer

California Institute of Technology

Pasadena, California

1966

(Submitted March 28, 1966)

ACKNOWLEDGMENTS

I wish to thank Professor Jerome L. Shapiro for his guidance during my entire stay at the Institute and particularly as my research advisor. Several suggestions were made concerning this work by Professor Harold Lurie to whom I am deeply indebted. Some direction in the area of numerical analysis was also provided by Professor Joel N. Franklin and the staff of the Computing Center, to whom I am grateful.

My graduate studies at the Institute were supported mainly by the California Institute of Technology through its program of Graduate Teaching Assistantships. An initial financial assistance was provided by NATO, the French Ministry of Foreign Affairs, The Alliance Francaise of New York and the Fulbright Commission for travel grants. To the administrators of all these sources, I wish to express my gratitude.

ABSTRACT

PULSED NEUTRON MEASUREMENTS IN TWO ADJACENT FINITE MEDIA

by Georges P. Giraudbit

The pulsed neutron technique has been used to investigate the decay of thermal neutrons in two adjacent water-borated water finite media. Experiments were performed with a 6 x 6 x 6 inches cubic assembly divided in two halves by a thin membrane and filled with pure distilled water on one side and borated water on the other side.

The fundamental decay constant was measured versus the boric acid concentration in the poisoned medium. The experimental results showed good agreement with the predictions of the time dependent diffusion model. It was assumed that the addition of boric acid increases the absorption cross section of the poisoned medium without affecting its diffusion properties: In these conditions, space-energy separability and the concept of an "effective" buckling as derived from diffusion theory were introduced. Their validity was supported by the experimental results.

Measurements were performed with the absorption cross section of the poisoned medium increasing gradually up to 16 times its initial value. Extensive use of the IBM 7090-7094 Computing facility was made to analyze properly the decay data (Frantic Code). Attention was given to the count loss correction scheme and the handling of the statistics involved. Fitting of the experimental results into the

analytical form predicted by the diffusion model led to

$$\Sigma_{av} = 4721 \text{ sec}^{-1} \quad (\pm 150)$$

$$D_o = 35972 \text{ cm}^2\text{sec}^{-1} \quad (\pm 800) \text{ for water at } 21^\circ\text{C}$$

$$C \text{ (given)} = 3420 \text{ cm}^4\text{sec}^{-1}$$

These values, when compared with published data, show that the diffusion model is adequate in describing the experiment.

TABLE OF CONTENTS

I INTRODUCTION

The behavior of a neutron-density field is described in the most general way by means of the well-known Boltzmann equation. Theoretically, this equation together with the adequate initial and boundary conditions is sufficient to define the neutron density in time, space and energy. However, the analytical treatment of the transport equation itself is so difficult in most cases that approximations have to be made. A standard treatment which has been used successfully in many instances is the so-called diffusion theory. In particular, diffusion theory has been used extensively to describe pulsed neutrons experiments. A pulsed neutron situation is one of the time-dependent problems which arises first, and therefore is of considerable interest.

In this situation, diffusion theory gives results of variable quality, according to the extent to which the underlying assumptions are met. Since the time when the diffusion model was first used, some improvements have been added to it, such as "diffusion cooling" effects. However, the basic approach remains the same.

Alternate treatments of the transport equation have been suggested, such as Fourier transforms techniques. In recent years, a complete rethinking of our interpretations of pulsed neutron experiments has been attempted, by trying to deal directly with the transport equation (see N. Corngold (1)).

---

(1) Noel Corngold: Theoretical Interpretation of Pulsed Neutron Phenomena - IAEA Symposium - Karlsruhe, Germany, May 1965.

Diffusion theory gives valuable results in two classes of problems:

a) Steady state for thermal homogeneous or heterogeneous systems. In the case of heterogeneous systems, diffusion theory is applicable in regions far from highly localized strong sources or sinks (such as boundaries or strong absorbers).

b) Time-dependent problem for homogeneous systems, in particular pulsed neutron experiments.

In these situations, boundary conditions can be introduced for use in finite size systems.

Since good results were obtained for these two problems, it was thought to test the diffusion model against one higher degree of difficulty, i. e. the time-dependent problem for a non multiplying finite heterogeneous system.

The practical way to evaluate diffusion theory in these conditions is to compare experimental results with the predictions of the theoretical model. Still, we have to define what we mean by "compare", "experimental results", and "predictions". To do so, we must select the physical system to be investigated and the methods of investigation.

It is known that the pulsed neutron technique is one of the simplest and most flexible methods of studying a time-dependent neutron field in a non multiplying medium. For convenience, relative simplicity and reliability, it has been chosen as method of investigation.

The choice of the physical system itself depends upon:

a. Its ability to be investigated by use of diffusion theory in order to predict the behavior of measurable quantities,

b. The simplicity of the experimental set-up, in order to isolate at best the quantities we want to measure, and

c. The possibility of checking the results against previously published data.

These conditions called for:

a. A simple geometry. We chose a cubic assembly made of two adjacent parallelepipeds of equal thickness.

b. A moderator of well known (absorption and diffusion) properties, for which diffusion theory gives reliable results in less complicated situations, such as pulsing of an homogeneous assembly (it would be quite inconsistent to check the validity of diffusion theory in a difficult situation when it does not give good results in a simpler one). Because of the amount of published data on water, it was decided to use water and water-boron solutions in the experiment.

c. A simple heterogeneity situation: Given two media, one can vary the absorption or diffusion properties or both. Here again, it is important to know a priori the characteristics of the two media. We chose pure distilled water in one medium against a boric acid aqueous solution in the other. Therefore, the heterogeneity lies essentially in the absorption properties of the two media. It is believed that the addition of a very strong absorber such as boric acid in very small quantities does not introduce a significant change in the diffusion properties of the poisoned medium.

It is then necessary to define what we meant by "compare the experimental results with the predictions of the theoretical model". In our situation, diffusion theory leads to the existence of time eigenvalues which describe the time decay of the neutron flux. It will also predict the dependence of the eigenvalues upon the degree of heterogeneity between the two media, i.e. the difference in absorption cross-sections resulting from the poisoning. When the poisoning is varied, the eigenvalues will change accordingly.

This is exactly what was done experimentally, i.e. investigate the decay of the neutron flux with respect to different poison concentrations in one of the two media. Since the theory leads to the existence of eigenvalues, we will seek the presence of such eigenvalues, in particular the fundamental mode. In fact, the "experimental results" should provide an answer to the two questions:

- Is there a fundamental mode?
- If a fundamental mode is reached, what is its decay constant?

Then, it is easy to "compare" the measured values of the fundamental decay constant with the predictions of the theory.

For consistency in the approach, it is important to note that we do not assume a priori the existence of discrete modes and associated eigenvalues, because a rigorous treatment using transport theory was not made to support this assumption. Therefore, we first look at the experimental time decay, and then identify a fundamental mode if the experimental data show one. On the other hand, to assume a priori the existence of such discrete modes would be to make a concession to diffusion theory, which is logically an inconsistent attitude.

II THE THEORETICAL MODEL: DIFFUSION THEORY

II. 1. The time dependent neutron transport theory.

The classical equation relating the behavior of a system containing many neutrons (i. e. from a statistical standpoint) to the interaction properties between the neutrons and the bulk media (such as absorption, scattering, etc.) can be written as follows, for a non-multiplying isotropic medium.

$$\frac{\partial N}{\partial t}(\vec{r}, v\vec{\Omega}, t) = -v\vec{\Omega}\cdot\nabla N - v\sigma_t(\vec{r}, v)N + \int dv' v' \int \sigma_s(\vec{r}, v') f(\vec{r}, v'\vec{\Omega}' \longrightarrow v\vec{\Omega}) N(\vec{r}, v'\vec{\Omega}', t) d\Omega' + S(\vec{r}, v\vec{\Omega}, t) \qquad \text{(II. 1. 1)}$$

t = time

$\vec{r}$ = position vector of a neutron

$\vec{v}$ = velocity vector of a neutron; $\vec{v} = v\vec{\Omega}$, $\vec{\Omega}$ = unit direction vector for the velocity

$N(\vec{r}, v\vec{\Omega}, t)\, dV\, dv\, d\Omega$ = probable number of neutrons at time t in the volume element dV about $\vec{r}$, with speed in dv about v in the direction $d\Omega$ about $\vec{\Omega}$.

$\sigma_t(\vec{r}, v)$ = Macroscopic cross-section (probability of interaction per unit path length), which is assumed to depend upon position and energy only. Similarly, σ_s and σ_a are the macroscopic cross sections for scattering and capture interactions respectively. $\sigma_t = \sigma_s + \sigma_a$.

$f(\vec{r}, v'\vec{\Omega}' \rightarrow v\vec{\Omega})dvd\Omega$ = Probability that a neutron, if it collides in dV about $\vec{r}$ with original velocity $v'\vec{\Omega}'$ will scatter into dv about v and $d\Omega$ about $\vec{\Omega}$.

$S(\vec{r}, v\vec{\Omega}, t)\, dV\, dv\, d\Omega\, dt$ = Probable number of neutrons emitted by independent sources in dV about $\vec{r}$, with speed dv about v in the direction $d\Omega$ about $\vec{\Omega}$, in the interval of time t, t + dt.

The neutron balance equation states that the time rate of change of the neutron density $\frac{\partial N}{\partial t}(\vec{r}, v\vec{\Omega}, t)$ is equal to the rate of removal of neutrons by leakage $(-v\vec{\Omega}.\nabla N)$ or capture and "scattering out" $(-v\sigma_t N)$ plus the rate of supplying by "scattering in" or external source term.

Classical boundary conditions are:

1. At the surface of a nonreentrant system, $N(\vec{r}, v\vec{\Omega}, t) = 0$ for all $\vec{\Omega}$ entering the system.

2. The number of neutrons coming directly (without collision) from infinity is zero.

3. At a point on an interface between two media, the number of neutrons leaving one medium with a certain velocity will enter the next medium with this velocity unchanged.

These can be simplified in most cases to:

1. $N(\vec{r}, v\vec{\Omega}, t) = 0$ for $\vec{r}$ on the surface and $\vec{\Omega}$ entering the system.

2. $\lim_{\vec{r} \to \infty} N(\vec{r}, v\vec{\Omega}, t) = 0$ if the sources are located in a finite region of space.

3. $N(\vec{r}, v\vec{\Omega}, t)$ is continuous at the interface.

We finally include the following assumptions:

The medium is homogeneous:

$$\sigma_t(\vec{r}, v) = \sigma_t(v)$$
$$f(\vec{r}, v\vec{\Omega}' \to v\vec{\Omega}) = f(v'\vec{\Omega}' \to v\vec{\Omega})$$

For a system containing several different homogeneous media, these assumptions hold within each medium.

The general problem mentioned above turns out to be very difficult, in particular since it is a time and energy dependent problem. One can think to remove the time dependence by applying a Laplace transform method, and the energy dependence by assuming a one-velocity model. Even under these circumstances, the problem remains very difficult, and further assumptions have to be made. These are the bases for the time-dependent diffusion approximation.

II. 2. The time-dependent diffusion approximation for the one velocity model.

In this section, we shall outline the kind of approximations leading to the time-dependent diffusion equation in the case of one velocity neutrons.

1. Neutrons are assumed to be monoenergetic.

$$f(v'\vec{\Omega}' \to v\vec{\Omega}) = f(\vec{\Omega}' \to \vec{\Omega}).\delta(v'-v) \qquad \text{(II. 2. 1)}$$

From the definition of the frequency function, it follows that

$$\int f(\vec{\Omega}' \to \vec{\Omega})\, d\Omega' = 1$$

2. Since one of the fundamental assumptions in this analysis is that the medium is homogeneous and isotropic, it follows that $f(\vec{\Omega}' \to \vec{\Omega})$ can be a function only of the angle between the directions $\vec{\Omega}$ and $\vec{\Omega}'$.

We write $\vec{\Omega}'.\vec{\Omega} = \mu_0$

$\eta(\mu_0;\vec{\Omega}')d\mu_0$ = Probability that a neutron moving in direction $\vec{\Omega}'$, when scattered, emerges with a new direction whose cosine lies in $d\mu_0$ about μ_0

Thus
$$f(\vec{\Omega}' \to \vec{\Omega}) = \frac{1}{2\pi}\,\eta(\mu_0;\vec{\Omega}') \qquad \text{(II. 2. 2)}$$

Equation (II. 1. 1) becomes

$$\frac{\partial N}{\partial t}(\vec{r},\vec{\Omega},t) = -v\vec{\Omega}.\nabla N - v\sigma_t N + \frac{1}{2\pi}\int v\sigma_s\,\eta(\mu_0;\vec{\Omega}')\,N(\vec{r},\vec{\Omega}',t)\,d\Omega' + S(\vec{r},\vec{\Omega},t) \qquad \text{(II. 2. 3)}$$

We furthermore introduce the neutron flux

$\Phi(\vec{r},\vec{\Omega},t) = vN(\vec{r},\vec{\Omega},t)$ leading to

$$\frac{1}{v}\frac{\partial \Phi}{\partial t}(\vec{r},\vec{\Omega},t) = -\vec{\Omega}.\nabla\phi - \sigma_t \Phi + \frac{\sigma_s}{2\pi}\int \eta(\mu_0;\vec{\Omega}')\,\Phi(\vec{r},\vec{\Omega}',t)\,d\Omega' + S(\vec{r},\vec{\Omega},t) \qquad \text{(II. 2. 4)}$$

II. 2. 1 The Expansion in Spherical Harmonics method.

A classical treatment of the transport equation, as described by many authors, (Meghreblian and Holmes (2), Davison (3)), consists in expanding the scattering function $f(\vec{\Omega}'\to\vec{\Omega})$, the neutron density $N(\vec{r},v\vec{\Omega},t)$ and the source term S in spherical harmonics.

Our purpose is not to give a detailed analysis of this rather complicated procedure. An extensive discussion can be found in the references previously mentioned (Meghreblian and Holmes, Davison).

Flux and source terms are expanded according to

$$\Phi(\vec{r},\vec{\Omega},t) = \sum_{n=0}^{\infty}\sum_{m=-n}^{n} \Phi_n^m(\vec{r},t)\, Y_n^m(\vec{\Omega}) \qquad \text{(II. 2. 1. 1)}$$

$$S(\vec{r},\vec{\Omega},t) = \sum_{n=0}^{\infty}\sum_{m=-n}^{n} S_n^m(\vec{r},t)\, Y_n^m(\vec{\Omega}) \qquad \text{(II. 2. 1. 2)}$$

where the $Y_n^m(\vec{\Omega})$ are a complete orthonormal set of complex functions such that:

$$\int_{\Omega} Y_\alpha^{\beta *}(\vec{\Omega}).Y_n^m(\vec{\Omega}) = \delta_n^\alpha.\delta_m^\beta \qquad \text{(II. 2. 1. 3)}$$

---

(2) Meghreblian and Holmes - Reactor Analysis - McGraw Hill (1960)

(3) B. Davison: Neutron Transport theory - Oxford Press (1957)

The scattering probability function is expanded into:

$$f(\vec{\Omega}'\to\vec{\Omega}) = \sum_{\ell=0}^{\infty}\sum_{\beta=-\ell}^{\ell} \eta_\ell \, Y_\ell^\beta(\vec{\Omega}) \cdot Y_\ell^{\beta *}(\vec{\Omega}') \qquad \text{(II. 2. 1. 4)}$$

The transport equation (II. 2. 4) can now be expressed in terms of the expansions. By furthermore using the orthogonality property (II. 2. 1. 3), one gets

$$\sum_{n,m} Y_n^m(\vec{\Omega})\left[\left(\frac{1}{v}\frac{\partial}{\partial t} + \vec{\Omega}.\nabla + \sigma_t - \sigma_s\eta_n\right)\phi_n^m(\vec{r},t) - S_n^m(\vec{r},t)\right] = 0 \qquad \text{(II. 2. 1. 5)}$$

This infinite set is separated into coupled equations in the harmonics ϕ_n^m and S_n^m by multiplying through by $Y_\alpha^{\beta *}$ and integrating over all $\vec{\Omega}$ with the aid of the orthogonality property.

The set of equations (II. 2. 1. 5) finally reduces to:

$$\begin{aligned}
&-\frac{1}{v}\frac{\partial}{\partial t}\phi_\alpha^\beta(\vec{r},t) - \sigma_t\phi_\alpha^\beta(\vec{r},t) + S_\alpha^\beta(\vec{r},t) + \sigma_s\eta_\alpha\phi_\alpha^\beta(\vec{r},t) = \\
&\quad F_{1,0}\frac{\partial}{\partial x}\phi_{\alpha+1}^\beta(\vec{r},t) \\
&\quad + F_{-1,0}\frac{\partial}{\partial x}\phi_{\alpha-1}^\beta(\vec{r},t) \\
&\quad + \frac{1}{2}\left(\frac{\partial}{\partial y} - i\frac{\partial}{\partial z}\right)\left[F_{-1,-1}\phi_{\alpha-1}^{\beta-1} - F_{+1,-1}\phi_{\alpha+1}^{\beta-1}\right] \\
&\quad + \frac{1}{2}\left(\frac{\partial}{\partial y} + i\frac{\partial}{\partial z}\right)\left[-F_{-1,1}\phi_{\alpha-1}^{\beta+1} + F_{1,1}\phi_{\alpha+1}^{\beta+1}\right]
\end{aligned} \qquad \text{(II. 2. 1. 6)}$$

where $\alpha = 0, 1, \ldots$ and β takes all values from $-\alpha$ to α. The F's are functions of α and β only.

The diffusion approximation is based upon the assumption that the neutron-flux distribution $\Phi(\vec{r},\vec{\Omega},t)$ is nearly isotropic. Analytically, this assumption is equivalent to the requirement that the series expansion for the flux (II. 2. 1. 1) be truncated to the first two terms, i. e. that $\alpha = 0, 1$ in (II. 2. 1. 6).

Therefore, (II. 2. 1. 6) will involve only Φ_0^0, Φ_1^{-1}, Φ_1^0 and Φ_1^1 all coefficients with higher indices being taken identically equal to zero. For consistency, we also require the source term to be isotropic, i.e. $S_\alpha^\beta \equiv 0$ except for S_0^0.

The system of equations (II. 2. 1. 6) reduces to four coupled partial differential equations, in which appear

$\eta_0 = 1$

$\eta_1 = \overline{\mu_0}$ = average value of the cosine of the scattering angle.

These equations can be greatly simplified in the following cases.

a) Steady state. (All derivatives with respect to time are set equal to zero.)

We define the total track length $\Phi(\vec{r})$ of all neutrons at speed v as

$$\phi(\vec{r}) = \int_\Omega \phi(\vec{r},\vec{\Omega})\, d\Omega$$

Similarly: $$S(\vec{r}) = \int_\Omega S(\vec{r},\vec{\Omega})\, d\Omega$$

Substituting into the reduced system of equations leads to

$$-\nabla . D\nabla\phi(\vec{r}) + \sigma_a \phi(\vec{r}) = S(\vec{r}) \qquad \text{(II. 2. 1. 7)}$$

with

$$D = \frac{1}{3(\sigma_t - \sigma_s \overline{\mu_0})} \qquad \text{(II. 2. 1. 8)}$$

which is the classical diffusion equation for the steady state.

b) One dimensional problems.

In the one dimensional problem, the space dependence can be described by means of a single variable x, therefore reducing very much the complexity of the expansions and of the system of equations.

The expansions of the flux and source term are:

$$\phi(x,\mu,t) = \sum_{n=0}^{\infty} \left(\frac{2n+1}{2}\right) \phi_n(x,t) P_n(\mu)$$

$$S(x,\mu,t) = \sum_{n=0}^{\infty} \left(\frac{2n+1}{2}\right) S_n(x,t) P_n(\mu)$$

where the $P_n(\mu)$ are the usual Legendre Polynomials leading to the system of coupled equations

$$-\frac{1}{v}\frac{\partial}{\partial t}\phi_\alpha - \sigma_t \phi_\alpha + S_\alpha + \sigma_s \eta_\alpha \phi_\alpha$$

$$= \left(\frac{\alpha+1}{2\alpha+1}\right)\frac{\partial}{\partial x}\phi_{\alpha+1} - \left(\frac{\alpha}{2\alpha+1}\right)\frac{\partial}{\partial x}\phi_{\alpha-1} \qquad \text{(II. 2. 1. 9)}$$

$\alpha = 0, 1, 2 \ldots$

Here again, the diffusion approximation which assumes the flux to be isotropic is equivalent to truncating the system of equations (II. 2. 1. 9) by restricting ϕ_α to be non zero only for $\alpha = 0, 1$, i.e.

$$\begin{cases} -\frac{1}{v}\frac{\partial \phi_0}{\partial t} - \sigma_a \phi_0 + S_0 = \frac{\partial \phi_1}{\partial x} \\ -\frac{1}{v}\frac{\partial \phi_1}{\partial t} - \sigma_t \phi_1 + \sigma_s \bar{\mu}_0 \phi_1 = \frac{\partial \phi_0}{\partial x}\cdot\frac{1}{3} \end{cases}$$

or, setting $\phi_0 = \phi$ and $S_0 = S$

$$\begin{cases} \left(\frac{1+3D\sigma_a}{v}\right)\frac{\partial\phi}{\partial t} + \frac{3D}{v^2}\frac{\partial^2\phi}{\partial t^2} = S - \sigma_a\phi + D\frac{\partial^2\phi}{\partial x^2} \\ D = \frac{1}{3(\sigma_t - \sigma_s\bar{\mu}_o)} \end{cases} \qquad \text{(II. 2. 2. 0)}$$

Equation (II. 2. 2. 0) is in its general form the so-called "telegraphist" equation. Its unique feature is that it describes physical phenomena which exhibit both wavelike characteristics and residual disturbance effects. The wavelike behavior is accounted for by the second order term in t, i.e. $\left(\frac{3D}{v^2}\frac{\partial^2\phi}{\partial t^2}\right)$. Wave effects propagate with a finite velocity, which is consistent with the fact that a perturbation cannot propagate faster than v, the velocity of the neutrons, since it is associated with the neutrons themselves.

However, after the passage of a "wave", the disturbance remains, and its effect is naturally described by the first-order term.

On the other hand, a pure diffusion phenomena which, by definition, involves only a first order term, will exhibit an "infinite" velocity of propagation of the perturbations. This is also an underlying character of the approximate diffusion equation for neutrons.

We wish to evaluate the circumstances under which the hybrid telegraphist equation (II. 2. 2. 0) reduces to the more trivial diffusion one. To do so, we must impose the condition that $v \to \infty$ (to meet the infinite velocity condition) while both vD and $\sigma_a v$ remain finite. (II. 2. 2. 0) can be written

$$\left[1 + \frac{3}{v^2}(\sigma_a v)(vD)\right]\frac{\partial n}{\partial t} + \frac{3}{v^2}(vD)\frac{\partial^2 n}{\partial t^2}$$
$$= S - (v\sigma_a)n - (vD)\frac{\partial^2 n}{\partial t^2} \qquad \text{(II. 2. 2. 1)}$$

where $n = \frac{1}{v}\phi$ is the neutron density.

Note that as $v \to \infty$, the terms $\frac{3}{v^2}(\sigma_a v)(vD)$ and $\frac{3}{v^2}(vD)$ tend towards zero as $\frac{1}{v^2}$, leading to:

$$\frac{\partial n}{\partial t} = S - \sigma_a v n + Dv\frac{\partial^2 n}{\partial x^2} \qquad \text{(II. 2. 2. 2)}$$

$$\text{or } \frac{1}{v}\frac{\partial \phi}{\partial t} = S - \sigma_a \phi + D\frac{\partial^2 \phi}{\partial x^2}$$

which is immediately identified as the classical time-dependent diffusion equation.

An alternate approach to reduce equation (II. 2. 2. 0) into (II. 2. 2. 2) is to assume that the term $\frac{3D}{v^2}\frac{\partial^2}{\partial t^2}$ is small compared to the other terms (i.e. $\frac{\partial^2 \phi}{\partial t^2}$ is of negligible order) and that $3D\sigma_a$ is $\ll 1$. In the case of water, when averages over the energy spectrum are taken:

$$\sigma_a = 0.0192 \text{ cm}^{-1}$$

$$D = 0.144 \text{ cm}$$

$$3D\sigma_a = 0.00832 \ll 1$$

Note that the one-dimensional problem mentioned above is in no way restricting the features of the first-order approximation. A complete treatment could have been carried out for the 4 equations truncated system (II. 2. 1. 6) which would have led to the same conclusions.

II. 2. 2. The approximations of time-dependent diffusion theory:

(one velocity model)

We write the elementary one velocity time-dependent diffusion equation for the total neutron flux $\phi(\vec{r},t)$ as:

$$\begin{cases} \frac{1}{v}\frac{\partial\phi}{\partial t}(\vec{r},t) = D\nabla^2\phi(\vec{r},t) - \sigma_a\phi(\vec{r},t) + S(\vec{r},t) \\ D = \frac{1}{3(\sigma_t - \sigma_s\bar{\mu}_0)} \end{cases} \qquad \text{(II. 2. 2. 3)}$$

The underlying assumptions are

a. Homogeneous isotropic medium

b. Monoenergetic neutrons

c. The neutron-flux distribution $\phi(\vec{r},\vec{\Omega},t)$ is nearly isotropic, allowing us to truncate the series expansion for the flux (II. 2. 1. 1) to the first two terms.

d. The source term $S(\vec{r},\vec{\Omega},t)$ is also isotropic.

e. The diffusion medium must have vanishingly small absorbtion cross section ($v\sigma_a$ remains finite when v increases).
This condition is well met for water which has a small $\frac{1}{v}$ dependent absorption cross section.

The diffusion medium must have a very large transport cross section $\sigma_{tr} = \sigma_t - \sigma_s\bar{\mu}_0$ in order to get $D = \frac{1}{3\sigma_{tr}}$ small with Dv remaining finite when v becomes very large.

II. 3 The time-dependent diffusion approximation for thermal neutrons

II. 3. 1 Introduction:

The next step in the treatment of the neutron transport equation is to include energy dependence of the neutrons. To do so, one must go back to the general form of the Boltzmann equation in an homogeneous isotropic non-multiplying medium:

$$\frac{1}{v}\frac{\partial}{\partial t}\phi(\vec{r},v\vec{\Omega},t) = -\sigma_t(v)\phi(\vec{r},v\vec{\Omega},t) - \vec{\Omega}\cdot\nabla\phi(\vec{r},v\vec{\Omega},t) + \int\int\sigma_s(v')f(v'\vec{\Omega}'\to v\vec{\Omega})\phi(\vec{r},v\vec{\Omega}',t)\,d\Omega'\,dv' + S(\vec{r},v\vec{\Omega},t) \qquad \text{(II. 3. 1. 1)}$$

One can then proceed in the same way described in Section (II. 2. 1), i. e. expand ϕ , S and f in space-energy spherical harmonics. If one is interested in the slowing down diffusion problem, the isotropic scattering in the center of mass system has to be assumed. Depending upon the extent of the approximations, one can derive the elementary slowing down and Fermi Age equations.

However, we shall not discuss the slowing down or the thermalization problems, because we deal essentially with a pulsed neutron situation where no sources are present during the decay, and the neutrons have reached thermal energies.

II. 3. 2. The case of thermal neutrons:

If the energy distribution of neutrons in a medium does not depend on position or direction of the neutrons, it is possible to describe the diffusion process by an energy independent one-group equation on which the cross-sections are suitable averages over the spectrum distribution. This space-energy separability will be

particularly valid at points far away from sources or localized sinks. Therefore, we can write:

$$\phi(\vec{r},v\vec{\Omega},t) = \phi(\vec{r},\vec{\Omega},t).F(v) \qquad \text{(II. 3. 2. 2)}$$

The situation described by (II. 3. 2. 2) is approximately realized in the case of thermal neutrons. For, if capture and escape are neglected, and no sources are present, then the neutrons will be in strict thermal equilibrium with the medium. It is known from the kinetic theory of gases that, regardless of the scattering law and the variations of the mean free path with energy, the neutron spectrum will be Maxwellian, i. e.

$$F(v) = Fv^2\, e^{-\frac{mv^2}{2kT}} \qquad \text{(II. 3. 2. 3)}$$

where m = mass of the neutron

T = Temperature of the medium

k = Boltzmann's constant

The energy spectrum is normalized, i. e.

$$\int_0^\infty F(v)\,dv = 1$$

This spectrum is independent of the position or direction of motion.

If the absorption of the neutrons and their escape from the medium are taken into account, then they will not be in strict thermal equilibrium, and (II. 3. 2. 3) will require modifications. However, two cases may occur:

a. If the absorption is very large, assumptions (II. 3. 2. 2) and (II. 3. 2 3) are no longer legitimate but, on the other hand, the thermal neutron population will be so small that its determination is of no interest.

b. If absorption is weak, the correction required for (II. 3. 2. 3) will be small. In addition, the escape of neutrons from the system can be regarded as a highly localized capture. Hence, except in the immediate vicinity of the boundaries, the effect of escape on the system will be like that of a weak absorber (i. e. the correction to (II. 3. 2. 3) will be small). Near the boundaries, this effect will be more important, and the extent of corrections to (II. 3. 2. 2) and(II. 3. 2. 3) will depend mainly on the rate of approach to thermal equilibrium from a distribution in the thermal energy range.

Since no exact results are available for a general configuration, it is hoped that (II. 3. 2. 2) and (II. 3. 2. 3) will hold even near the boundaries. Thus, thermal neutrons can be treated by one-group theory, even if σ_a and σ_s may vary appreciably with energy.

The second interesting character of a thermal neutron population applies to the scattering function $f(v'\vec{\Omega}' \rightarrow v\vec{\Omega})$

The effects which should be taken into account are the molecular binding and the thermal motion of the atomic nuclei. They will both tend to make the scattering isotropic in the laboratory system, since the thermal motion is random, and the molecular binding can be accounted for in first approximation by ascribing to the nucleus a mass greater than its real mass. Isotropic scattering in the L-system leads to

$$f(v'\vec{\Omega}' \rightarrow v\vec{\Omega}) = f(v' \rightarrow v)\frac{1}{4\pi} \qquad \text{(II. 3. 2. 4)}$$

(II. 3. 2. 4) will be valid for most neutron-nuclei interactions, except collisions with very light nuclei such as protons or deuterons.

For isotropic scattering in the L-system, $\overline{\mu}_o$, average cosine of the scattering angle $\vec{\Omega}'.\vec{\Omega}$ should be equal to zero, i.e. $(1-\overline{\mu}_o)$ should be equal to 1. A first approximation to the treatment of scattering leads to $\overline{\mu}_o = \frac{2}{3A}$ where A is the atomic weight of the moderator. Such typical values (4) are given, showing the extent of the approximation of isotropic scattering.

Atomic weight A	Element	$(1-\overline{\mu}_o)$
1	H	0.3386
18	H_2O	0.676
20	D_2O	0.884
4	He	0.8334
7	Li	0.9047

All values above Zn (A = 65) are above 0.990, leading to fairly good isotropic scattering in the laboratory system for "heavy moderator".

II. 3. 3. One group time dependent diffusion equation for thermal neutrons.

We first introduce the space energy separability assumption (II. 3. 2. 2) into the transport equation.

The general time-dependent transport equation is

$$\frac{1}{v}\frac{\partial\phi}{\partial t}(\vec{r},v\vec{\Omega},t) = -\vec{\Omega}.\nabla\phi(\vec{r},v\vec{\Omega},t) - \sigma_t(v)\,\phi(\vec{r},v\vec{\Omega},t) + \iint\sigma_s(v')\,f(v'\vec{\Omega}'\rightarrow v\vec{\Omega})\,\phi(\vec{r},v'\vec{\Omega}',t)\,d\Omega'\,dv' + S(\vec{r},v\vec{\Omega},t) \qquad \text{(II. 3. 3. 1)}$$

(4) Reactor Physics Constants. ANL 5800 (1963).

The space-energy separability (II. 3. 2. 2) is written:

$$\begin{cases} \phi(\vec{r},v\vec{\Omega},t) = \phi(\vec{r},\vec{\Omega},t)\cdot F(v) \\ S(\vec{r},v\vec{\Omega},t) = S(\vec{r},\vec{\Omega},t)\cdot G(v) \\ \sigma_s(v')\, f(v'\vec{\Omega}'\to v\vec{\Omega}) = \sigma_s(v'\to v)\, f(\vec{\Omega}'\to\vec{\Omega}) \end{cases} \qquad \text{(II. 3. 3. 2)}$$

where $\sigma_s(v'\to v)$ is the energy scattering kernel

$F(v)$ and $G(v)$ are normalized energy spectra.

(II. 3. 3. 1) becomes:

$$\frac{F(v)}{v}\frac{\partial\phi}{\partial t}(\vec{r},\vec{\Omega},t) = -F(v)\vec{\Omega}\cdot\nabla\phi(\vec{r},\vec{\Omega},t) - \sigma_t(v)F(v)\,\phi(\vec{r},\vec{\Omega},t) + \int_0^\infty \sigma_s(v'\to v)F(v')\,dv' \int f(\vec{\Omega}'\to\vec{\Omega})\,\phi(\vec{r},\vec{\Omega}',t)\,d\Omega' + G(v)\,S(\vec{r},\vec{\Omega},t) \qquad \text{(II. 3. 3. 3)}$$

Integrating (II. 3. 3. 3) over all energies, i. e. all v's, we get

$$\frac{1}{v^*}\frac{\partial\phi}{\partial t}(\vec{r},\vec{\Omega},t) = -\vec{\Omega}\cdot\nabla\phi(\vec{r},\vec{\Omega},t) - \sigma_t^*\,\phi(\vec{r},\vec{\Omega},t) + \sigma_s^* \int f(\vec{\Omega}'\to\vec{\Omega})\,\phi(\vec{r},\vec{\Omega}',t)\,d\Omega' + S(\vec{r},\vec{\Omega},t) \qquad \text{(II. 3. 3. 4)}$$

where

$$\begin{cases} \dfrac{1}{v^*} = \displaystyle\int_0^\infty \frac{F(v)}{v}\, dv \\ \sigma_t^* = \displaystyle\int_0^\infty \sigma_t(v)\, F(v)\, dv \\ \sigma_s^* = \displaystyle\int_0^\infty\int_0^\infty \sigma_s(v' \to v)\, F(v')\, dv'\, dv \end{cases}$$

Equation (II. 3. 3. 4) is immediately identified with equation (II. 2. 4) applying to the monoenergetic case.

$\frac{1}{v^*}$, σ_t^*, σ_s^* are averages over the energy spectrum, while $\Phi(\vec{r}, \vec{\Omega}, t)$ and $S(\vec{r}, \vec{\Omega}, t)$ designate thermal flux and source.

Note that

$$\sigma_s^* = \int_0^\infty\int_0^\infty \sigma_s(v' \to v)\, F(v')\, dv'\, dv$$

$$= \int_0^\infty F(v')\, dv' \int_0^\infty \sigma_s(v' \to v)\, dv$$

$$= \int_0^\infty F(v')\, \sigma_s(v')\, dv'$$

with $\displaystyle\int_0^\infty \sigma_s(v' \to v)\, dv = \sigma_s(v')$

It is now possible to treat equation (II. 3. 3. 4) in exactly the same way equation (II. 2. 4) was studied. In particular, we derive the one group time-dependent diffusion equation for thermal neutrons according to section (II. 2. 1).

$$\begin{cases} \frac{1}{v^*}\frac{\partial \phi}{\partial t} = D^* \nabla^2 \phi(\vec{r},t) - \sigma_a^* \phi(\vec{r},t) + S(\vec{r},t) \\ \\ D^* = \frac{1}{3(\sigma_t^* - \sigma_s^* \bar{\mu}_0)} \end{cases} \qquad \text{(II. 3. 3. 5)}$$

where $\phi(\vec{r}, t)$ and $S(\vec{r}, t)$ are total thermal neutron flux and source term.

Equation (II. 3. 3. 5) is valid under exactly the same conditions mentioned in Section (II. 2. 2), to which should be added the space-energy separability conditions (II. 3. 3. 2).

Note that we did not introduce directly condition (II 3. 2. 4) of isotropic scattering, requiring

$$f(\vec{\Omega}' \to \vec{\Omega}) = \frac{1}{4\pi} \qquad \text{(II. 3. 2. 4)}$$

We shall see how this condition compares with the more general procedure of truncating the system of equations (II. 2. 1. 6) to the first two terms. This is equivalent to keeping only the first two terms in the Legendre polynomial expansion of $f(\Omega' \to \Omega)$

We recall that we wrote (II. 2. 2)

$$f(\vec{\Omega}' \to \vec{\Omega}) = \frac{1}{2\pi} \eta(\mu_0; \vec{\Omega}')$$

We expanded $\eta(\mu_0; \vec{\Omega}')$ into $\sum_{n=0}^{\infty} \left(\frac{2n+1}{2}\right) \eta_n P_n(\mu_0)$ leading to the first two terms

$$\eta_0 = 1$$

$$\eta_1 = \bar{\mu}_0$$

$$\eta(\mu_0;\vec{\Omega}') = \frac{1}{2}\left[1 + 3\bar{\mu}_0\mu_0\right]$$

$$f(\vec{\Omega}'\to\vec{\Omega}) = \frac{1}{4\pi}\left[1 + 3\bar{\mu}_0\mu_0\right] \qquad \text{(II. 3. 3. 6)}$$

which is what was really used in the derivation of (II. 3. 3. 5). We see that the L-system isotropy condition (II. 3. 2. 4) is more restricting than (II. 3. 3. 6), since it assumes $\bar{\mu}_0 = 0$

II. 3. 4 Time and energy dependent diffusion equation.

In (II. 3. 3), we introduced space energy separability and nearly isotropic scattering in the laboratory system (i. e. we wrote $\sigma_s(v') f(v'\vec{\Omega}'\to v\vec{\Omega}) = \sigma_s(v'\to v) f(\vec{\Omega}'\to\vec{\Omega})$ where $f(\vec{\Omega}'\to\vec{\Omega})$ was truncated to the first two terms).

Here, we assume isotropic scattering only, i. e. condition (II. 3. 2. 4) which is written

$$\sigma_s(v') f(v'\vec{\Omega}'\to v\vec{\Omega}) = \frac{1}{4\pi}\sigma_s(v'\to v) \qquad \text{(II. 3. 4. 1)}$$

With this assumption, and under the general conditions of (II. 2. 2), we are led to the following time and energy dependent diffusion equation:

$$\begin{cases} \dfrac{1}{v}\dfrac{\partial\phi}{\partial t}(E,\vec{r},t) = -\sigma_a(E)\phi(E,\vec{r},t) + D(E)\nabla^2\phi(E,\vec{r},t) \\ \qquad\qquad + L\phi + S(E,\vec{r},t) \\ \text{with} \quad L\phi = \displaystyle\int_0^\infty \sigma_s(E'\to E)\phi(E',\vec{r},t)\,dE' - \sigma_s(E)\phi(E,\vec{r},t) \end{cases} \qquad \text{(II. 3. 4. 2)}$$

where:

-v has been replaced by the energy variable E for convenience

-$L\phi$ is the thermalization operator.

Because of the assumption of isotropic scattering, $\bar{\mu}_0 = 0$ and

$$D(E) = \frac{1}{3\sigma_t(E)} \qquad \text{(II. 3. 4. 3)}$$

Furthermore, we can assume space-energy separability, i. e.

$$\begin{cases} \phi(E,\vec{r},t) = \phi(E)\,\phi(\vec{r},t) \\ S(E,\vec{r},t) = S(E)\,S(\vec{r},t) \end{cases} \qquad \text{(II. 3. 4. 4)}$$

where ϕ (E) and S(E) are normalized energy spectra.

Integrating equation (II. 3. 4. 2) over all energies leads to

$$\begin{cases} \frac{1}{v^*}\frac{\partial \phi}{\partial t}(\vec{r},t) = -\sigma_a^*\,\phi(\vec{r},t) + D^*\nabla^2\phi(\vec{r},t) + S(\vec{r},t) \\ D^* = \frac{1}{3\sigma_t^*} \end{cases} \qquad \text{(II. 3. 4. 5)}$$

equivalent to equation (II. 3. 3. 5).

Similarly, $\frac{1}{v^*}$, σ_a^* and σ_t^* denote averages over the spectrum (E), and we used the fact that $\int_0^\infty \sigma_s(E' \to E)\,dE = \sigma_s(E')$

II. 4. The thermal neutron energy spectrum.

II. 4. 1. General considerations:

So far, we introduced the concept of a neutron energy spectrum through the assumption of space-energy separability. In this section, we shall survey briefly and qualitatively some of the classical qualities of energy spectra:

We first refer to the ideal case of an infinite homogeneous non-absorbing medium: No absorption, no leakage and no sources are present. The neutrons are in thermal equilibrium with the nuclei of the moderator. As seen in Section (II. 3. 2), the neutron spectrum will be Maxwellian, i. e.

$$F(v) = F v^2 e^{-\frac{mv^2}{2kT_o}} \qquad \text{(II. 3. 2. 3)}$$

where T_o is the temperature of the moderator.

We mention briefly some of the properties of this spectrum which will be useful in the future.

a) Energy variable:

dN = number of neutrons per unit volume with energies in $(E, E+dE)$

$$dN = N(E)dE = \frac{2\pi N}{(\pi kT_o)^{\frac{3}{2}}} e^{-\frac{E}{kT_o}} \sqrt{E}\, dE$$

$$N = \int_o^\infty N(E)\, dE \qquad \text{(II. 4. 1. 1)}$$

$$\frac{N(E)\, dE}{N} = \frac{2}{\sqrt{\pi}} e^{-\frac{E}{kT_o}} \sqrt{\frac{E}{kT_o}}\, \frac{dE}{kT_o}$$

Average energy

$$\overline{E} = \frac{\int E\, N(E)\, dE}{N} = \frac{3}{2} kT_o$$

Most probable energy $E_{T_o} = kT_o$

For the flux $\Phi(E) = v N(E)$

$$\frac{\Phi(E)\, dE}{\Phi} = \frac{E}{E_{T_o}^2}\, e^{-\frac{E}{kT_o}}\, dE \qquad \text{(II. 4. 1. 2)}$$

$$\Phi = \int_o^\infty N(v)\, v\, dv = N\bar{v} = \frac{2}{\sqrt{\pi}} N v_{T_o}$$

b) Velocity variable:

$$\frac{N(v)\, dv}{N} = \frac{4}{\sqrt{\pi}} \left(\frac{m}{kT_o}\right)^{\frac{3}{2}} v^2\, e^{-\frac{mv^2}{2kT_o}}\, dv$$

Most probable velocity: $v_{T_o} = \sqrt{\frac{2kT_o}{m}}$

Average velocity: $\bar{v} = \frac{2}{\sqrt{\pi}} v_{T_o}$

$$(\bar{v})^2 = \frac{4}{\pi} v_{T_o}^2 \qquad \overline{(v^2)} = \frac{3}{2} v_{T_o}^2$$

Example:

$T_o = 293.6^\circ K\ (20.4^\circ C)$

$E_{T_o} = kT_o = 0.0253$ eV

$v_{T_o} = 2200$ m/s $= v_o$

This spectrum is an equilibrium spectrum, i. e. from a macroscopic standpoint, the net statistical average change in energy of the neutrons is zero. This is more accurately expressed by the principle

of detailed balance which says that in equilibrium as many neutrons make transitions from the energy E to the energy E' as make transitions from the energy E' to the energy E.

If we call M(E) the Maxwellian normalized probability distribution function, and remembering that energy transfer takes place through collisions with the nuclei of the moderator, we request:

$$M(E')\,\sigma_s(E' \to E) = M(E)\,\sigma_s(E \to E') \qquad \text{(II. 4. 1. 3)}$$

The Maxwellian spectrum will suffer alterations from the non-ideal case when neutrons are removed (by absorption or leakage) or added (source term), according to the way the amounts deducted or added are distributed over the spectrum. However, when the distributions from a Maxwellian spectrum are small, one can use a small perturbations approach, and assume that the neutron energy spectrum is Maxwellian with a shifted effective neutron temperature T_n.

The concept of effective neutron temperature has been proven useful in many circumstances, and gives an easy evaluation of the average energy of a given spectrum. By reference to the ideal case of the true equilibrium where the effective neutron temperature T_n is equal to the moderator temperature T_o, it will be proper to talk of "heated" ($T_n > T_o$) or "cooled" ($T_n < T_o$) spectrum.

Obviously, the spectrum is unaffected if the rate of removal or addition of neutrons per unit neutron density does not depend upon the energy of these neutrons. The only effect is to change the total neutron population normalization factor, without altering the spectrum

itself. In particular, this property is independent of the "shape" of the spectrum.

However, if the removal or addition processes discriminate neutrons with respect to their energy, the average energy (i.e. the effective neutron temperature T_n) will change accordingly. Two cases are of practical importance.

- Non-stationary case:

When no sources are present, the rates of removal of neutrons per unit neutron density are classically given by:

. $R_a = v\sigma_a(v)$ for absorption

. $R_d = vD(v)B^2$ where $B^2 = -\frac{\nabla^2 \Phi(\vec{r}, t)}{\Phi(\vec{r}, t)}$ for diffusion leakage.

In most cases, B^2 is assumed to be a constant, i.e. it is space independent.

In the case of water, or boron, the absorption cross section $\sigma_a(v)$ is well described by a $\frac{1}{v}$ law over the thermal range of energies. Hence, $v\sigma_a(v)$ is constant, and the absorption term does not alter the spectrum.

. The situation is different for the leakage term. $D(v)$ is not $\frac{1}{v}$ dependent; the over-all removal term $vD(v)B^2$ depends upon the spectrum and B^2 itself. The situation is such that the more energetic neutrons preferentially leak out of the medium. This preferential leakage leads to a "cooling" of the spectrum which is more pronounced the weaker the energy coupling of the neutron gas to the moderator.

- Stationary case:

Here, sources are present. They are generally slowing down sources distributed usually according to a 1/E law above thermal energies. When coupled with the diffusion effect of those (above thermal energies) neutrons, they produce a "heating" of the spectrum because the average energy of the neutrons arriving into each volume element is larger than that of the neutrons being absorbed there.

II. 4. 2. Elementary treatment of diffusion cooling or diffusion heating.

We consider the time and energy dependent diffusion equation(II. 3. 4. 2) without source term, i. e.

$$\begin{cases} \frac{1}{v}\frac{\partial \phi}{\partial t}(E,\vec{r},t) = -\Sigma_a(E)\,\phi(E,\vec{r},t) + D(E)\nabla^2\phi(E,\vec{r},t) + L\phi \\ L\phi = \int_0^\infty \Sigma_s(E'\to E)\,\phi(E',\vec{r},t)\,dE' - \Sigma_s(E)\phi(E,\vec{r},t) \end{cases} \qquad \text{(II. 4. 2. 1)}$$

Note: In the remaining part of this work, we will write

σ = Microscopic cross section

Σ = Macroscopic cross section

We follow a classical approach described by Beckurts (5), i. e. we assume space energy separability

$$\phi(E,\vec{r},t) = \phi(E)\,\phi(\vec{r},t) \qquad \text{(II. 4. 2. 2)}$$

Integrating (II. 4. 2. 1) over all energies, and making use of (II. 4. 2. 2)

---

(5) K. H. Beckurts and K. Wirtz: Neutron Physics (1964).

$$\frac{1}{\bar{v}} \frac{\partial \phi}{\partial t}(\vec{r},t) = -\bar{\Sigma}_a \phi(\vec{r},t) - \bar{D} \nabla^2 \phi(\vec{r},t) \qquad \text{(II. 4. 2. 3)}$$

where $\bar{\Sigma}_a$ and $\bar{D}$ are averages over the spectrum.

We introduce a balance equation for the energy density

$$n(\vec{r},t)\,\bar{E} = \int_0^\infty \frac{1}{v} \phi(E,\vec{r},t)\, E\, dE \qquad \text{(II. 4. 2. 4)}$$

Multiplying (II. 4. 2. 1) by E and integrating over all energies gives:

$$\frac{\bar{E}}{\bar{v}} \frac{\partial \phi}{\partial t}(\vec{r},t) = -\bar{\Sigma}_a E_a \phi(\vec{r},t) + \bar{D} E_D \nabla^2 \phi(\vec{r},t) \qquad \text{(II. 4. 2. 5)}$$

$$+ \phi(\vec{r},t) \int_0^\infty E \left\{ \int_0^\infty \Sigma_s(E' \to E) \phi(E')\, dE' - \Sigma_s(E) \phi(E) \right\} dE$$

where

$$E_a = \frac{\int_0^\infty E \Sigma_a(E) \phi(E)\, dE}{\int_0^\infty \Sigma_a(E) \phi(E)\, dE}$$

$$E_D = \frac{\int_0^\infty E D(E) \phi(E)\, dE}{\int_0^\infty D(E) \phi(E)\, dE}$$

For $\frac{1}{v}$ absorption, $E_a = \bar{E}$ (II. 4. 2. 6)

We also have:

$$\int_0^\infty E \left\{ \int_0^\infty \Sigma_s(E' \to E)\,\phi(E')\,dE' - \Sigma_s(E)\,\phi(E) \right\} dE$$

$$= \int_0^\infty \int_0^\infty (E - E')\,\Sigma_s(E' \to E)\,\phi(E')\,dE\,dE'$$

combining (II. 4. 2. 3) and (II. 4. 2. 5), we get

$$\overline{D}\,\frac{\nabla^2\phi}{\phi}\,(E_D - \overline{E}) = \int_0^\infty \int_0^\infty (E' - E)\,\Sigma_s(E' \to E)\,\phi(E')\,dE\,dE' \qquad \text{(II. 4. 2. 7)}$$

a) If $\frac{\nabla^2\phi}{\phi} = 0$ (no diffusion), we request the double integral on the right hand side of (II. 4. 2. 7) to vanish. This is accomplished if $\phi(E)$ is a Maxwellian spectrum.

$$\phi(E) = \frac{E}{(kT_o)^2}\, e^{-\frac{E}{kT_o}} = M(E) \qquad \text{(II. 4. 2. 8)}$$

where T_o correspond to the neutron temperature in an infinite, $\frac{1}{v}$ absorber, source-free medium. According to Section (II. 4. 1), the neutron temperature is equal to the moderator temperature.

b) If $\frac{\nabla^2\phi}{\phi_1} \neq 0$, and remembering that $(E_D - \overline{E}) \neq 0$ (otherwise, D would be $\frac{1}{v}$ dependent), the left hand side of (II. 4. 2. 7) is different from zero. Depending on the sign of $\frac{\nabla^2\phi}{\phi}$, each volume element either loses or gains energy through diffusion. This energy must be gained or lost through collisions with the atoms of the moderator, i. e. $\phi(E)$ must depart from an equilibrium spectrum.

We now make the fundamental assumption that the new spectrum is Maxwellian with a shifted effective neutron temperature $T \neq T_o$. Then:

$$\begin{cases} E_a = \overline{E} = \dfrac{3kT}{2} \\ E_D = \dfrac{1}{\overline{D}} \displaystyle\int_o^\infty E\, D(E) \frac{E}{(kT)^2}\, e^{-\frac{E}{kT}}\, dE \end{cases} \qquad \text{(II.4.2.9)}$$

as

$$\overline{D} = \int_o^\infty D(E) \frac{E}{(kT)^2}\, e^{-\frac{E}{kT}}\, dE$$

$$\frac{d\overline{D}}{dT} = \int_o^\infty D(E) \left\{ \frac{-2E}{(kT)^2 T}\, e^{-\frac{E}{kT}} + \frac{E}{(kT)^2} \frac{E}{kT^2}\, e^{-\frac{E}{kT}} \right\} dE$$

$$= -\frac{2\overline{D}}{T} + \frac{1}{kT^2}\, \overline{D}.E_D$$

$$E_D = kT^2 \left[\frac{2}{T} + \frac{d\overline{D}}{\overline{D}} \cdot \frac{1}{dT} \right]$$

$$= 2kT + kT^2 \frac{d(\mathrm{Log}\,\overline{D})}{dT}$$

$$E_D - \overline{E} = \frac{kT}{2} + kT^2 \frac{d(\mathrm{Log}\,\overline{D})}{dT}$$

$$= \frac{kT}{2} \left\{ 1 + 2\, d(\mathrm{Log}\,\overline{D}) \frac{T}{dT} \right\}$$

$$E_D - \overline{E} = \frac{kT}{2} \left\{ 1 + 2 \frac{d(\mathrm{Log}\,\overline{D})}{d(\mathrm{Log}\,T)} \right\} \qquad \text{(II.4.3.0)}$$

As $T \sim T_o$, we can make a linear Taylor expansion of the shifted spectrum around T_o:

$$\Phi(E) = M(E) + \frac{T-T_o}{T_o}\left(\frac{E}{kT_o} - 2\right) M(E) \qquad \text{(II. 4. 3. 1)}$$

with M(E) given by (II. 4. 2. 8).

The right hand side of (II. 4. 2. 7) becomes

$$\int_o^\infty\int_o^\infty (E'-E)\,\Sigma_s(E'\to E)\,\Phi(E')\,dE'dE$$

$$= \frac{T-T_o}{kT_o^2}\int_o^\infty\int_o^\infty E'(E'-E)\,\Sigma_s(E'\to E)\,M(E')\,dE'dE \qquad \text{(II. 4. 3. 2)}$$

as $$\int_o^\infty\int_o^\infty (E'-E)\,\Sigma_s(E'\to E)\,M(E')\,dE'dE = 0$$

The new double integral is expressed in terms of the mean square energy loss M_2 defined as:

$$M_2 = \frac{1}{(kT_o)^2}\int_o^\infty\int_o^\infty (E'-E)^2\,M(E')\,\sigma_s(E'\to E)\,dE'dE \qquad \text{(II. 4. 3. 3)}$$

$$= \frac{1}{(kT_o)^2}\iint (E'^2 - 2EE' + E^2)\,M(E')\,\sigma_s(E'\to E)\,dE'dE$$

$$= \frac{1}{(kT_o)^2}\left\{\iint E'(E'-E)\,M(E')\,\sigma_s(E'\to E)\,dE'dE + \iint E(E-E')\,M(E')\,\sigma_s(E'\to E)\,dE'dE\right\} \qquad \text{(II. 4. 3. 4)}$$

We now make use of the principle of detailed balance introduced in Section (II. 4. 1):

$$M(E')\sigma_s(E' \to E) = M(E)\sigma_s(E \to E')$$

The second integral in (II. 4. 3. 4) becomes:

$$\iint E(E-E')\,M(E')\,\sigma_s(E' \to E)\,dE'dE$$

$$= \iint E(E-E')\,M(E)\,\sigma_s(E \to E')\,dE'\,dE$$

$$= \iint E'(E'-E)\,M(E')\,\sigma_s(E' \to E)\,dE'\,dE \qquad \text{by interchanging E and E'.}$$

Finally $$M_2 = \frac{2}{(kT_o)^2} \iint E'(E'-E)M(E')\sigma_s(E' \to E)\,dE'\,dE \qquad \text{(II. 4. 3. 5)}$$

By writing $\Sigma_s = N\sigma_s$ where N = number of atoms per unit volume, (II. 4. 2. 7) becomes:

$$\bar{D}\frac{\nabla^2\phi}{\phi}\,\frac{kT}{2}\left[1 + 2\,\frac{d(\log \bar{D})}{d(\log T)}\right] = \frac{1}{2}\,k(T-T_o)\,NM_2 \qquad \text{(II. 4. 3. 6)}$$

By setting $T \sim T_o$ in the left hand side of (II. 4. 3. 6) leads to

$$\frac{T-T_o}{T_o} = \bar{D}\,\frac{\nabla^2\phi}{\phi}\;\frac{1 + 2\,\dfrac{d(\log \bar{D})}{d(\log T)}}{NM_2} \qquad \text{(II. 4. 3. 7)}$$

Study of $\dfrac{\nabla^2\phi}{\phi}$ leads to two interesting cases:

a) Non-stationary case:

We seek solutions to (II. 4. 2. 3) in the form

$$\phi(\vec{r},t) = R(\vec{r})\, e^{-\lambda t} \qquad \text{(II. 4. 3. 8)}$$

$R(\vec{r})$ must then satisfy $\nabla^2 R + B^2 R = 0$ with the condition that the flux vanishes at some extrapolated boundary. B^2 is called "buckling" and describes the geometrical dependence of the medium.

The time eigenvalue λ is given by

$$\lambda = \overline{v}\overline{\Sigma}_a + \overline{D}\,\overline{v}\; B^2 \qquad \text{(II. 4. 3. 9)}$$

. $\overline{v}\overline{\Sigma}_a$ corresponds to the average rate of removal of neutrons by absorption. For a $\frac{1}{v}$ absorber, $\overline{v}\overline{\Sigma}_a = \overline{v\Sigma}_a = v_o \Sigma_a(v_o) =$ CONSTANT.

. $\overline{D}\overline{v}$ describes the average rate of removal of neutrons by diffusion out of the medium. It depends on the spectrum and B^2 (through II. 4. 3. 7). In particular:

$$\frac{T-T_o}{T_o} = -\overline{D}B^2\, \frac{1+2\,\frac{d(\mathrm{Log}\overline{D})}{d(\mathrm{Log}T)}}{NM_2} \qquad \text{(II. 4. 4. 0)}$$

$$\overline{D}\,\overline{v}(T) = \overline{D}\,\overline{v}(T_o) + (T-T_o)\,\frac{d(\overline{D}\overline{v})}{dT}$$

We set:

$$\begin{cases} \overline{D}\,\overline{v}(T_o) = D_o \\ C = T_o \overline{D}\; \dfrac{d(\overline{D}\overline{v})}{dT}\; \dfrac{1+2\,\frac{d(\mathrm{Log}\overline{D})}{d(\mathrm{Log}T)}}{NM_2} \end{cases} \qquad \text{(II. 4. 4. 1)}$$

leading to:

$$\begin{cases} \overline{D}\overline{v} = D_o - CB^2 \\ \lambda = \overline{\Sigma}_a \overline{v} + D_o B^2 - CB^4 \end{cases} \qquad \text{(II. 4. 4. 2)}$$

Differentiating (II. 4. 4. 0) with respect to T, and making use of definition (II. 4. 4. 1) gives

$$C = \frac{v\overline{D}^2}{2NM_2} \left(1 + 2\,\frac{d(\mathrm{Log}\,\overline{D})}{d(\mathrm{Log}\,T)}\right)^2 \qquad \text{(II. 4. 4. 3)}$$

C is called the "diffusion cooling" factor. Its significance is seen through equation (II. 4. 4. 0) which can be written

$$T - T_o = -CB^2\,\frac{dT}{d(\overline{D}\overline{v})} \qquad \text{(II. 4. 4. 4)}$$

$$T = T_o \left\{1 - \exp\left(\frac{\overline{D}\overline{v}}{CB^2}\right)\right\} \qquad \text{(II. 4. 4. 5)}$$

If $C = 0$, it is seen that $T = T_o$: No cooling.

If $C > 0$, $T < T_o$: Diffusion cooling occurs.

The interpretation of the diffusion cooling effect follows from Section (II. 4. 1). Since Dv depends on the spectrum and B^2, it is found that the rate of removal of neutrons with large velocities is larger than for those with small velocities. The equilibrium spectrum is no longer conserved as neutrons leak out. When the new spectrum is compared to a Maxwellian one, the effective neutron temperature T is less than the moderator temperature T_o.

Beckurts (6) gives some values of C calculated for water according to the method of effective neutron temperature. M_2 was computed from various scattering models.

$\frac{d(\text{Log } \overline{D})}{d(\text{Log } T)}$	$\overline{D}$ (cm)	C ($cm^4\ sec^{-1}$)	M_2 from
		3400	Nelkin Model
$\frac{1}{2}$	0.144	2650	A = 1 Monoatomic gas
		4250	A = 18

As will be seen later in Chapter III, these results are reasonably consistent with published experimental values.

Note that the value $\frac{d(\text{Log } \overline{D})}{d(\text{Log } T)}$ comes from the elementary formula

$$\frac{\overline{D}}{\overline{D_o}} = \left(\frac{T}{T_o}\right)^{\frac{1}{2}} \qquad \text{(II.4.4.6)}$$

This was considered by Antonov (7) who refers to a description given by Von Dardel where he assumes that the transport mean free path λ_t is independent of the neutron energy. Von Dardel and Sjostrand (8) put $\lambda_t \simeq \lambda_s$ and get

$$\frac{\overline{D}}{\overline{D_o}} = \left(\frac{T}{T_o}\right)^{\frac{1}{2}} \frac{\lambda_s(T)}{\lambda_s(T_o)} \qquad \text{(II.4.4.7)}$$

(6) K. H. Beckurts and K. Wirtz: Neutron Physics (1964).

(7) Antonov and al: Vol. V, P/661, USSR.

(8) Von Dardel and Sjostrand: Phys. Rev. 94, 1272, (1954).

Antonov points out that the last approximation may be inaccurate in many cases.

The energy dependence of the diffusion coefficient D given by (II.4.4.6) is a first approximation for water, which has strongly energy dependent scattering properties. On the other hand, for graphite or beryllium, D(E) is nearly constant, so that $\frac{d(\text{Log } \overline{D})}{d(\text{Log } T)} = 0$, leading to

$$C = \frac{\overline{v}\,\overline{D}^2}{2NM_2}$$

b) Stationary case:

Here, $\phi(\vec{r}, t) = R(\vec{r})$ only, and (II.4.2.3) leads to

$$\begin{cases} \nabla^2 R - \dfrac{R}{L^2} = 0 \\ L^2 = \dfrac{\overline{D}}{\overline{\Sigma}_a} \end{cases} \qquad \text{(II.4.4.8)}$$

(II.4.3.8) becomes:

$$\frac{T-T_0}{T_0} = \overline{\Sigma}_a \frac{1 + 2\,\dfrac{d(\text{Log}\,\overline{D})}{d(\text{Log}\,T)}}{NM_2} \qquad \text{(II.4.4.9)}$$

By analogy with (II.4.4.2), we write

$$\overline{D}\,\overline{v} = D_0 + \frac{C}{L^2} \qquad \text{(II.4.4.10)}$$

i.e. diffusion heating occurs, as mentioned in Section (II.4.1).

II.4.3. Other treatments.

So far, we described the classical approach through the concept of effective neutron temperature. This concept has been often criticized, and should be considered as elementary. The weakness of the scheme is its a priori assumption on the shape of the spectrum.

However, most authors agree that it gives valuable information in the case of water, where the absorption is near $\frac{1}{v}$ and the leakage can be kept reasonable as long as the medium is not too small. The situation is less ideal in the case of graphite, where it is even difficult to separate space and energy variables.

Alternate methods have been suggested which give a more complete description. Without details, we mention:

- The method of Laguerre Polynomials:

It carries out the expansion of λ to higher powers of B^2. It is verified that the method of effective neutron temperature gives consistent results with the polynomial method when the last is carried to order B^4 only.

- Direct treatment of the transport operation:

The transport equation in a homogeneous, source free, isotropically scattering medium in plane geometry is:

$$\frac{1}{v}\frac{\partial \phi}{\partial t}(E,\mu,x,t) = -\Sigma_t(E)\,\phi(E,\mu,x,t) - \mu\frac{\partial \phi}{\partial x}(E,\mu,x,t)$$

$$+ \frac{1}{2}\int_0^{\infty}\int_{-1}^{+1}\Sigma_s(E'\to E)\,\phi(E',\mu',x,t)\,dE'\,d\mu' \qquad \text{(II. 4. 5. 0)}$$

where $\mu = \cos\theta$ (θ = scattering angle).

In the non-stationary case, we seek solutions in the form:

$$\phi(E,\mu,x,t) = \phi(E,\mu,x)\,e^{-\alpha t} \qquad \text{(II. 4. 5. 1)}$$

and

$$\left(\Sigma_t(E) - \frac{\alpha}{v}\right)\phi(E,\mu,x) = -\mu\frac{\partial\phi}{\partial x} + \frac{1}{2}\int_0^{\infty}\int_{-1}^{+1}\Sigma_s(E'\to E)\,\phi(E',\mu',x)\,dE'\,d\mu' \qquad \text{(II. 4. 5. 2)}$$

which is an eigenvalue equation for the time decay parameter α.

We shall not enter into the mathematical arguments used to describe the set of eigenvalues. To describe the energy spectrum itself, we follow a procedure described by Beckurts and Wirtz (9), i. e. introduce the Fourier transform

$$\phi(E,\mu,B) = \int_{-\infty}^{\infty}\phi(E,\mu,x)\,e^{-iBx}\,dx \qquad \text{(II. 4. 5. 3)}$$

satisfying

$$\left(\Sigma_t(E) - \frac{\alpha}{v}\right)\phi(E,\mu,B) = iB\mu\,\phi(E,\mu,B) + \frac{1}{2}\int_0^{\infty}\int_{-1}^{1}\Sigma_s(E'\to E)\,\phi(E',\mu',B)\,dE'\,d\mu' \qquad \text{(II. 4. 5. 4)}$$

Integrating (II. 4. 5. 4) over all μ and introducing

$$\phi(E,B) = \int_{-1}^{+1}\phi(E,\mu,B)\,d\mu \qquad \text{(II. 4. 5. 5)}$$

---

(9) Beckurts and Wirtz - Neutron Physics (1964).

leads to:

$$\phi(E,B) = \frac{1}{B}\ \text{Arctan}\left\{\frac{B}{\Sigma_t(E) - \frac{\alpha}{v}}\right\} \int_0^\infty \Sigma_s(E' \to E)\,\phi(E',B)\,dE' \qquad \text{(II.4.5.6)}$$

The last integral equation has been solved numerically for α and the spectrum $\phi(E, B)$ by Honeck (10), whose results will be reported later. However, it can be shown that $\phi(E, B)$ can be expanded into the following power series:

$$\begin{cases} \phi(E,B) = M(E) + B^2\,\phi_2(E) + B^4\phi_4(E) - \cdots \\ \lambda \quad = \lambda_0 + D_0 B^2 \quad - CB^4 \quad + FB^6 \quad \cdots \end{cases} \qquad \text{(II.4.5.7)}$$

which, when substituted into equation (II.4.5.6) leads to:

$$D_0 = \frac{\int_0^\infty \frac{1}{3\Sigma_s(E)}\,M(E)\,dE}{\int_0^\infty \frac{1}{v}\,M(E)\,dE} \qquad \text{(II.4.5.8)}$$

$$C = \underbrace{\frac{\int_0^\infty \left(\frac{D_0}{v} - \frac{1}{3\Sigma_s(E)}\right)\phi_2(E)\,dE}{\int_0^\infty \frac{1}{v}\,M(E)\,dE}}_{C_D} + \underbrace{\frac{\int_0^\infty \frac{1}{3\Sigma_s^2(E)}\left\{\frac{4}{15\Sigma_s(E)} - \frac{D_0}{v}\right\}M(E)\,dE}{\int_0^\infty \frac{1}{v}\,M(E)\,dE}}_{C_t} \qquad \text{(II.4.5.9)}$$

(10) Honeck, H., BNL719, 1186 (1962).

The first term (C_D) is identical with the result found by the method of Laguerre Polynomials mentioned earlier. It describes a diffusion cooling effect.

The second term (C_t) represents a purely theoretical correction to the results of elementary diffusion theory. For a heavy gas ($A \gg 1$), $C_D \gg C_t$ which makes the transport correction a negligible factor.

The calculations carried out by Honeck for water at 20°C give:

$D_o = 37,460 \ cm^2 \ sec^{-1}$

$C = C_D + C_t = 2878 \ cm^4 \ sec^{-1}$ with $\frac{C_t}{C_D} = -0.057$

$F = 270 \ cm^6 \ sec^{-1}$

All calculations were performed according to the Nelkin model for scattering in water.

II. 5. The two media problem:

II. 5. 1. Introduction.

We finally give a description of the experimental situation we encountered:

We are concerned with a cubic assembly divided in two halves (see Fig. II. 5. 1). One of them contains pure distilled water. The other contains pure distilled water poisoned with small amounts of boric acid (BO_3H_3) whose effect is essentially to increase the absorption coefficient. Relying on experimentally measured cross sections (11), it is reasonable to assume that water and boric acid solutions have $\frac{1}{v}$ dependent absorption cross sections.

A fast neutron source is placed near the assembly (see Fig. II. 5. 1). The assembly is surrounded by a cadmium shielding allowing only fast neutrons to enter, and a very absorbing medium (borated water) to minimize back scattering effects. These fast neutrons (14 Mev) are thermalized within the assembly and provide pulsed slowing-down sources distributed within the medium.

In half assembly I : Properties Σ_1, D_1

In half assembly II : Properties Σ_2, D_2

it is assumed that $D_1 \simeq D_2$, and $\Sigma_2 = (1+\alpha)\Sigma_1$ where α is the "poisoning" factor.

Theoretically, the situation described above is a very difficult problem if one attempts to find an analytical solution to the transport equations in the two media. Since no such solution exists to our

---

(11) Reactor Physics Handbook - ANL 5800.

FIG II 5l

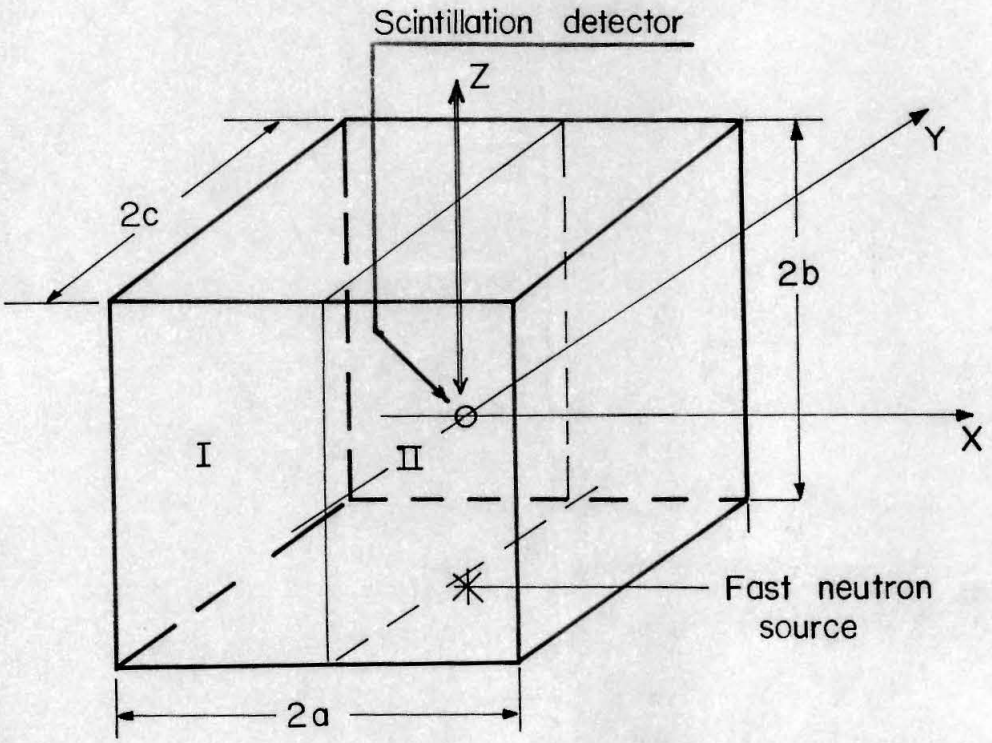
Scintillation detector
Z
Y
2c
2b
X
I
II
Fast neutron
source
2a

knowledge, it is the exact purpose of this work to test experimentally the predictions of an approximate theory which, because it is simplified, does not pretend to give a priori a detailed picture of the phenomena.

It is of interest to look briefly upon the work of R. C. Erdmann (12), who derived an exact solution for the time dependent monoenergetic neutron transport in two adjacent semi-infinite media. Isotropic scattering in the L-system, was assumed, and an isotropic plane source placed at the interface ($x = 0$) was delivering nonenergetic neutrons in a short burst at time $t = 0$.

Although this situation is quite different from ours, the evolution of the neutron current at the interface, and the flux shape near the interface pointed out two areas of investigation: On a short time scale, the scattering process is initially dominant, i.e. neutrons will travel from the medium with the larger to the region with the smaller cross section. On the other hand, the absorption is a long term effect, i.e. after some time, the neutrons travel from the region with small to the region with large absorption cross-section. Hence, if absorption and scattering cross section are larger in one medium then in the other, a reversal of the neutron current at the interface will occur.

As far as we are concerned, the short-time investigation is of no interest, since we change only the absorption properties in our experiment. Moreover, the evolution of the neutron current at the

---

(12) R. C. Erdmann: Time dependent monoenergetic neutron transport in two adjacent semi-infinite media. Thesis - California Institute of Technology (1966).

interface will certainly be masked by the finite length of the burst, the thermalization time, the fact that the slowing down sources are distributed over the assembly, and the over-all difficulties of measuring directional neutron current. At best, we could detect wave effects due to the relative position of the source and detector, under non-idealized and poor conditions.

Hence, as mentioned previously, we focused our attention on the long time range investigation, i.e. the die-away of the thermal neutron flux.

II. 5. 2 Solution in the diffusion approximation:

We first assume that diffusion theory holds in the two media I and II to describe the decay of a thermalized flux in the absence of sources.

Medium I $\Phi_1(E,\vec{r},t), \Sigma_{a_1}(E), D_1(E), \vec{B}_1 \qquad \vec{r} \in I$

Medium II $\Phi_2(E,\vec{r},t), \Sigma_{a_2}(E), D_2(E), \vec{B}_2 \qquad \vec{r} \in II$

$\vec{B}$ = External boundary of the assembly = $\vec{B}_1 + \vec{B}_2$

$\vec{C}$ = interface.

We assume isotropic scattering, and write (II. 3. 4. 2) in each medium.

$$\begin{cases} \frac{1}{v}\frac{\partial \Phi_1}{\partial t}(E,\vec{r},t) = -\Sigma_{a_1}(E)\,\Phi_1(E,\vec{r},t) + D_1(E)\nabla^2\Phi_1(E,\vec{r},t) + L_1\Phi_1 \\ \frac{1}{v}\frac{\partial \Phi_2}{\partial t}(E,\vec{r},t) = -\Sigma_{a_2}(E)\,\Phi_2(E,\vec{r},t) + D_2(E)\nabla^2\Phi_2(E,\vec{r},t) + L_2\Phi_2 \end{cases} \qquad \text{(II. 5. 2. 1)}$$

$L\,\Phi$ = Thermalization operator

$$L_{1,2}\,\Phi_{1,2} = \int_0^\infty \Sigma_{s_{1,2}}(E' \to E)\,\Phi_{1,2}(E,\vec{r},t)\,dE' - \Sigma_{s_{1,2}}(E)\,\Phi_{1,2}(E,\vec{r},t) \qquad \text{(II. 5. 2. 2)}$$

II. 5. 2. 2. The assumptions.

a) The space energy separability:

. The energy spectrum is space and time independent in each medium, i. e.

$$\Phi(E,\vec{r},t) = \varphi(E)\,\Phi(\vec{r},t)$$
$$\int_0^\infty \varphi(E)\,dE = 1 \qquad \text{(II. 5. 2. 3)}$$

As mentioned previously in Section (II. 3. 2), space-energy separability is valid for thermal neutrons far away from localized sources or sinks such as external boundaries where the Milne condition applies (i. e. no neutrons return into the medium). Williams (13) showed that, for water slabs, the spectrum is strongly distorted near the surface owing to the different leakage probabilities for neutrons at different energies. Nevertheless, William's results show that, if the assembly is large with respect to the transport mean free path of neutrons at different energies, space-energy separability is valid in most of the interior. We extend it into all the medium.

---

(13) M. R. Williams: Space energy separability in pulsed neutron systems. Brookhaven Conference on Neutron Thermalization (1962) - Reactor Science and Technology 1963, Vol. 17, pp. 55 to 66.

b) External boundary condition:

A classical derivation from the Milne problem is the concept of an extrapolated distance d at which the "extrapolated" flux vanishes. For monoenergetic neutrons or σ_{tr} = constant:

$d = 0.7104\ \lambda_{tr}$ $\quad\lambda_{tr}$ = transport mean free path.

The energy dependent Milne problem is very difficult because of the space dependence of the energy spectrum mentioned above. For $\frac{1}{v}$ dependence of σ_{tr}, rigorous treatment leads to $d = 0.76\ \lambda_{tr}\ (v_o)$.

. Gelbard and Davis (14) numerically solved the problem for $\phi(E, x)$ and the fundamental decay constant λ in the case of water slabs of variable thickness a. By fitting λ into the form $\lambda = \lambda_o + D_o B^2 - CB^4$ with $B^2 = \left(\frac{\pi}{a+2d}\right)^2$, they solved for $d = \frac{1}{2}\left(\frac{\pi}{B} - a\right)$ leading to:

$d = 0.76\ \overline{\lambda_{tr}}$	for	$B^2 = 0$
$d = 0,75\ \overline{\lambda_{tr}}$		$B^2 = 0.1\ cm^{-2}$
$d = 0,74\ \overline{\lambda_{tr}}$		$B^2 = 0,2\ cm^{-2}$

which shows good agreement with Kiefhaber's (15) results. These results are classically used in the calculation of the geometrical buckling B^2 for pulsed neutron work on water. We therefore assume that there exists an extrapolated boundary at which the extrapolated thermal fluxes vanish, i.e.

$$\phi_{1,2}\left(\vec{B}_{1,2}, t\right) = 0 \qquad \text{(II.5.2.4)}$$

---

(14) Gelbard and Davis: NSE 13, 237 (1962).

(15) Kiefhaber, E.: NSE 18, 404 (1964)

c) The interface ($\vec{c}$) conditions.

(i) The flux is continuous at the interface ($\vec{c}$)

$$\Phi_1(E,\vec{c},t) = \Phi_2(E,\vec{c},t) \qquad \text{(II. 5. 2. 5)}$$

Assuming that assumption (a) is still valid at the interface, we request:

$$\varphi_1(E)\,\Phi_1(\vec{c},t) = \varphi_2(E)\,\Phi_2(\vec{c},t) \qquad \text{(II. 5. 2. 6)}$$

which leads to

$$\begin{cases} \varphi_1(E) = \varphi_2(E) \\ \Phi_1(\vec{c},t) = \Phi_2(\vec{c},t) \end{cases} \qquad \text{(II. 5. 2. 7)}$$

(ii) The net neutron current is continuous:

In the framework of diffusion theory, the net neutron current is $\vec{J} = -D.\nabla\Phi$

Hence: (II. 5. 2. 8)

$$D_1(E)\nabla\Phi_1(E,\vec{c},t) = D_2(E)\nabla\Phi_2(E,\vec{c},t)$$

or

$$D_1(E)\varphi_1(E).\nabla\Phi_1(\vec{c},t) = D_2(E)\varphi_2(E).\nabla\Phi_2(\vec{c},t)$$

It is seen that a corollary of assumption (a) and conditions (c) is the indentity of the two energy spectra in media I and II, i. e.

$$\varphi_1(E) = \varphi_2(E) \qquad \text{(II. 5. 2. 9)}$$

d) In both media I and II, the absorption cross-sections are $\frac{1}{v}$ dependent. This is a classical assumption for both water and boron.

e) The diffusion properties in both media are identical, i.e.

$$D_1(E) = D_2(E) \qquad \text{(II. 5. 3. 0)}$$

This assumption is justified since we are doing a poisoning experiment by adding a very strong absorber (boric acid) in very small quantities. It hardly affects the scattering cross section while drastically increasing the absorption cross section.

f) The common spectrum $\varphi(E)$ may be described by a Maxwellian distribution with an effective neutron temperature T. The shift of T from the moderator temperature T_o is accounted for by introduction of a diffusion cooling term C. The fact that there is a common energy spectrum coupled with assumption (e) is sufficient to insure C to be independent of the poisoning, since it involves only the variations of the diffusion coefficient with energy.

This assumption is quite valid since the spectrum does not depend on the absorption properties because they are $\frac{1}{v}$ dependent (hence it does not depend upon the poisoning). As about the scattering properties, they do not depend on the poisoning because of assumption (e). Therefore, as long as the spectra in I and II are concerned, the medium appears homogeneous from a scattering properties standpoint, which reinforces the needed condition $\varphi_1(E) = \varphi_2(E)$ and helps fulfill the space energy separability at the interface.

While these assumptions have to be stated independently, the validity of one of them depends upon the others. For instance, the validity of (f) is reinforced by (d), (e) and corollary (II. 5. 2. 9). We will say that, in our case, the assumptions are very well conditioned.

This explains the over-all validity of the diffusion model which was demonstrated later by the experimental results.

Note that if we had introduced a change in the diffusion properties of the media, it would have been practically impossible to retain assumption (a), because the energy spectra had to be different in each half far from the interface and external boundaries, while being equal at the interface. In such conditions, space-energy separability is very likely to fail.

II.5.2.3. Analytical solution:

With the assumptions mentioned in (II.5.2.2), and by integrating (II.5.2.1) over all energies, we get:

$$\begin{cases} \dfrac{\partial \Phi_1}{\partial t}(\vec{r},t) = D\upsilon\nabla^2\Phi_1(\vec{r},t) - \upsilon\Sigma_1\Phi_1(\vec{r},t) \\ \dfrac{\partial \Phi_2}{\partial t}(\vec{r},t) = D\upsilon\nabla^2\Phi_2(\vec{r},t) - \upsilon\Sigma_2\Phi_2(\vec{r},t) \end{cases} \qquad \text{(II.5.3.1)}$$

where all values refer to averages over the common energy spectrum we assume separation of variables.

$$\Phi_1(x,y,z,t) = X_1(x).Y_1(y).Z_1(z).T_1(t)$$

$$\Phi_2(x,y,z,t) = X_2(x).Y_2(y).Z_2(z).T_2(t)$$

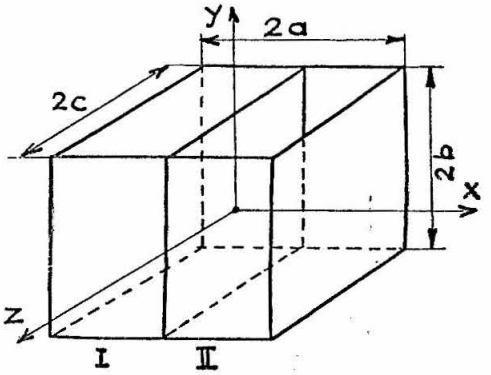

where a, b, c denote extrapolated boundaries.

Interface conditions:

i) Flux must be continuous for all y, z, t

$$\phi_1(o,y,z,t) = \phi_2(o,y,z,t)$$

$$\begin{cases} X_1(o) = X_2(o) \\ Y_1(y) = Y_2(y) & \text{Same y dependence} \\ Z_1(z) = Z_2(z) & \text{Same z dependence} \\ T_1(t) = T_2(t) & \text{Same t dependence} \end{cases}$$

So we can write

$$\phi_1 = X_1 YZT$$

$$\phi_2 = X_2 YZT$$

ii) $\vec{J} = -D\nabla\phi$ must be continuous at the interface, i. e.

$$\frac{dX_1}{dx}(0) = \frac{dX_2}{dx}(0)$$

Outer boundaries.

$X_1(-a) = 0$

$X_2(+a) = 0$

$Y(\pm b) = 0$

$Z(\pm b) = 0$

With these conditions, (II. 5. 3. 1) becomes

$$\begin{cases} -\frac{T'}{T} = \lambda = \Sigma_1 v - Dv\left(\frac{X''_1}{X_1} + \frac{Y''}{Y} + \frac{Z''}{Z}\right) \\ -\frac{T'}{T} = \lambda = \Sigma_2 v - Dv\left(\frac{X''_2}{X_2} + \frac{Y''}{Y} + \frac{Z''}{Z}\right) \end{cases}$$

Thus, because of the separation of variables:

$$\begin{cases} \dfrac{X''_1}{X_1} = -\omega_1^2 \\ \dfrac{X''_2}{X_2} = -\omega_2^2 \\ \dfrac{Y''}{Y} = -\mu^2 \\ \dfrac{Z''}{Z} = -\nu^2 \end{cases}$$

We solve easily for T, Y, Z

$$\begin{cases} T(t) = e^{-\lambda t} \\ Y(y) = \cos \dfrac{m\pi y}{2b} \qquad \mu^2 = \left(\dfrac{m\pi}{2b}\right)^2 \qquad m = 1, 2, \ldots \\ Z(z) = \cos \dfrac{n\pi z}{2c} \qquad \nu^2 = \left(\dfrac{n\pi}{2c}\right)^2 \qquad n = 1, 2, \ldots \end{cases}$$

The eigenvalue equations are:

$$\begin{cases} \lambda = \Sigma_1 v - Dv\left\{\dfrac{X''_1}{X_1} + \dfrac{Y''}{Y} + \dfrac{Z''}{Z}\right\} \\ \lambda = \Sigma_2 v - Dv\left\{\dfrac{X''_2}{X_2} + \dfrac{Y''}{Y} + \dfrac{Z''}{Z}\right\} \end{cases} \qquad \text{(II. 5. 3. 2)}$$

For X_1 and X_2, we have the following problem

$$\begin{cases} \dfrac{X''_1}{X_1} = -\omega_1^2 \\ \dfrac{X''_2}{X_2} = -\omega_2^2 \end{cases} \qquad \begin{cases} X_1(-a) = 0 \\ X_2(+a) = 0 \end{cases} \qquad \begin{cases} X_1(0) = X_2(0) \\ X'_1(0) = X'_2(0) \end{cases}$$

while (II. 5. 3. 2) requires

$$\omega_1^2 - \omega_2^2 = - \frac{\Sigma_1 - \Sigma_2}{D} \qquad \text{(II. 5. 3. 3)}$$

Now, the physical situation guides us to understand the nature of ω_1^2 and ω_2^2

a) If the two media are the same, i. e. $\Sigma_1 = \Sigma_2 = \Sigma$

$$\omega_1^2 = \omega_2^2 = \frac{1\pi}{2a}$$

$$X_1(x) = X_2(x) = \cos \frac{1\pi x}{2a}$$

$$\lambda_{1mn} = \Sigma v + Dv B^2_{1mn}$$

with $B^2_{1mn} = \left(\frac{1\pi}{2a}\right)^2 + \left(\frac{m\pi}{2b}\right)^2 + \left(\frac{n\pi}{2c}\right)^2$ (II. 5. 3. 4)

The fundamental mode is given by

$$\lambda_{111} = \Sigma v + Dv B^2_{111} \qquad \text{(II. 5. 3. 5)}$$

$$\phi(x, y, z, t) = \sum_{1, m, n \geq 1} A_{1, m, n} \cos \frac{1\pi x}{2a} \cos \frac{m\pi y}{2b} \cos \frac{n\pi z}{2c} e^{-\lambda_{1mn} t}$$

The x-dependence of the fundamental mode of the flux is shown in Fig. (II. 5. 3. a).

b) It is now clear that, by continuity, a slight increase in Σ_2 for instance will lead to trigonometric solutions for $X_1(x)$ and $X_2(x)$ of the form

$$\begin{cases} X_1(x) = a_1 \sin \omega_1 (x+a) \\ X_2(x) = a_2 \sin \omega_2 (x-a) \end{cases}$$

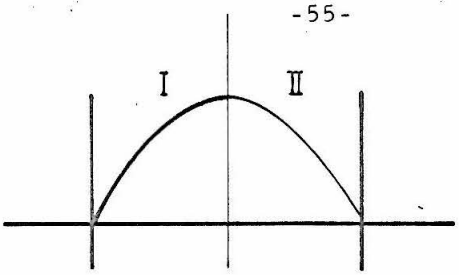

$a = 0$

$$X_1 = X_2 = a \cos \frac{\pi x}{2a}$$

FIG. II 53a

TRIGONOMETRIC SOLUTION

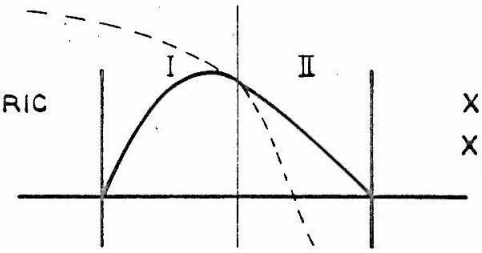

$0 < a < a_c$

$$X_1 = a_1 \sin \omega_1 (x + a)$$
$$X_2 = a_2 \sin \omega_2 (x - a)$$

FIG. II 53b

HYPERBOLIC SOLUTION

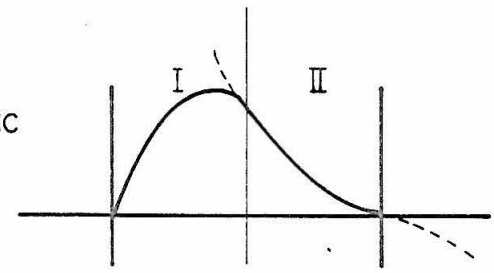

$a_c < a$

$$X_1 = a_1 \sin \omega_1 (x + a)$$
$$X_2 = a_2 \sinh \omega_2 (x - a)$$

FIG. II 53c

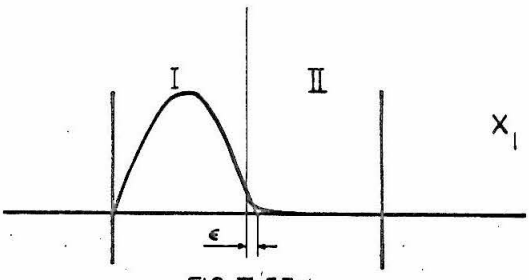

$a \rightarrow \infty$

$$X_1 = a_1 \sin \frac{\pi}{a+\epsilon} (x + a)$$

FIG. II 53d

The x dependence of the flux is shown in Fig. (II. 5. 3. b).

We define a poisoning factor α such that

$$\Sigma_2 = \Sigma_1 (1 + \alpha) \qquad \text{i. e. } \Sigma(\text{boron}) = \alpha\Sigma_1$$

One sees that, as Σ_2 increases, the flux shape becomes so asymmetric that it is no longer possible to fulfill the equality of slopes at x = 0 with a trigonometric solution in region II. This is because $\omega_2^2 < 0$, i. e. ω_2 is imaginary, leading to a hyperbolic solution of the form

$$X_2 = a_2 \sinh \omega_2 (x+a)$$

c) Hyperbolic solution: See Fig. (II. 5. 3. c).

d) For very large boron concentrations, region II becomes a black absorber, i. e. no neutron return from medium II.

We then approach the situation of Fig. (II. 5. 3. d), with a vacuum condition at the interface.

II. 5. 2. 3. 1 Trigonometric solution.

Formulas for $X_1(x)$ and $X_2(x)$ satisfying external boundary conditions $X_1(-a) = X_2(+a) = 0$ are

$$X_1(x) = a_1 \sin \omega_1 (x+a) \qquad x \leq 0$$

$$X_2(x) = a_2 \sin \omega_2 (x-a) \qquad x \geq 0$$

with $$\omega_2^2 = \omega_1^2 + \frac{\Sigma_1 - \Sigma_2}{D}$$

$$\omega_2^2 = \omega_1^2 + P^* \qquad P^* = \frac{\Sigma_1 - \Sigma_2}{D}$$

Continuity of flux at the interface:

$$X_1(0) = X_2(0) \longrightarrow a_1 \sin \omega_1 a = -a_2 \sin \omega_2 a \qquad \text{(II. 5. 3. 6)}$$

Continuity of current:

$$X'_1(0) = X'_2(0) \longrightarrow a_1 \omega_1 \cos \omega_1 a = a_2 \omega_2 \cos \omega_2 a \qquad \text{(II. 5. 3. 7)}$$

(II. 5. 3. 6) and (II. 5. 3. 7) give:

$$\frac{\tan \omega_1 a}{\omega_1} = - \frac{\operatorname{tg} a\sqrt{\omega_1^2 + p^*}}{\sqrt{\omega_1^2 + p^*}} \qquad \text{(II. 5. 3. 8)}$$

Assume $\Sigma_2 > \Sigma_1$

$$\Sigma_2 = (1 + \alpha)\Sigma_1$$

introduce the auxiliary variable $\Omega = a\omega_1$

and solve for ω_1 vs α

$$\begin{cases} \dfrac{\tan \Omega}{\Omega} = - \dfrac{\tan \sqrt{\Omega^2 + p}}{\sqrt{\Omega^2 + p}} \\ p = - \dfrac{\alpha \Sigma_1}{D} a^2 \\ \Omega = a\omega_1 \end{cases} \qquad \text{(II. 5. 3. 9)}$$

This solution is possible as long as $\Omega^2 + p \geq 0$ corresponding to $\alpha \leq \alpha_c$ where α_c denotes a critical concentration for which $\Omega^2 + p = 0$.

If $\Omega^2 + p = 0$

$$\frac{\operatorname{tg} \Omega}{\Omega} = - \frac{\operatorname{tg}(0)}{(0)} = - 1$$

or $\operatorname{tg} \Omega = - \Omega$

$$\Omega = 2.0288$$

$$\alpha_c = \frac{(2.0288)^2 D}{\sum_1 a^2}$$

II. 5. 2. 3. 2. Hyperbolic solution:

For $\alpha > \alpha_c$, we have an hyperbolic solution in the poisoned medium

$$\begin{cases} \omega_1^2 > 0 & \longrightarrow X_1(x) = a_1 \sin \omega_1 (x + a) \quad x < 0 \\ \omega_2^2 = \omega_1^2 + p < 0 & \longrightarrow X_2(x) = a_2 \sinh |\omega_2| \ (x - a) \quad x > 0 \end{cases}$$

Continuity of flux and current at the interface give

$$a_1 \sin \omega_1 a = - a_2 \sinh |\omega_2| \ a$$

$$\omega_1 a_1 \cos \omega_1 a = a_2 \omega_2 \cosh |\omega_2| \ a$$

$$|\omega_2| = \sqrt{- (\omega_1^2 + p)}$$

leading to:

$$\begin{cases} \dfrac{\tan \Omega}{\Omega} = - \dfrac{\tanh \sqrt{-(\Omega^2+p)}}{\sqrt{-(\Omega^2+p)}} \\ p = -\dfrac{\alpha \Sigma_1}{D} a^2 \\ \Omega = a\omega_1 \end{cases} \qquad \text{(II. 5. 4. 0)}$$

II. 5. 2. 3. 3. Numerical solutions:

Solutions (II. 5. 3. 9) and (II. 5. 4. 0) were solved numerically, giving ω_1 vs α for selected values of Σ_1, a, D. It is then trivial to derive the decay constant λ by writing

$$\begin{cases} B^2 = \omega_1^2 + \left(\dfrac{\pi}{2b}\right)^2 + \left(\dfrac{\pi}{2c}\right)^2 & = \text{"effective buckling"} \\ & \quad \text{in region I} \\ \lambda = \Sigma_1 v + DvB^2 - CB^4 \end{cases}$$

when the cooling factor C has been introduced to take into account the distortion from the pure Maxwellian spectrum. This addition is legitimate by assumption (f).

Small perturbations calculations around $\alpha = 0$ were performed in the trigonometric range. When $\alpha = 0$, $\omega_1 = \omega_2 = \dfrac{\pi}{2a}$. We then introduce perturbed eigenvalues

$$\begin{cases} \omega_1 = \dfrac{\pi}{2a} (1 + \varepsilon_1) \\ \omega_2 = \dfrac{\pi}{2a} (1 + \varepsilon_2) \end{cases}$$

$$\lambda = \frac{\Sigma_1 + \Sigma_2}{2} v + Dv \left\{ \frac{\omega_1^2 + \omega_2^2}{2} + \left(\frac{\pi}{2b}\right)^2 + \left(\frac{\pi}{2c}\right)^2 \right\}$$

It was found

$$\begin{cases} \lambda \simeq \dfrac{\Sigma_1 + \Sigma_2}{2} v + Dv \left\{ \dfrac{1}{2} \left(1 + \sqrt{1 - \dfrac{K^2}{4}}\right)\left(\dfrac{\pi}{2a}\right)^2 + \left(\dfrac{\pi}{2b}\right)^2 + \left(\dfrac{\pi}{2c}\right)^2 \right\} \\ K = \dfrac{\Sigma_1 - \Sigma_2}{D} \left(\dfrac{2a}{\pi}\right)^2 \end{cases}$$

if $\Sigma_2 = \Sigma_1 (1+\alpha)$

for small poisonings $\alpha \ll 1$

$$K = \frac{-\alpha \Sigma_1}{D} \left(\frac{2a}{\pi}\right)^2 = k\alpha$$

$$\sqrt{1 - \frac{K^2}{4}} \simeq 1 - \frac{k^2 \alpha^2}{8}$$

$$\lambda \simeq \Sigma_1 v \left(1 + \frac{\alpha}{2}\right) + Dv \left\{ \left(\frac{\pi}{2a}\right)^2 \left(1 - \frac{k^2 \alpha^2}{8}\right) + \left(\frac{\pi}{2b}\right)^2 + \left(\frac{\pi}{2c}\right)^2 \right\}$$

$$\simeq \frac{\Sigma_1 + \Sigma_2}{2} v + Dv B^2 (\alpha = 0) + 0 (\alpha^2)$$

$$\frac{d\lambda}{d\alpha} (\alpha = 0) = \frac{\Sigma_1 v}{2}$$

For small poison concentration, λ varies linearly with the average absorption cross section. The slope at the origin $\alpha = 0$ was verified with the numerical calculations.

II. 5. 2. 3. 4. Validity of the use of the diffusion cooling term.

Essentially, the mathematical problem has been to solve for effective buckling $B^2_{1,2}$ in regions I and II. We wrote

$$B_1^2 = \omega_1^2 + \left(\frac{\pi}{2b}\right)^2 + \left(\frac{\pi}{2c}\right)^2$$

$$B_2^2 = \omega_2^2 + \left(\frac{\pi}{2b}\right)^2 + \left(\frac{\pi}{2c}\right)^2$$

and derived an expression connecting ω_1^2 and ω_2^2 by requiring the same decay constants in the two regions, i.e.

$$\lambda = \Sigma_1 v + D v B_1^2 = \Sigma_2 v + D v B_2^2$$

$$\omega_2^2 = \omega_1^2 + \frac{\Sigma_1 - \Sigma_2}{D}$$

One may ask what happens if, for consistency with the final calculations, one adds the cooling factor CB^4, i.e.: What is the influence of the diffusion cooling on the effective bucklings B_1^2 and B_2^2 ?

Writing $\lambda = \Sigma_1 v + D v B_1^2 - C B_1^4 = \Sigma_2 v + D v B_2^2 - C B_2^4$

gives

$$(\Sigma_1 - \Sigma_2) + D(\omega_1^2 - \omega_2^2) - \frac{C}{v}\left\{(\omega_1^4 - \omega_2^4) + 2(\omega_1^2 - \omega_2^2)\left[\left(\frac{\pi}{2b}\right)^2 + \left(\frac{\pi}{2c}\right)^2\right]\right\} = 0$$

$$\begin{cases} C\omega_2^4 + 2\gamma\omega_2^2 + \delta = 0 \\ \gamma = \left[\left(\frac{\pi}{2b}\right)^2 + \left(\frac{\pi}{2c}\right)^2\right] C - \frac{Dv}{2} \\ \delta = -\left[C\omega_1^4 + 2\gamma\omega_1^2 + (\Sigma_2 - \Sigma_1) v\right] \end{cases}$$

Since the expansion is carried towards the B^4 term, and B^2 is always small (0.1 to 0.3 cm^{-2}), we see that the cooling factor CB^4 is not going to perturb significantly the ω_1^2 vs ω_2^2 equation. In particular, if we write

$$\frac{C}{2\gamma}\,\omega_2^4 + \omega_2^2 + \frac{\delta}{2\gamma} = 0$$

$$\frac{C}{2\gamma} \simeq -\frac{C}{D\upsilon} \ll 1 \qquad \text{and, a posteriori } \frac{C}{2\gamma}\omega_2^4 \ll \omega_2^2$$

III NUMERICAL SOLUTIONS

Numerical calculations of the λ vs α law (i.e. decay constant of the fundamental mode versus poisoning factor) were performed using different sets of published data and the analysis given in Chapter II.

III. 1. Experimental parameters.

. In our experiment, we pulsed a 6 x 6 x 6 inches assembly, divided in its center by a thin membrane.

. The extrapolation distance d was chosen according to the Gelbard and Davis calculations. See Section (II. 5. 2. 2) for

$0.12 < B^2 < 0.22$ (in cm^{-2})

$$d = 0.75\ \overline{\lambda_{tr}}$$

$\overline{\lambda_{tr}} = 0.434 \pm 0.001$ cm at $21^{\circ}C$ is recommended by Berkurts (16).

$d = 0.325$ cm

. Water temperature = $21^{\circ}C \pm 1^{\circ}C$.

. Assuming a Maxwellian distribution at the water temperature ($21^{\circ}C$)

$$\bar{v} = \frac{2}{\sqrt{\pi}} \sqrt{\frac{T}{T_o}}\ v_o$$

$v_o = 2200$ m/sec at $T_o = 293.6^{\circ}K$ ($20.4^{\circ}C$)

$\bar{v} = 2.485 \pm 0.003\ 10^5$ cm/sec

---

(16) Beckurts: Neutron Physics, Page 374.

. Extrapolated dimensions

$a = b = c = 7.62$ cm

$\tilde{a} = \tilde{b} = \tilde{c} = 7.945$ cm

III. 2. Absorption and diffusion properties for water.

In this compilation, we used the basic data $\overline{\Sigma_a v}$, $D_o (= \overline{D}.\overline{v})$ and C as published by several authors rather than partial data like $\overline{\Sigma_a}$ or $\overline{D}$. This is because these parameters are directly derived from $\lambda = \Sigma_a v + D_o B^2 + CB^4$ in pulsed neutron measurements. We assume

$$\overline{\Sigma_a v} = \overline{\Sigma_a} \cdot \overline{v}$$

$$D_o = \overline{D} \cdot \overline{v}$$

to derive $\overline{\Sigma_a}$ and $\overline{D}$, and take into account eventual temperature corrections for D_o and C only.

There exist many formulae giving the dependence of D_o with respect to the moderator temperature. As we are interested only in a small variation with respect to published data at 22°, we use the formula given by Dio and Schoffer (17)

$$\overline{D}_o = 3.505.10^4 + (T-19)\ (130 \pm 30) \quad cm^2 sec^{-1}$$

between 19 and 75°C. It gives an increase of 130 $cm^2\ sec^{-1}$ per °C, or 0.37 (±0.09)% per °C from the value at 19°C. This formula agrees

---

(17) W. H. Dio and E. Schoffer. Nuclear Phys. 6: 175-176 (1958).

with measurements by Kuchle (18) at 22°C, who found a temperature coefficient of 0.37%/°C.

Selected values taken from literature are reproduced in Table III. 2, together with their corrected values at 21°C. Since we take $\bar{v}$ rather than $\overline{\Sigma_a}$ as reference in the product, $\overline{\Sigma_a v}$, we give the resulting values of $\overline{\Sigma_a} = \frac{\overline{\Sigma_a v}}{\bar{v}}$ and σ_a (2200 m/sec) derived from $\overline{\Sigma_a}$. It is interesting to note that these σ_a's agree quite well with the best published value $\sigma_a(2200) = 0.654$ (±0.006) barns (Beckurts (19)).

We feel that the last published data (Kuchle, Lopez and Beyster, Beckurts) are the most reliable up to date. The range of buckling included in these data makes a good basis for comparison. Fig. (III. 2.2 abc) shows the results in the form of curves fitted to these sets of data.

III. 3. Boron dosimetry.

Boric acid (BO_3H_3) in crystalline form was used for poisoning. We took the following data.

. Molecular weight of BO_3H_3 = 61.84 gr.

. Solubility in water at 21°C: 51.5 g per liter.

Since a poisoning corresponding to $\alpha = 1$ requests 3 g/liter of H_2O, the maximum possible poisoning ratio is: $\alpha_{maxi} \simeq 17$.

a) Poisoning doses: In first approximation, we took

$$\left.\begin{array}{l} \cdot\ \sigma_a\ (H_2O) = 0.66 \text{ barns} \\ \sigma_a\ (BO_3H_3) \simeq \sigma_a(B) = 755 \text{ barns} \end{array}\right\} \text{at 2200 m/sec}$$

---

(18) Kuchle: NSE 8, No. 1, 88, (1960).

(19) Beckurts and Wirtz. Neutron Physics, Page 408 (1964).

MEASURED VALUES OF ABSORPTION AND DIFFUSION

PROPERTIES OF WATER AT 21°C ($\bar{v}$ = 2,485 m/sec)

Authors	Size of Medium (B^2 in cm^{-2})	Year	$\bar{\Sigma}_a \bar{v}$ (sec^{-1})	$\bar{\Sigma}_a$ ($10^{-2} cm^{-1}$) σ_a(2200) in barns	22°C		Corrected 21°C	
					D_o($cm^2 sec^{-1}$)	C($cm^4 sec^{-1}$)	D_o($cm^2 sec^{-1}$)	$\bar{D}$ (cm)
Von Dardel & Sjostrand	$0.1<B^2<0.7$	1954	4892	1.9686 (0.664)	36,340 ±750	7,300 ±1,500	36,210 ±750	0.1457
Antonov et al.	Cylinder Dia=18.6 cm h=2.75 to 20 cm	1955	4831	1.9441 (0.656)	35,000 ±1000	4,000 ±1000	35,000 ±1000	0.1418
Bracci and Coceva	$0.09<B^2<0.96$	1956	4950	1.9919 (0.672)	34,850 ±1,100	3,000 ±1,000	34,850 ±1,100	0.1402
Dio	---	1959	4808	1.9348 (0.653)	35,450 ±600	3,700 ±700	35,320 ±600	0.14213
Kuchle	---	1960	4785	1.9255 (0.650)	35,400 ±700	4,200 ±800	35,270 ±700	0.14193
Lopez and Beyster	$0.02<B^2<0.42$	1962	4768	1.9187 (0.648)	36,892 ±400	5,116 ±776	36,762 ±400	0.1479
Beckurts	Compiling of recent results	1965	4782 ±15	1.9243 (0.650)	35,630 ±80 at 20°C	3,420 ±170	35,760 ±80	0.1439

TABLE III. 2

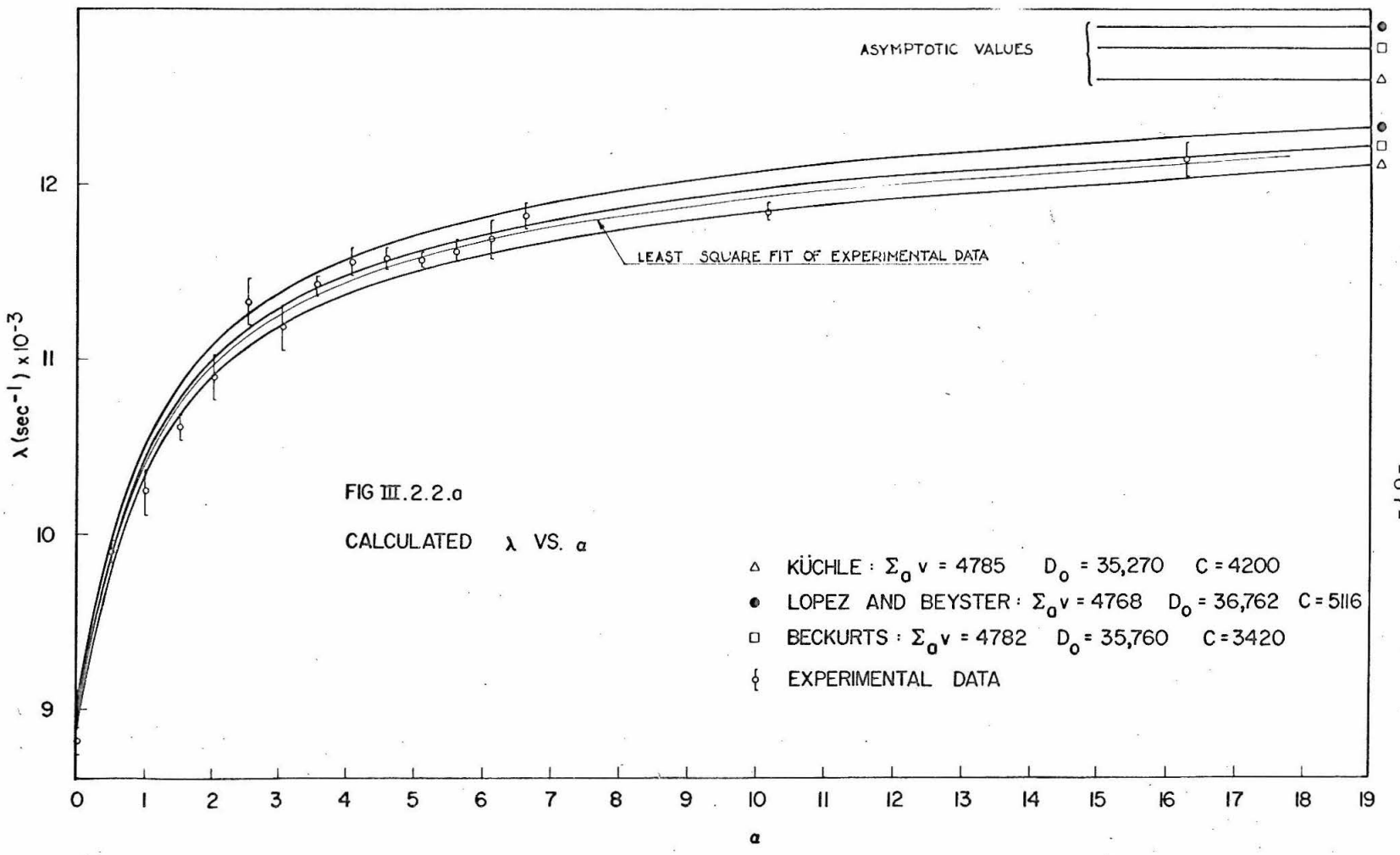

FIG III.2.2.a

CALCULATED λ VS. α

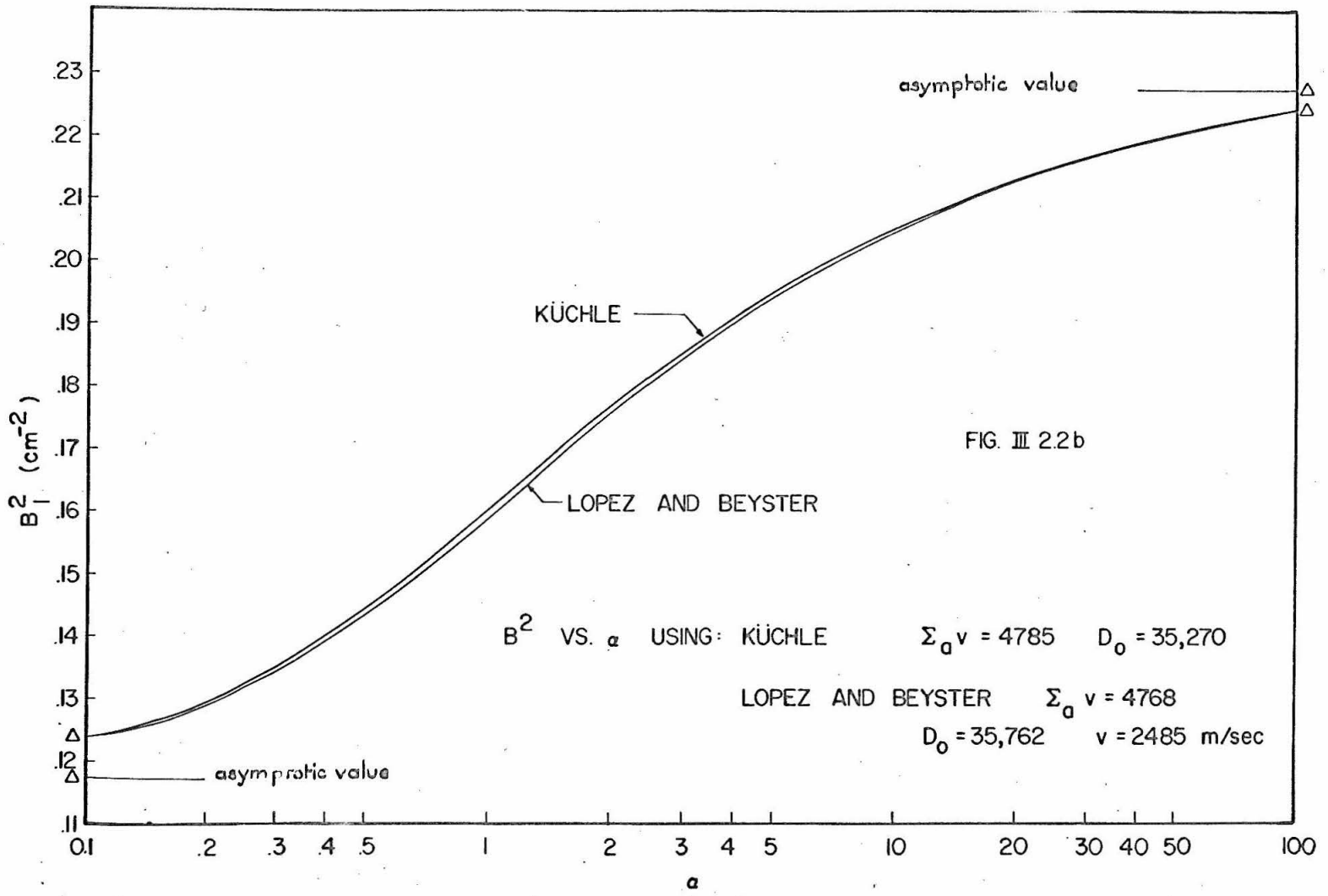
asymptotic value
KÜCHLE
LOPEZ AND BEYSTER
FIG. III 2.2b
B^2 VS. α USING: KÜCHLE $\Sigma_a v = 4785$ $D_0 = 35{,}270$
LOPEZ AND BEYSTER $\Sigma_a v = 4768$
$D_0 = 35{,}762$ $v = 2485$ m/sec
asymptotic value
B_1^2 (cm^{-2})
α
.23
.22
.21
.20
.19
.18
.17
.16
.15
.14
.13
.12
.11
0.1
.2
.3
.4
.5
1
2
3
4
5
10
20
30
40
50
100

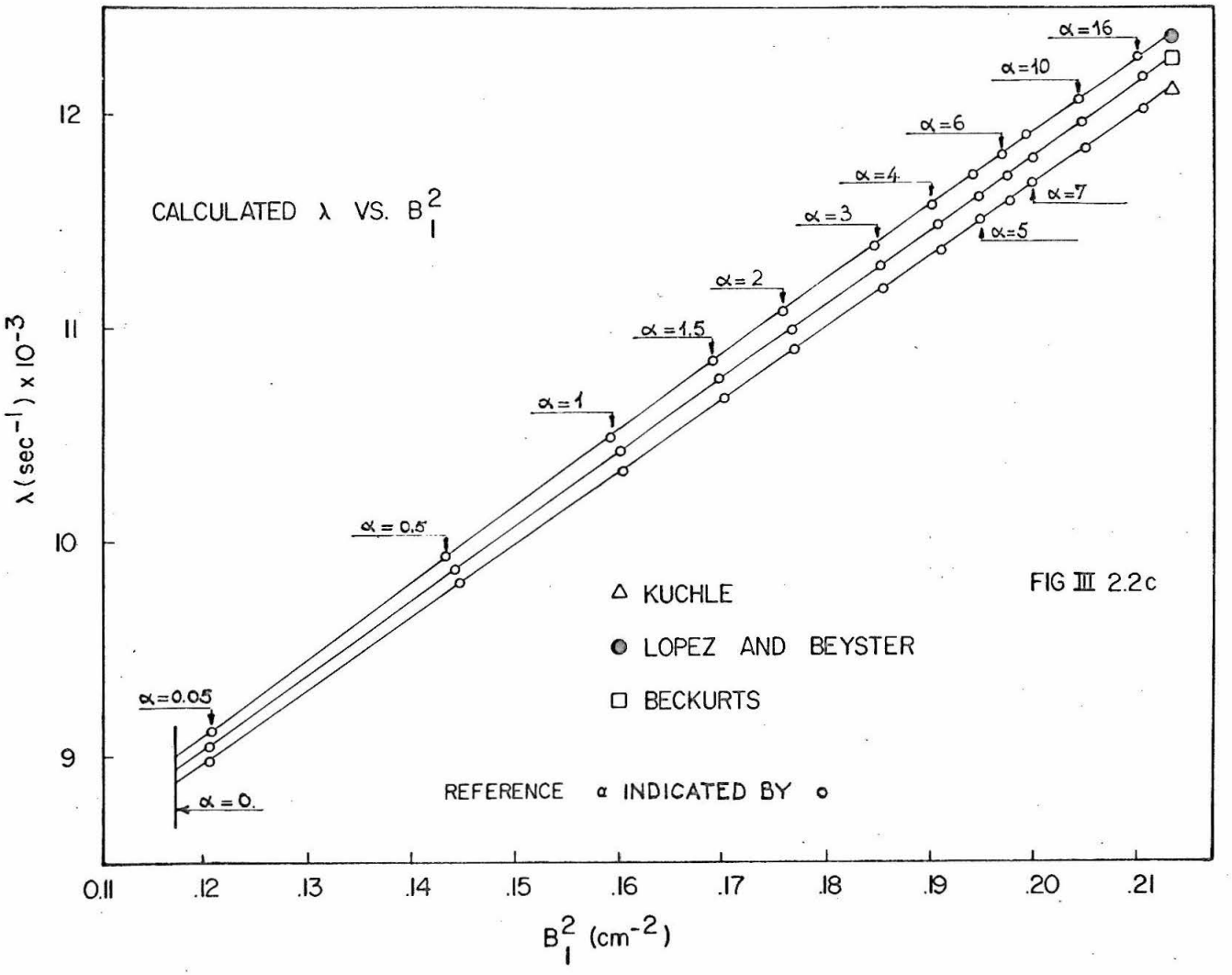
CALCULATED λ VS. B_1^2
$\lambda (sec^{-1}) \times 10^{-3}$
$B_1^2 (cm^{-2})$
α = 16
α = 10
α = 6
α = 4
α = 7
α = 3
α = 5
α = 2
α = 1.5
α = 1
α = 0.5
α = 0.05
α = 0.
△ KUCHLE
● LOPEZ AND BEYSTER
□ BECKURTS
REFERENCE α INDICATED BY o
12
11
10
9
0.11
.12
.13
.14
.15
.16
.17
.18
.19
.20
.21

FIG III 2.2c

as referenced in (20).

with $H_2O = 18$

$BO_3H_3 = 61.84$

This leads to a poisoning addition of

$m = 3.003269 \text{ mg/cm}^3$ for $\alpha = 1$

The volume to poison is $V = 1786.1097 \text{ cm}^3$, i.e. requiring

$M = 5.364169$ g of BO_3H_3 for $\alpha = 1$.

Poisoning was performed on this basis with α varying by steps of 0.5 from 0 to 6.5, then for $\alpha = 10$ and $\alpha = 16$.

b) More accurate data was later introduced with:

$H_2O = 18.016$ $\quad \sigma_a(H_2O) = 0.654 \pm 0.006$ barn.

$BO_3H_3 = 61.84$ $\quad \sigma_a(B) = 760.8 \pm 1.9$ barn for natural boron (19.81% of B^{10}) (21)

These new values lead to:

$$\alpha = 1 \times \frac{760.8}{755} \times \frac{18.016}{18} \times \frac{0.660}{0.654} = 1.01783$$

for $M = 5.364169$ g of BO_3H_3 as added.

These corrections have been taken into account in the data processing.

---

(20) Meghreblian and Holmes: Nuclear reactor theory.

(20) Reactor Physic Constants: ANL 5800, Page 30 (1963).

(21) Prasdocimi and Deruytter: The Absorption cross section of Boron. J. Nucl. Energy A & B, 17, 83 (1963).

IV DESCRIPTION OF THE EXPERIMENTAL SET-UP

A conventional source of 14 MeV neutrons was used to pulse the assembly, which was surrounded with cadmium and boron. A thermal neutron scintillation detector (1/4" in diameter) was connected to proper amplifiers and discriminator before feeding a 256 channel analyzer.

IV. 1. The pulsed neutron generator:

In this experiment, we used the Model 9505 Neutron Generator manufactured by the Texas Nuclear Corporation of Austin, Texas. Neutrons are produced by bombarding deuterium or tritium targets with deuterons, according to the following reactions:

- $D_2 + D_2 \rightarrow n_1 + He_3 + 3.267$ MeV
- $D_2 + T_3 \rightarrow n_1 + He_4 + 17.577$ MeV

For the "thick" targets supplied with the accelerator, the D-D reaction will yield neutrons of 2.86 MeV energy and the D-T reaction will yield neutrons of 14.74 MeV at 0° with respect to the incident neutron beam. Since the targets supplied with the accelerator are "thick" relative to the range of the incident deuterons, deuterons of all energies from zero to the incident bombarding energy will yield neutrons which will introduce an energy spread of the neutrons. In all our experiments, we used the (D-T) reaction.

The accelerator produces ion beams (deuterons) up to 1500 microamperes under 150 kilovolts, (continuous beam). In the pulsed mode, the beam is deflected by means of a pulser and chopper monitored from an external console, where the frequency and the pulse width may be adjusted.

As far as this experiment is concerned, the accelerator, when operating under normal conditions, was able to produce a sufficiently strong neutron flux with very small background between pulses (i.e. when the beam is deflected). This last feature was particularly appreciated, since it is known that certain pulsed neutron facilities may produce unwanted neutrons due to secondary interactions when the beam is turned off. This situation was not detected in our experiments.

IV. 2. General configuration of the experimental set-up.

The general pulsed neutron source and pulsed assembly configuration is described below.

a) The water container:

The water container is made of aluminum, with walls 3 mm thick and a dividing foil (0.8 mm thick) whose absorption effects were neglected.

The internal dimensions are 6 x 6 x 7 inches (±0.2 mm) allowing a 6 x 6 x 6 inches water volume. It is internally coated with a protective spray to minimize corrosion by water.

The container, open at the top, is entirely coated externally (top included) with cadmium (1 mm thick) whose role is to absorb most incoming or outcoming thermal neutrons, thus minimizing the hazard of slow reflected neutrons.

b) The surrounding shielding:

When an experiment is performed, the whole assembly is shielded with highly absorbing boron everywhere, except on the bottom face which is closely exposed to fast neutrons. A large thickness of borated water surrounds the ensemble. This configuration minimizes backscattering effects.

IV. 3. The scintillation detector.

The Model DS8-10 Neutron scintillation detector set manufactured by the Nuclear Chicago Corporation was used in all experiments.

IV. 3. 1. The neutron probe:

The SN-6 neutron probe consists of an aluminium housing, 5/16" outside diameter and 42" long, a light pipe, a thermal neutron crystal, and a probe adapter cap. The light pipe is a polished lucite rod for optical coupling between the crystal and the photomultiplier tube.

The thermal neutron crystal is a disc of plastic 1/4" in diameter and 3/16" thick. The plastic contains 95% enriched boron-10 and silver-activated zinc sulfide (ZnS(Ag)). The phosphor is also coated on the grooved front face of the disc.

When a capture takes place, α particles are emitted through the standard (n, α) reaction, causing in turn the nearby phosphor to scintillate.

The counting efficiency and discrimination against γ rays of such crystals is described by W. J. Price (22). The crystal responds to fast neutrons and gammas. Fast neutrons will create recoil protons, while gammas may strip orbital electrons. Both may cause the phosphor to scintillate. However, since the ionization effect is much greater for α particles than for other particles, it is possible to discriminate against fast neutrons and gamma rays.

---

(22) W. J. Price: Nuclear Radiation Detection, Page 298 (1958).

The energy dependence of the cross section σ for the $B^{10}(n,\alpha)$ reaction is found to have the $\frac{1}{v}$ dependence up to about 100 eV and is commonly written

$$\sigma(v) = \sigma_o \frac{v_o}{v} \qquad \text{(IV. 3. 1. 1)}$$

Price (23) gives σ_o = 4010 barns at $v_o = 2.2 10^5$ cm/sec.

The reaction rate (reactions per sec) in B^{10} is

$$R = \int_o^\infty \Sigma(E)\,\phi(E)\,dE$$

if $\phi(E)$ is assumed to be constant inside the crystal.

If the neutron spectrum lies within 0-100 eV, (IV. 3. 1. 1) is valid, and we get

$$R = \int_o^{100\,eV} \Sigma(E)\,\phi(E)\,dE$$

$$= \Sigma_o v_o \int_o^{100\,eV} n(E)\,dE$$

$$R = \Sigma_o v_o N$$

N is the total number of neutrons per unit volume.

Such a detector measures effectively a neutron density, independently of energy. Assuming a Maxwellian spectrum with average velocity $\bar{v}$, the total flux is

---

(23) W. J. Price: Nuclear Radiation Detection (1958).

$$\bar{\Phi} = N\bar{v} = \frac{R\bar{v}}{\Sigma_a v_o}$$

In our experiment, the flux is assumed to be Maxwellian, with $\bar{v}$ held constant corresponding to the moderator temperature. Therefore, the output of the detector can be interpreted as either neutron density or neutron flux.

It is reasonable to assume, in our case, the following:

a) The extra absorption introduced into the system by the detector is negligible, because of the size of the crystal and properties of the casing which are very close to that of water.

b) The probe itself has practically no dead-time. This is because the principal decay component of ZnS (Ag) has a decay constant of approximately 0.04 μ sec. There is a significant advantage for very short resolving times.

c) We are able to make a fair gamma discrimination. It is known that fast neutrons may induce secondary γ-rays in water, thus affecting the measurements. We did not find any such significant effect in all the experiments.

d) The crystal does not get saturated at high counting rates.

IV. 3. 2 Position of the neutron probe:

The probe was located in the assembly in a way such that the effect of higher harmonics was minimized.

It was placed in the half-tank containing the pure distilled water, at the center of the Y and Z coordinates (see Fig. II. 4. 1) i.e. Y=Z=0.

The position of the probe along the X axis was adjusted accordingly with the boron poison concentration in the opposite half-tank, in such a way that it was always positioned approximately where the first spatial harmonic of the flux in the pure water was maximum. (See the schematic x-dependence vs poisoning on Fig. II.4.2 abcd). This means practically that the probe is placed at X = 0 for no poison ($\alpha = 0$) and placed at $X = -\frac{a}{2}$ for the maximum poison concentration.

In general, $X(\phi \text{maxi}) = \frac{1}{2}\left(\frac{\pi}{\omega_1} - a\right)$ where ω_1 vs. α was known approximately from the theoretical calculations.

IV.3.2. The photomultiplier:

The photomultiplier (Nuclear Chicago Part number VTK-1692) consists of 10 stages, cesium-antimony dynodes. The current gain is approximately 300,000 at the final dynode.

IV.3.3. The preamplifier:

The preamplifier, directly connected to the photomultiplier, consists of 3 transistor stages. The positive pulse from the photomultiplier tube is coupled to an emitter-follower connected transistor, which delivers a 7 to 10 μ sec positive pulse with low impedance (150 ohms). This first stage output is A-C coupled to a common emitter amplifier which is direct coupled to an emitter-follower.

The output of the amplifier has an overall gain of 20 and an output impedance of 150 ohms.

IV.4. The count-recording apparatus.

The output from the pre-amplifier is connected to the apparatus described in Fig. (IV.2.1).

Pulses are fed into the amplifier of the Model 181-A Decade Scaler (Nuclear-Chicago) which is used also as a power supply for the scintillation detector. The output of the 181-A is sent to a discriminator and ultimately to the model CN-110 transistorized multi-channel pulse analyzer system (Technical Measurement Corporation), equipped with the Time of Flight Logic Unit Model 211.

Dead time of the scintillation detector- Model 181-A - Discriminator set was measured and found to be close to 5 μsec. This is in agreement with the value given by the constructor for the 181-A.

However, this equipment had a very important disadvantage: The amplifier was found to be unable to handle reliably the high counting rate that occurs immediately after the neutron pulse. This effect introduced unwanted changes in the over-all efficiency of the apparatus which was difficult to take into account by a standard correction. Therefore, we had to limit the length and strength of the neutron bursts to minimize this saturation effect. This also "diluted" any short-time phenomena right after the end of the pulse, and contributed to the failure of its investigation.

The CN 110 equipped with the Model 211 Time of flight logic unit was used as follows:

- 256 adjacent channels
- channel width = 8 μsec
- No delay

Characteristics of the pulse generator were:

- Frequency = 450 or 475 cps
- Pulse width = 50 or 75 μsec

FIG. IV 2.1

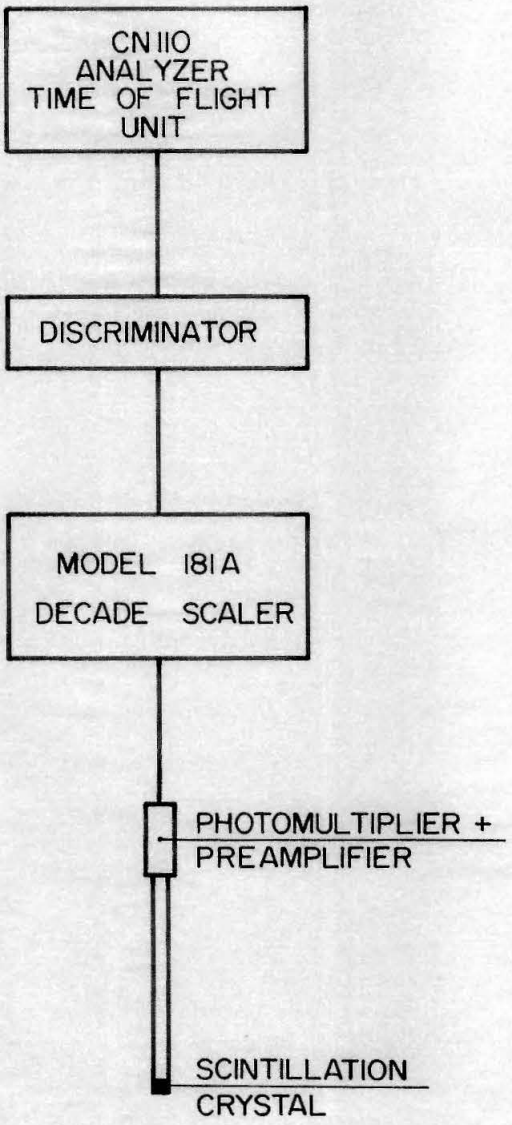
CN 110
ANALYZER
TIME OF FLIGHT
UNIT
DISCRIMINATOR
MODEL 181A
DECADE SCALER
PHOTOMULTIPLIER +
PREAMPLIFIER
SCINTILLATION
CRYSTAL

This provided a good picture of the pulse, and insured that each pulse decayed to the background level before another pulse was generated.

The total number of pulses (N) in a given experiment was also recorded.

V THE ANALYSIS OF EXPERIMENTAL DECAY CURVES

V.1. The Frantic Code:

The Frantic Program for Analysis of Experimental Growth and decay curves, developed at the Laboratory for Nuclear Science of the Massachusetts Institute of Technology, was used extensively throughout the experiments. (IBM 7090-7094)

Many authors make reference of methods to perform least square analysis of multicomponent exponentially decaying data in the assumed form $F(t) = \sum_{i=1}^{N} A_i e^{-\lambda_i t}$

Among them, the Behrens' method (24) gives good results for one component + unknown background. However, it was felt that, to improve the flexibility of the code, a real multicomponent scheme should be used. The Frantic code, modified for our specific use (including new count losses corrections) was shown to give fairly consistent and reliable results. It has been tested under many conditions, the most difficult arising with the 4 component analysis of a pulsed flux in graphite. Because it is based on an iterative method, there are times when convergence is not reached, and the method fails. However, this occurs essentially in the analysis of components with very close decay constant, or very slowly decaying components.

A short description of the iterative procedure is given in Appendix A1, together with ways of estimating the goodness of fit.

---

(24) D. J. Behrens - The fitting of exponential decay curves to the results of counting experiments. AERE T/R.629.

V.2. Corrections for count losses.

Two kinds of dead times were accounted for in the analysis:

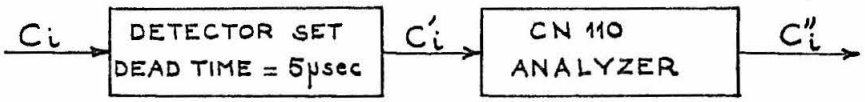

C''_i = Recorded counts in channel i at the output of the analyzer (known)

C'_i = Expected number of incoming counts in channel i

C_i = Expected number of counts

The CN110 Analyzer and the detector set (probe + amplifiers + discriminator) have quite different types of count losses processes.

V.2.1. Dead-time of the CN110 Analyzer:

When fitted with the Model 211 Time of Flight Logic Unit, the analyzer has a basic dead time of 16 μsec for recording of a count. In fact, the inoperative period may vary, since the recording of a count triggers an advance in the address of the next available channel. A complete description of the process is given in Appendix A2.

Assuming that the distribution of incoming counts in channel i is a Poisson distribution characterized by an average λ_i, the formula for the expected number of incoming counts in channel i is:

$$C'_i = -N \operatorname{Log}\left[1 - \frac{C''_i}{N - \sum_{j=i-n}^{i-1} C''_j}\right] \qquad (V.2.1.1)$$

N = Number of pulses

C''_i = Number of recorded counts in channel i after N pulses

C'_i = Expected number of incoming counts in channel i after N pulses

$n = \frac{16}{\ell}$ where ℓ is the channel length in microseconds. ($\ell \leqslant 16$ μsec)

This formula was first published without proof by Mills, Allen, Selig and Cadwell (25). A proof is given in Appendix A2.

As a channel length of 8 μsec was used in all experiments, n = 2, and formula (V. 2. 1. 1) becomes

$$C'_i = -N \operatorname{Log}\left[1 - \frac{C''_i}{N - (C''_{i-2} + C''_{i-1})}\right] \qquad \text{(V. 2. 1. 2)}$$

where C''_{i-2} and C''_{i-1} are the recorded counts in channels i-2 and i-1 respectively.

V. 2. 2. Dead-time of the detector.

As mentioned already, the dead-time of the detector amplifier set was found to be approximately 5 μsec. An accurate treatment of the dead time correction connecting C_i to C'_i is very difficult because:

. The source has a rapidly changing strength

. We know only the recorded counts C''_i in the analyzer, and this information is related to C'_i through the approximate assumption that the output pulses from the detector follow a Poisson distribution over a channel length.

(25) Mills, Allen, Selig, Cadwell - Neutron and gamma ray die-away in an heterogeneous system. Nuclear Applications Vol. 1, 4 (August 65).

It is clear that, as in the case for the CN110 Analyzer, a problem arises when the dead time of the detector is of the same order of magnitude than the measuring time (channel length). For a dead time $\tau = 5$ μsec and a measuring time $\ell = 8$ μsec, the maximum number of detected counts will be 2, regardless of the total number of generating counts. In addition, what happens in a given channel depends strongly on the detected events in the previous one.

However, it is felt that this problem arises mostly when the count-rate is extremely high. In most of our experiments, the peak count rate was voluntarily limited in order to give a maximum of 10^5 counts for 10^7 pulses, i.e. 10^{-2} counts per channel per pulse or 1.2510^5 cps for a 8 μsec channel length.

In such conditions, we believe it is legitimate to make a standard dead time correction as follows:

N = number of pulses (e.g. 10^7)

ℓ = channel length (e.g. 8.10^{-6} sec)

$N\ell$ = Total measuring time (e.g. 80 sec)

τ = Dead time of the detector (e.g. $5\ 10^{-6}$ sec)

$$C_i = \frac{C'_i}{1 - \frac{C'_i}{N\ell}\tau}$$

For $C'_i = 10^5$ counts, and our indicative values, we get

$C_i = 10^5\ (1 + 0.00625)$ i.e. a correction less than 1% at worst.

These two dead-time corrections were taken into account by the modified Frantic Code. Their effect is to give a better exponential behavior over the first channels. The analysis was carried over the C_i's.

V.2.4. Validity of the Poisson distribution assumption.

This treatment relies on the assumption that the counts incoming into the analyzer follow a Poisson distribution over a channel width. The physical process involved may be compared to radioactive disintegrations. By looking at the works of D. J. Behrens (26), R. Peierls (27), A. Ruark and L. Devol (28), it appears that such an assumption is legitimate if:

a) The source strength does not vary appreciably over a channel length of time. The total number N of neutrons which may give raise to a count is very large with respect to n, the number of counts appearing over a channel length. Therefore, we may apply the Poisson approximation to the binomial distribution of appearing counts.

b) The detector has zero dead-time.

Assumption (a) deals with the statistical model used. When we look at a multichannel picture, this is as if we were to assume

---

(26) D. J. Behrens. Notes on the nature of experiments, the statistics of counting and the fitting of exponential decay curves to the results of counting experiments. A.E.R.E. T/R.629 (1951)

(27) R. Peierls. Statistical Error in Counting Experiments, Proc. Roy. Society (London) A149 (1935).

(28) A. Ruark and L. Devol., General theory of fluctuations in Radioactive Disintegrations. Phy. Review 49 (1936).

that the smooth exponential decay curve is broken into steps, each step corresponding to an individual constant source over a channel length. Since after all we deal only with a correction term, it may be assumed that the variations of the source strength over the channel length introduced a higher order error that was not taken into account.

Assumption (b) is felt to be legitimate, for while the detector has a finite dead time, the maximum count-rate is so small (10^{-2} counts per channel) that it is not expected to affect in a sensible way the overall correction.

Some remarks on the probability distribution functions in decay processes are given in Appendix A3.

V.3. The fundamental decay mode analysis.

We feel that one of the critical points of every pulsed neutron experiment lies in a proper selection of the portion of the decay data to be analyzed. Assuming that a proper numerical analysis method and a correct count losses correction scheme are available, it is frequent to find more than 5% variation in the determination of the fundamental decay mode. This uncertainty lies in the selection of the part of data to be analyzed. Thus, given a set of data, the critical questions are:

. Where should the analysis start? (i.e. with respect to the end of the burst).

. Where should the analysis end?

It turns out that some of the discrepancies between published results may be attributed to the different individual answers given by each author. It is difficult to derive a 100% effective criterion to recognize "best fits" for some of these criteria may lead to contadictory answers.

We first selected a basic amount of data as follows:

All our experiments were performed with 256 (8 μsec) channels and no delay time. As decay goes on, we selected data starting at the first channel containing less than 10^5 counts. The experiments were carried long enough and in such a way that this channel number lies between 30 and 40, providing an approximate waiting time of 190 to 270 μsec for a pulse width of 50 μsec. Then, all the data were taken up to channel 256.

This usually provided a decay over 5 decades and 100 channels, leaving approximately 100 channels of background. This background measurement, besides providing an accurate estimation of the background level (of very little interest), was essentially used to check that no slowing decaying or increasing component of small amplitude was present, such as accelerator generated background.

Fig. (V.3.a) is a typical example of such data for $\alpha = 0.508$.

These basic data were then numerically least-squares fitted to one decaying component and a constant background ($\lambda = 0$) of unknown amplitude. The starting channel was changed by steps of 5, and the end channel was adjusted over the background range. In this way, we analyzed different portions of the basic data, keeping track of λ, $\sigma(\lambda)$, and the variance of the fit (VAR). From many experiments, we observed:

a) The selection of the end point is of no significant importance:

Fig. (V.3.b) shows the change in λ and VAR when the end channel was reduced by steps of 5 over the background range. As

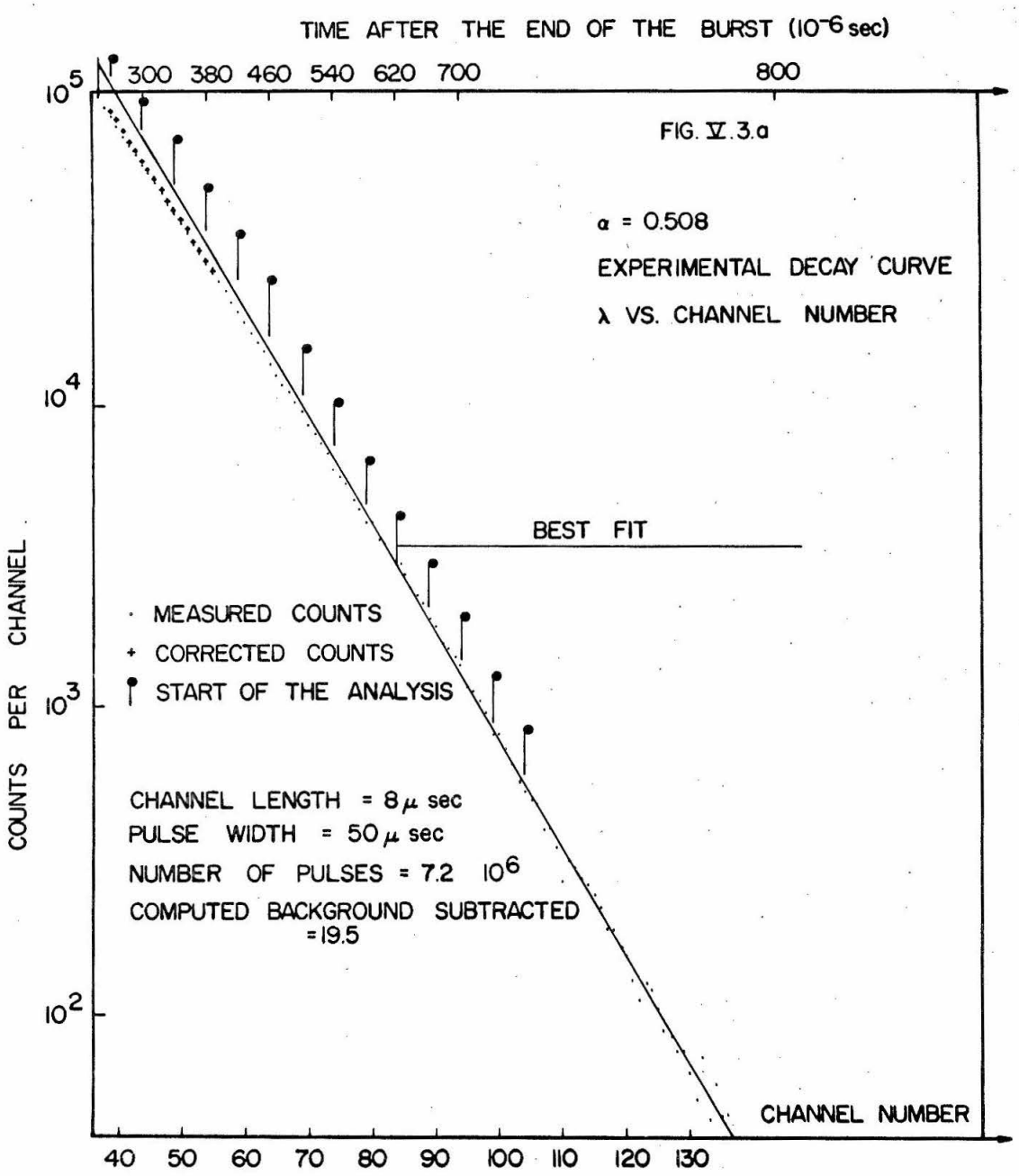
TIME AFTER THE END OF THE BURST (10^{-6} sec)
300 380 460 540 620 700 800
10^5
10^4
10^3
10^2
COUNTS PER CHANNEL
FIG. V.3.a
α = 0.508
EXPERIMENTAL DECAY CURVE
λ VS. CHANNEL NUMBER
BEST FIT
· MEASURED COUNTS
+ CORRECTED COUNTS
START OF THE ANALYSIS
CHANNEL LENGTH = 8 μ sec
PULSE WIDTH = 50 μ sec
NUMBER OF PULSES = 7.2 10^6
COMPUTED BACKGROUND SUBTRACTED
=19.5
CHANNEL NUMBER
40 50 60 70 80 90 100 110 120 130

can be seen, this change never exceeded 0.15% for λ, which is quite reasonable. Including more background data does not affect λ, but improves the accuracy in the background level, in which we are not interested. However, since there is no disadvantage in including very much background data, we did so in all the analysis, i.e. included all the background data.

b) The selection of the starting point is very important.

As can be seen in Fig. (V.3.a), it takes a relatively long time for the fundamental mode to be truly established, i.e. for the background corrected decay curve (on semi-log plot) to be a true straight line, with statistical fluctuations evenly scattered as time goes on. Fig. (V.3.a) shows also the effect of the count-loss correction factor. However, this "straightening" of the curve is insufficient to provide a real straight line all over the decay curve.

Thus, we believe strongly in the need for a complete detailed picture of the decay process from the end of the burst down to the background level. We believe it is also important to gather sufficient information on the background itself (i.e. at least 50 channels) in order to make sure that it is reached and does not vary slowly because of backscattering or improper shut off of the beam of the accelerator. This calls for a truly multichannel analyzer with at least 100 channels. If these conditions are not met, the experimenter using a simplified analyzer (as those with 20 channels) will analyze an incomplete portion of the decay, and therefore be unable to decide whether the fundamental mode has been reached or not. (For instance, one could be tempted to analyze the first 3 decades of the typical decay shown in Fig. (V.3.a),

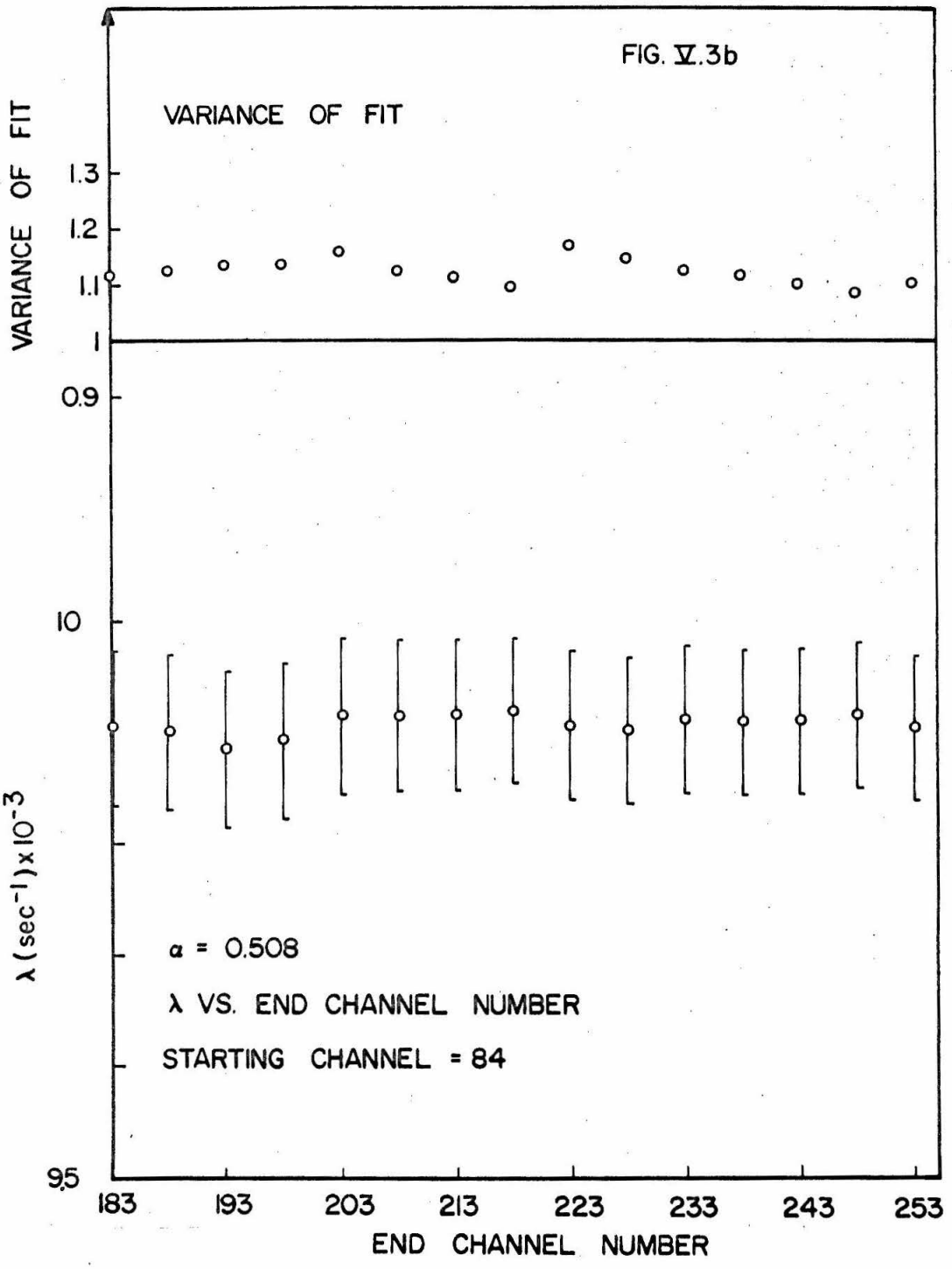
FIG. V.3b
VARIANCE OF FIT
VARIANCE OF FIT
1.3
1.2
1.1
1
0.9
10
9.5
λ (sec⁻¹) x 10⁻³
α = 0.508
λ VS. END CHANNEL NUMBER
STARTING CHANNEL = 84
183
193
203
213
223
233
243
253
END CHANNEL NUMBER

and would derive a wrong result.)

Assuming that we have the necessary detailed picture of the decay process, it is then necessary to select the proper starting point where the fundamental mode is believed to be reached. The best way to do it is to perform many analysis by varying the starting point, and keep track of λ, $\sigma(\lambda)$ and the variance of fit (VAR). When the fundamental mode is reached, λ should not vary whatever posterior portion of the data is analyzed.

Fig. (V.3.c) shows how λ and VAR change when this method was applied to data in Fig. (V.3.a). If the analysis is begun too soon, λ is underestimated, and the weighted variance of the fit relatively large. When the beginning of the analysis is delayed more and more λ increases while the closeness of fit improves (i.e. the weighted variance of the fit decreases). Ultimately, λ reaches an equilibrium level from which it does not change. From there, we can say that the fundamental mode has been reached. The variance of fit has also improved by reaching a minimum.

This behavior allows us to select the "best fit", i.e. the one leading to a minimum variance when the fundamental mode has been reached. From Fig. (V.3.c), it can be seen that the fundamental mode was reached at about channel 84, i.e. 620 μsec after the end of the burst. The calculated decay curve has been plotted on Fig. (V.3.a), and shows that the statistical variations are evenly distributed along it.

Fig. (V.3.c) also shows that, after the fundamental mode has been reached, the decay constant may suffer some fluctuations (in this particular case, it dropped). This may occur when the starting

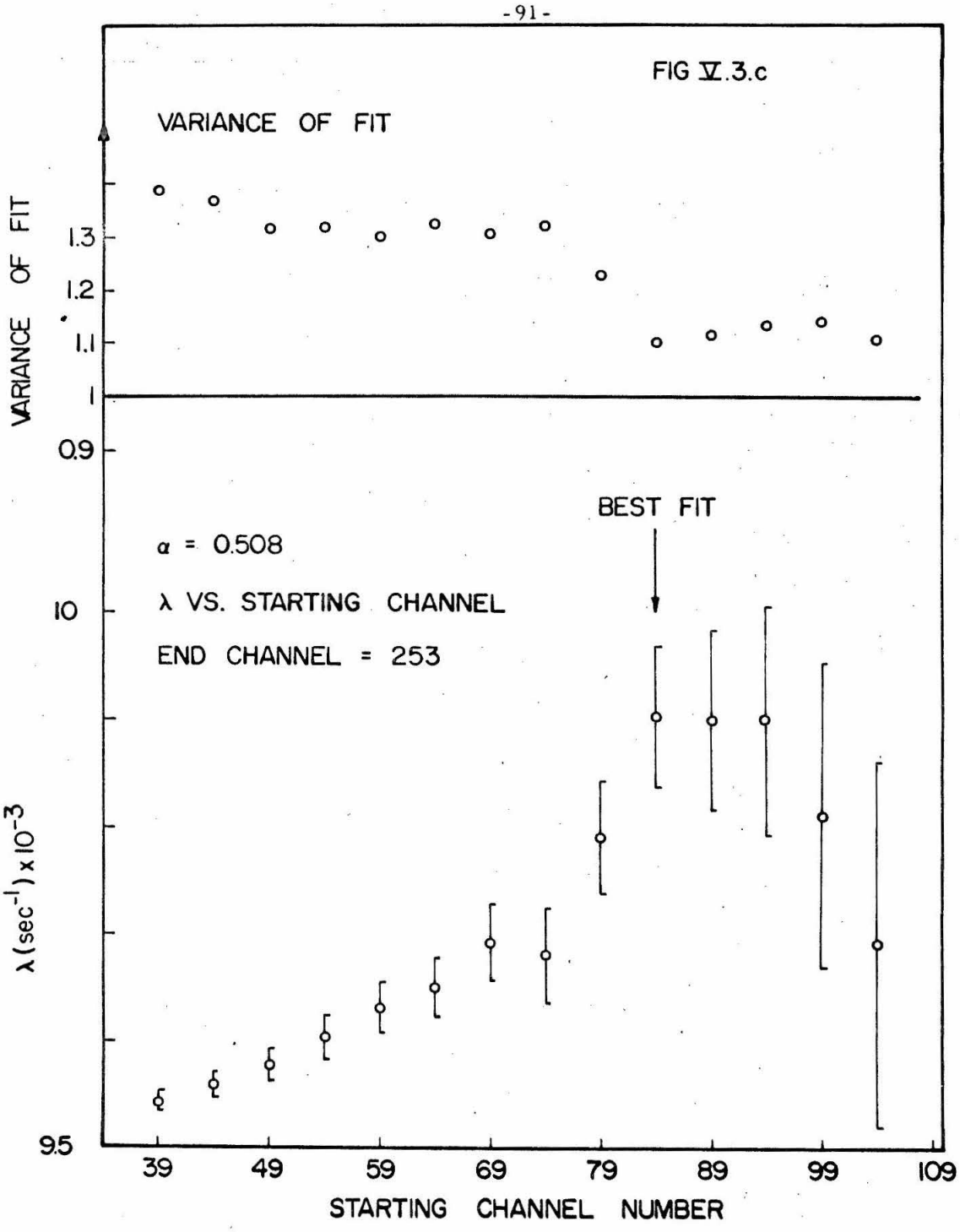
FIG V.3.c
VARIANCE OF FIT
VARIANCE OF FIT
1.3
1.2
1.1
1
0.9
BEST FIT
α = 0.508
λ VS. STARTING CHANNEL
END CHANNEL = 253
10
λ (sec⁻¹) x 10⁻³
9.5
39
49
59
69
79
89
99
109
STARTING CHANNEL NUMBER

channel is so delayed that only a very small portion of the end of the decay is analyzed against a long tail of background. These random fluctuations should be charged to poor statistics, since they result from analysis covering less than 1 decade, on counts subject to relatively large statistical fluctuations. This is why the best fit is often chosen as the first occurring after reaching of the fundamental mode.

In all our experiments, such an analysis was performed. Data were analyzed using 13 to 15 starting points, depending how fast the decay was. The last starting point was fixed by the fact that the remaining data should cover one decade at least (from 300 to 30 counts for instance). The average time required to reach the fundamental mode was of the order of 600 μsec, and often more.

From there, the "best fit" was chosen according to the following criteria:

- The fundamental mode has been reached (i.e. λ does not change appreciably as the starting point is more delayed)
- The variance of the fit is minimum
- The standard deviation $\sigma(\lambda)$ is the smallest available.

The two first criteria were weighted equally and were given priority to select the proper decay constant. If these were insufficient to choose from the different potentially eligible λ, then the last criterion was applied to make the final decision.

In the case given in Fig. (V.3.c), the situation happened to be ideal, i.e. the different criteria led to compatible answers. There were cases when the choice was not so clear, and a careful weighting of these factors had to be made. Most of the time, the reaching of

the fundamental mode criterion was given final priority.

From all the experiments, it appears that λ could be determined within 0.7% for 10 out of 16 cases, and the overall accuracy is of the order of 1%.

VI RESULTS

VI. 1. Experimental results:

Table VI. 1 shows the experimental results obtained for different values of the poisoning parameter α. These experimental results were derived in the following conditions:

a) Determination of α: The poisoning factor α was taken "a priori" according to section III. 3.

b) Determination of λ: The fundamental mode decay constant was chosen according to the numerical analysis described in Chapter 5. The "best fit" was chosen by optimizing the following criteria:

- Variance of the fit
- Behavior of λ versus the portion of data to be analyzed
- Good statistical distribution of the deviations between calculated and experimental curve.

The apparent numerical accuracy of these results is purely fictitious, and should be attributed to the data processing method.

c) Determination of the standard deviation $\sigma(\lambda)$:

This result is generated by the Frantic code, and gives only an evaluation of how well the calculated curve fits the data when statistical weights are used. Thus, this standard deviation describes how much confidence should be put in the fit. We believe that the standard deviation associated with the experiment and the fit should be taken larger than σ given in Table VI. 1.

TABLE VI. 1

Least-square fit:

$\lambda = 4792 + 34,800\ B^2_{\text{eff.}}$

α	Experimental λ (sec^{-1})	$\sigma(\lambda)$ (sec^{-1})	Calculated λ (sec^{-1})	Calculated B^2 (cm^{-2})
0	8824.	83	8873.	0.11726
0.509	9903.	64	9845	0.14519
1.018	10256	141	10395	0.16100
1.527	10613	76	10740	0.17091
2.036	10900	126	10971	0.17756
2.545	11333	134	11136	0.18230
3.054	11188	130	11268	0.18608
3.562	11437	46	11372	0.18908
4.071	11559	77	11458	0.19154
4.580	11585	59	11530	0.19362
5.089	11571	38	11592	0.19540
5.598	11620	63	11646	0.19695
6.107	11691	113	11689	0.19819
6.616	11826	71	11734	0.19948
10.178	11850	47	11942	0.20546
16.285	12151	97	12135	0.21101

In Table VI. 1, an experimental value has been omitted: $\alpha = 7.125$ $\lambda = 11488\ \text{sec}^{-1}$ $\sigma = 84.33\ \text{sec}^{-1}$. This value falls so much under the general curve that its deviation can be explained only by an experimental inconsistency. We believe that, in this case, the relatively large amount of boric acid was not fully dissolved in the water. As a consequence, the boron concentration suffered a large error.

This value was not considered in the data evaluation.

VI. 2. The data evaluation.

We first plot λ versus α, and expect to find a curve similar to those obtained using a priori values for $\Sigma_a v$, D_o and C taken in the literature. This appears to be the case, and we can estimate roughly the experimental scattering of points to be within 1% of the λ value.

However, we would like to have a better estimation of the goodness of data, i. e. we would like to find the best parameters $\Sigma_a v$ and D_o which, when used to generate the λ versus α curve according to the analysis given in Section II.5.2, minimize the quantity:

$$\chi^2 = \sum_{i=1}^{n} \frac{(y_i - Y_i)^2}{\sigma_i^2}$$ where

n = number of data points

Y_i = experimental value of λ

σ_i = standard deviation associated with Y_i

y_i = calculated value of λ

Here, the σ_i's enter as weighting factors. Thus, their absolute value is not of primary importance; it is rather their relative amplitude which counts. This relative amplitude is given by the Frantic Code, and tabulated in Table VI. 1.

The general accuracy of the results leads us to believe that the introduction of an unknown cooling factor C in the fit is purely artificial, since this correction term is of the same order that the experimental error (i.e. $\simeq 100\ \text{sec}^{-1}$). We will attempt a two parameter fit, and write

$$\overline{\Sigma_a v} = A_o$$
$$\overline{D_o} = A_1$$
$$\lambda = y$$

For a given amount of boric acid added, the poisoning factor α depends on the ratio of the absorption cross sections of water and boric acid. If $(\Sigma_a v)_{H_2O}$ is allowed to vary in the fit, α will vary accordingly. However, since $(\Sigma_a)_{H_2O}$ is not expected to vary in large proportions in the course of the fit, we take as constant reference the ratio $\frac{(\Sigma_a)_{H_2O}}{(\Sigma_a)_{BO_3H_3}}$ rather than $(\Sigma_a)_{BO_3H_3}$ alone. Thus, α is taken constant a priori.

VI. 2. 1. Two parameter fit without the introduction of the cooling factor:

We attempt the following fit

$$y\left(\alpha(A_o), A_o, A_1\right) = A_o + A_1 B^2\left(\alpha(A_o), A_o, A_1\right)$$

where B^2 denotes the effective buckling as calculated in Section II.4.2.3. Because $B^2 = \omega_1^2(\alpha, A_o, A_1) + \left(\frac{\pi}{2b}\right)^2 + \left(\frac{\pi}{2c}\right)^2$ is NOT linear in A_o and A_1, we cannot make a unique least-squares analysis as in the case of polynomial fitting.

With α held constant when A_o and A_1 are allowed to vary, we have

$$y(A_o, A_1) = A_o + A_1 B^2(\alpha, A_o, A_1)$$

We chose to perform an iterative least square analysis as follows:

a) We give first guesses for A_o and A_1 denoted by $A_o^{(o)}$ and $A_1^{(o)}$, and compute $B^2(\alpha, A_o^{(o)}, A_1^{(o)})$ which is then known and denoted by $B^2_{(o)}(\alpha)$. It is then trivial to make a least square analysis of the experimental data in the form

$$y(\alpha) = A_o + A_1 B^2_{(o)}(\alpha)$$

This least-square analysis leads to an improved set of coefficients $A_o^{(1)}$ and $A_1^{(1)}$, and a given $\chi^2_{(1)}$. This is known as an iteration.

b) These improved values $A_o^{(1)}$ and $A_1^{(1)}$ are then substituted into $B^2(\alpha, A_o^{(1)}, A_1^{(1)})$ leading to a new $B^2_{(1)}(\alpha)$. A polynomial fitting is performed with

$$y(\alpha) = A_o + A_1 B^2_{(1)}(\alpha)$$

leading to new improved values $A_o^{(2)}$ and $A_1^{(2)}$ of the coefficients, together with a new improved $\chi^2_{(2)}$.

c) The iterative process is continued (i.e. put $A_o^{(2)}$ and $A_1^{(2)}$ in B^2, derive $B^2_{(2)}$, find improved $A_o^{(3)}$, $A_1^{(3)}$, $\chi^2_{(3)}$ and so on) until both $A_o^{(i)}$, $A_1^{(i)}$ and $\chi^2_{(i)}$ do not vary by more than 10^{-6} from one iteration to another. Then, convergence is achieved.

Theoretically, this process offers no guarantee of convergence and stability. We cannot influence any of them, for they are contained in the non-linear function B^2 of α, A_o, A_1. However, one can get a crude idea of the convergence feasibility by looking at the dependence of λ and B^2 vs A_o and A_1. When $\frac{A_o}{A_1}$ decreases, B^2 decreases (see Fig. III. 2. 2. b) while λ increases (Fig. III. 2. 2. a). This reverse effect is believed to provide the necessary convergence and stability.

Numerical calculations were performed on the IBM 7090-7094, and led to the following results:

. Number of iterations needed to satisfy the convergence criterion = 6.

. $A_o = \Sigma_a v = 4792\ (\pm 150)\ \text{sec}^{-1}$

. $A_1 = D_o = 34,800\ (\pm 800)\ \text{cm}^2\text{sec}^{-1}$

. $\chi^2 = \sum_1^n \frac{(y_i - Y_i)^2}{\sigma_i^2} = 18.22$ for 16 points.

The values given in parentheses give estimates of the standard deviation of the parameters as computed from the least-squares analysis. They are relatively large. This is due mainly to the rather small range of buckling values available, rather than to the over all accuracy of the experimental results (in which $\sigma(\lambda) \backsimeq 100\ \text{sec}^{-1}$).

Dividing χ^2 by the number of degrees of freedom = Number of points – number of unknown parameters = 14

leads to a variance of fit

$$\text{VAR} = \frac{\chi^2}{\text{NF}} = 1.30 \text{ which is reasonable.}$$

We were therefore able to represent our experimental data in the best analytical form.

$$\lambda = 4792 + 34800\ B^2 \quad (\alpha, 4792, 34800) \qquad \text{(VI. 2. 1)}$$

Fig. (VI. 2. a) and (VI. 2. b) show λ (α) and λ (B^2) as determined experimentally and fitted by formula (VI. 2. 1). Local values as calculated are given in table (VI. 1). We can see that the agreement is very good between the experiment and the idealized curve.

It is of interest to compare this two parameter fit with values given for water in literature. We found

$$\overline{\Sigma_a v} = 4792 \quad (\pm 150)\ \text{sec}^{-1}$$

$$\overline{D_o} = 34,800\ (\pm 800)\ \text{cm}^2\ \text{sec}^{-1}$$

It is clear that the value $\overline{\Sigma_a v} = 4792\ \text{sec}^{-1}$ agrees pretty well with the value found by Kuchle ($\overline{\Sigma_a v} = 4785\ \text{sec}^{-1}$) and Beckurts ($\overline{\Sigma_a v} = 4782\ \text{sec}^{-1}$).

On the other hand, $\overline{D_o}$ is consistently underestimated. This is because, in first approximation, we did not take into account the cooling factor C. Therefore, when fitting a parabola with a straight-line as we did, we had to reduce the slope corresponding to $B^2 = 0$.

However, the result on D_o can be improved by the following first order approximation:

Suppose we write $\lambda = \Sigma_a v + (D_o - CB^2)\ B^2$

Since the range of buckling is very small (from 0. 12 to 0. 21 cm^{-2}), it can be expected that (D_o - CB^2) will not vary appreciably over this range. We may then take the cooling factor C a priori as given in the

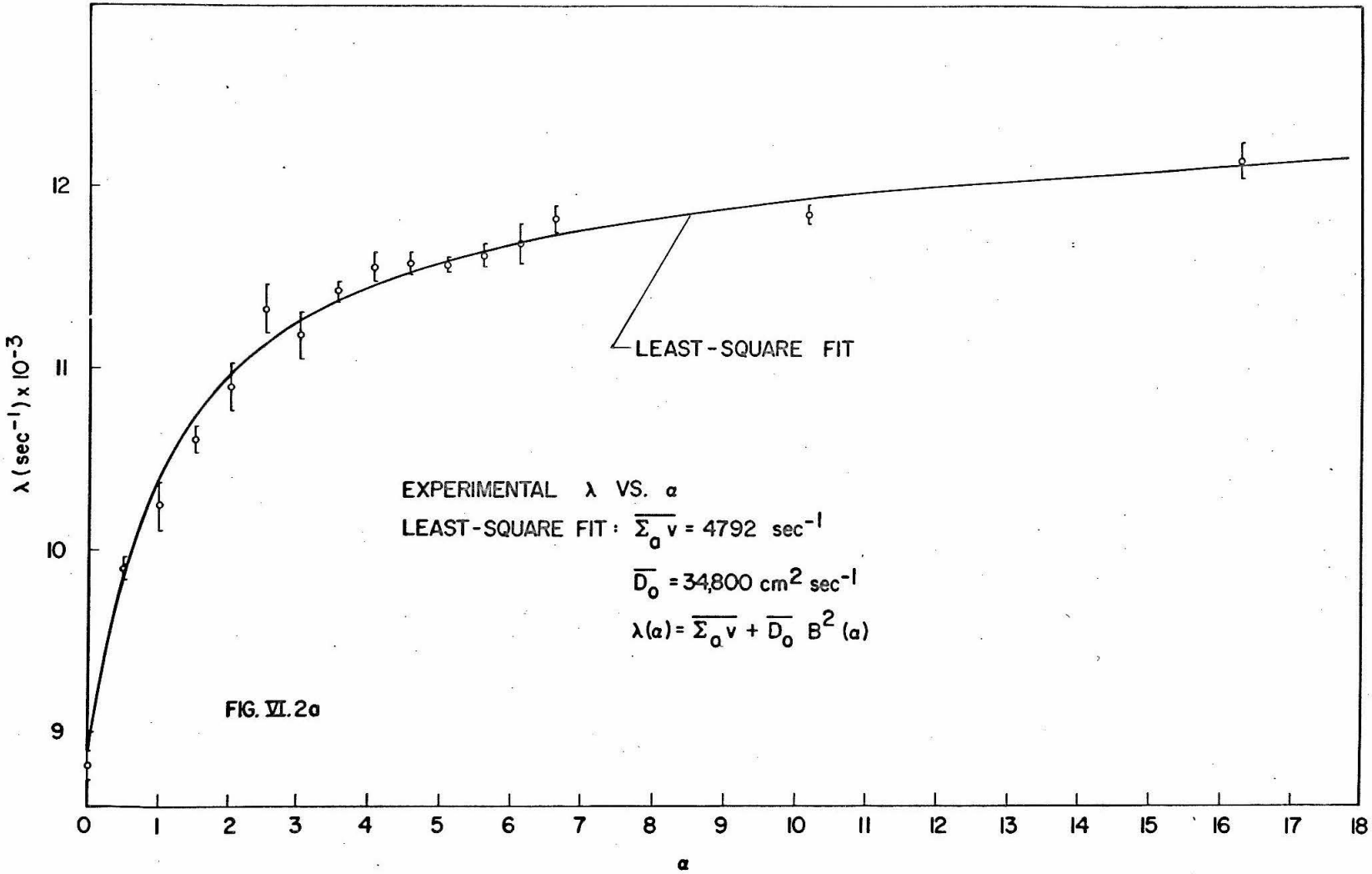
λ (sec⁻¹) x 10⁻³
12
11
10
9
0
1
2
3
4
5
6
7
8
9
10
11
12
13
14
15
16
17
18
α
LEAST-SQUARE FIT
EXPERIMENTAL λ VS. α
LEAST-SQUARE FIT : $\overline{\Sigma_a v}$ = 4792 sec⁻¹
$\overline{D_0}$ = 34,800 cm² sec⁻¹
λ(α) = $\overline{\Sigma_a v}$ + $\overline{D_0}$ B² (α)

FIG. VI.2a

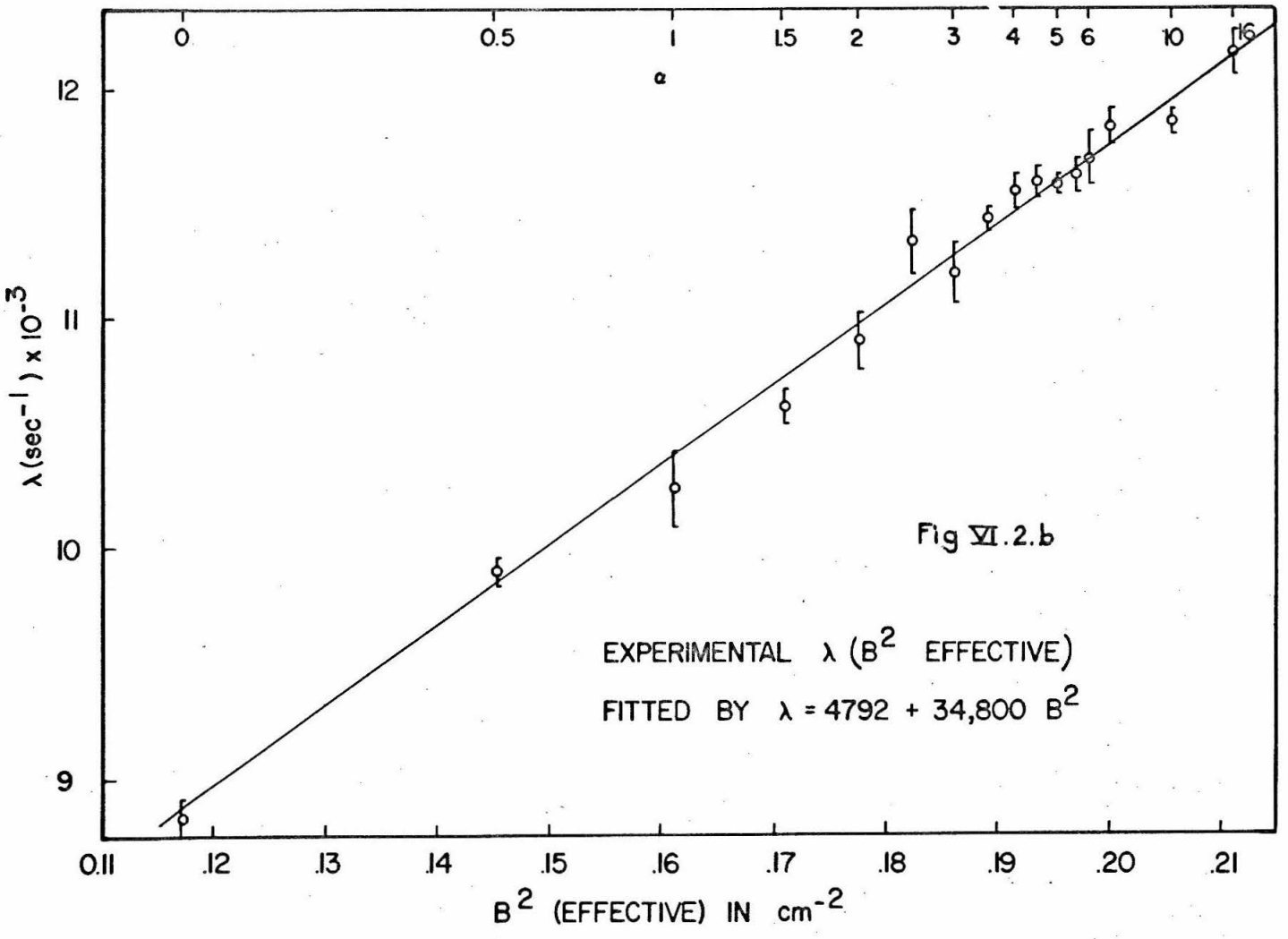
0
0.5
1
1.5
2
3
4
5
6
10
16
α
12
11
10
9
λ(sec⁻¹) x 10⁻³
0.11
.12
.13
.14
.15
.16
.17
.18
.19
.20
.21
B² (EFFECTIVE) IN cm⁻²
EXPERIMENTAL λ (B² EFFECTIVE)
FITTED BY λ = 4792 + 34,800 B²

Fig VI.2.b

literature, and identify $\overline{\Sigma_a v}$ and $(D_o - CB^2)$ with A_o and A_1 respectively.

a) . $C = 4200\ cm^4\ sec^{-1}$ (Kuchle)

$(D_o - CB^2) = A_1 = 34,800$

$B^2 = 0.12\ cm^{-2} \longrightarrow D_o = 35,300\ cm^2 sec^{-1}$

$B^2 = 0.21\ cm^{-2} \longrightarrow D_o = 35,680\ cm^2 sec^{-1}$

to be compared with $D_o = 35,270\ cm^2 sec^{-1}$ given by Kuchle

b) . $C = 3420\ cm^4 sec^{-1}$ (Beckurts)

$B^2 = 0.12\ cm^{-2} \longrightarrow D_o = 35,210\ cm^2 sec^{-1}$

$B^2 = 0.21\ cm^{-2} \longrightarrow D_o = 35,500\ cm^2 sec^{-1}$

to be compared with $D_o = 35,760\ cm^2 sec^{-1}$ given by Beckurts

These values are well within 1% of the published values.

VI. 2. 2. Two-parameter fit with introduction of the cooling factor:

In order to get a better estimate of the effect of a given cooling factor C (taken from the literature, and held constant) introduced in a two parameters fit, least-squares analysis of experimental data was performed using the iterative procedure introduced earlier. Given C, the problem is then to fit the quantity $y = \lambda + CB^4$ into the form $A_o + A_1 B^2$, where A_o and A_1 are unknown.

The iterative process is the following:

. Give first estimates $A_o^{(o)}$, $A_1^{(o)}$

. Compute $B^2_{(o)}$ as $B^2\ (\alpha,\ A_o^{(o)},\ A_1^{(o)})$

. Fit $y^{(o)} = \lambda$ (experimental) + $CB^4_{(o)}$ into $A_o^{(1)} + A_1^{(1)} B^2_{(o)}$.
Extract $A_o^{(1)}$ and $A_1^{(1)}$.

. Reset, i.e. plug the new estimates $A_o^{(1)}$ and $A_1^{(1)}$ into $B^2(\alpha, A_o^{(1)}, A_1^{(1)}) = B^2_{(1)}$ and continue along the same line.

When χ^2, A_o and A_1 reach a stable value, convergence is achieved.

Table VI. 2. 2 shows the results obtained by this method, using selected values of C taken from literature.

Table VI. 2. 2.

REFERENCE DATA				LEAST-SQUARE FIT OF EXPERIMENTAL DATA		
Author	$\Sigma_a v$ (sec^{-1})	D_o $cm^2 sec^{-1}$	Common C $cm^4 sec^{-1}$	$\Sigma_a v$ (sec^{-1})	D_o ($cm^2 sec^{-1}$)	χ^2
			0	4792 (±150)	34,800 (±800)	18.22
Beckurts	4782 (±15)	35760 (±80)	3420 (±170)	4722 (±150) (-1.25%)	35,972 (±800) (+0.60%)	19.04
Kuchle	4785	35270 (±700)	4200 (±800)	4710 (±150) (-1.55%)	36,207 (±800) (+2.65%)	19.24
Lopez and Beyster	4768	36762 (±400)	5116 (±780)	4698 (±150) (-1.45%)	36,488 (±800) (+2.0%)	19.59

Reference data: See Table III. 2. Values in parentheses give published error estimates on the parameters.

Experimental data: Values in parentheses give standard deviations and deviations (in %) of the least-squares fitted parameters from published corresponding parameters.

As could have been expected, the introduction of a fixed cooling factor in the fitting of our given experimental data had the following effects:

(1) Increase D_o as C increases

(2) Decrease $\Sigma_a v$ as C increases

(3) Increase X^2 as C increases: This is because the experimental data do not exhibit a "cooling" component, i.e. a flattening of the λ vs B^2 curve as B^2 increases. On the contrary, it would rather show the inverse effect on the rather small range of buckling which was investigated. This contradiction should probably be charged to experimental errors.

Table VI. 2. 2 also shows that except in the fitting without cooling factor, $\Sigma_a v$ is underestimated (-1. 5% at worse) while D_o is overestimated (+2. 65% maxi).

Again, it is likely that no physical reason is responsible for that, but rather the lack of experimental data on a wider range of buckling.

We are inclined to think that, considering the extent of the approximations which were made and the many factors entering in the experiment, such results, which are purely indicative of the goodness of the method, are reasonably good and consistent. In particular, it is worth pointing out that the range of available bucklings (0. 12 to . 21 cm^{-2}) is very small compared with the much larger ranges over which absorption and diffusion parameters are usually determined ($\sim$ 0 up to 0. 8 cm^{-2}, i.e. 8 times more).

VI. 3. Interpretation of the experimental results.

So far, it can be said that the overall experimental results are in good agreement which theoretical predictions based on a simple diffusion model. Our data evaluation consisted of two steps, which are closely related:

a) Set up a theoretical model, derive predictions using previously published data on absorption and diffusion properties of water, and compare the results of the experiment with these predictions: The maximum deviation which was observed was of the order of 2% on λ, and is believed to be a reasonable order of accuracy for such an experiment. (In fact, most experimental points lie within 1% of the announced values.)

b) Starting from the experimental data, assume a priori that they follow the diffusion model, and derive the "best" absorption and diffusion parameters which should be "plugged in" the model to describe them. It was shown that this analysis led to values of $\Sigma_a v$ and D_o quite close to those given in reference (within a tolerance of 1 to 2%).

This leads to more confidence that the theory itself matches the experimental results.

However, it should be remembered that the primary purpose of this work is not to determine neutron properties for water, but to check a theoretical model. This method is believed to be undesirable for the determination of absorption or diffusion properties, since the range of available bucklings is limited, and the results require a rather complicated mathematical scheme for the analysis.

VII CONCLUSION

Before summarizing the evaluation of results, we feel that it is of value to point out several remarks concerning pulsed neutron measurements in general which have been learned through the experience of this work:

It appears that the pulsed neutron technique, when used with appropriate care, is able to provide valuable and reliable information. To do so, we believe that the following conditions must be met:

1. The experimental set-up:

a) The neutron source should be strong and should provide adequate flexibility for proper selection of pulse width and repetition rate. In particular, it should not produce unwanted background when the beam is turned off: This can be accomplished by pulsing the extraction voltage of the ion source together with the beam deflecting plates.

b) The detector set must be able to handle high count rates occurring during the pulse, i.e. have a nearly constant efficiency regardless of the count rate. Its dead time should be kept as small as possible, in particular when small channel widths are used.

c) The analyzer should have enough channels to cover all the time history of a pulse. It is recommended to gather information on the background itself in order to make sure that it has been reached and that no significant backscattering effects take place.

2. The decay analysis:

The selection of the portion of data to be analyzed (corresponding to the reaching of the fundamental mode) is an extremely critical

factor and calls for an adequate data processing facility. Care should be taken in the count-loss correction scheme and in the use of a numerical code for experimental decay analysis. We believe that the data interpretation is one of the most important points of the pulsed neutron technique. Therefore, it is absolutely necessary to define a consistent and reliable method for data analysis, in order to get comparable and consistent results. Under these conditions, and assuming that the raw data are of good quality the fundamental decay constant can be determined within 0.5%.

As far as the diffusion model is concerned, we believe that its use is valid under the present circumstances, i.e. when the absorption properties only are changed. The experimental results agree fairly well with the predictions of our model within experimental errors. When fitted into the form predicted by diffusion theory, the measurements lead to

$$\Sigma_a v = 4721 \text{ sec}^{-1} \quad (\pm 150)$$

$$D_o = 35972 \text{ cm}^2 \text{sec}^{-1} \quad (\pm 800 \text{ for water at } 21^\circ\text{C})$$

$$C \text{ (given)} = 3420 \text{ cm}^4 \text{ sec}^{-1}$$

which, when compared to published data, reinforce the confidence in the adequacy of the theoretical model.

We believe that the accuracy of our measurements could be improved by further refinements in the evaluation of the poisoning factor and, eventually, by a two components decay analysis.

The validity of diffusion theory in the actual experiment is not surprising since we changed essentially the absorption properties without altering the diffusion ones. In addition, a $\frac{1}{v}$ dependence of the

absorption cross-sections does not affect the energy spectrum, allowing us to assume with reason a unique energy spectrum for the whole assembly. The diffusion theory underlying assumptions have not been violated; this explains the agreement between the experiment and the theory.

Possible extensions of this investigation would be to introduce a change in the scattering properties of the two media (for instance: water against hydrocarbon). Such a situation is more difficult, because one cannot assume identical energy spectra in both media. Moreover, it is doubtful that the space-energy separability condition would be valid, because the interface condition asks for identical spectra while the interior conditions requires different spectra. To treat this case, it will be useful to refer to the work of R. C. Erdmann mentioned earlier to evaluate the qualitative effects of scattering and absorption heterogeneities.

VIII APPENDIX

APPENDIX A1. THE FRANTIC CODE

This code processes raw counting data and fit to these data, by the least-squares techniques, equations for multiple exponential growth and decay.

If one forces a set of data to assume the form $F(t) = \sum_{j=1}^{N} A_j e^{-\lambda_j t}$, the problem is then to determine the optimum A_j's and λ_j's minimizing the "variance of the fit"

$$VAR = \frac{1}{NF} \sum_{i=1}^{N} W_i \left[y_i - \sum_{j=1}^{k} A_j e^{-\lambda_j t_i} \right]^2$$

where

k = number of components

N = number of data points

NF = number of degrees of freedom = N - number of unknown parameters

y_i = data to be analyzed

W_i = weighting factors

A_j, λ_j = unknown parameters

. Several options are available to compute W_i. As customary in least-squares methods involving data obeying nuclear statistics, we chose the option calculating the weight according to $W_i = \frac{1}{Y_i}$.

. One or more parameters can be held constant in the course of the analysis. In particular, a constant background of unknown strength is entered with $\lambda = 0$.

. The signs of parameters may be held constant.

In order for a least-squares analysis to be applicable, there must exist a set of simultaneous equations which are linear in the parameters which are to be determined. The number of equations in the set must be at least as large as the number of unknown parameters. When these conditions are met, a unique solution exists and the values of the parameters can be determined by a Unique Least-Squares Analysis.

For instance, in trying to fit experimental data into the form $F(t) = \sum_{j=1}^{k} A_j e^{-\lambda_j t}$, the resulting equations are linear in A_j's while they are not linear with respect to the decay constants λ_j's. Therefore, the least-squares method is NOT directly applicable to the determination of the λ's, and there may exist a series of minima in the variance of fit.

In order to use the least-squares method, the equations must be made linear. One method of linearization consists of expanding each expression in a first-order Taylor series about the point defined by previous estimates of the parameters. Keeping only first order terms provides a set of simultaneous equations which are linear in the first power of the Δ terms (i.e. differences between the estimates of the parameters and the actual values), but not necessarily linear in the original parameters themselves. However, this set of equations can be least-squares analyzed and leads to a unique solution for the increments Δ for which the previous estimates must be corrected in order to minimize the variance.

Of course, since all higher-order terms of the Taylor expansion are neglected one cannot expect to find immediately the correct Δ terms which will lead to the best λ's. It is necessary to repeat the process many times until some convergence criterion is met. This process is known as an Iterative Least-Squares Analysis.

In the Frantic Code, original estimates can be supplied as initial data, or calculated by the code itself (Subroutine GUESS). Then, the Code begins the iteration process, and keeps track of the evolution of the variance of the fit VAR. The convergence criterion is that the variance VAR should not vary by more than 10^{-6} from its previous value. Then, results of the last iteration are printed, together with statistical data such as X^2, an histogram of the durations between calculated and experimental data, standard deviations on the parameters, etc.

The Code is able to accommodate 400 data points with a maximum of 10 components.

Note: Statistical weights.

In the code, we use the following local weight:

$$W_i = \frac{1}{\sigma_i^2}$$

with

$$\sigma_i^2 = \sigma^2(C)_i + \sigma^2(B)_i + \sigma^2(\tau_d)_i + \sigma^2(DT)_i$$

$$\sigma^2(C)_i = \left(\frac{\sqrt{C_i}}{DT_i}\right)^2$$ uncertainty in count rate (C_i = number of counts DT_i = counting time)

$$\sigma^2(B)_i = \frac{B}{DT_i}$$ uncertainty in background B

$\sigma^2(\mathcal{Z}d)_i$ from uncertainty in dead time factor $\sigma(\mathcal{Z}d)$

$\sigma^2(DT)_i$ from uncertainty in counting interval.

-Interpretation of the results.

. The goodness of fit:

The goodness of fit is described mainly by the calculated values of the weighted variance of fit (VAR) and X^2. The variance of fit is the sum of the weighted squares of the residuals divided by the degrees of freedom, where each weighted residual is expressed in units of its individual σ. The σ values include uncertainty in the observed count-rate, background, dead-time, and counting interval (see above).

The value of (VAR) is also the square of the standard deviation of the distribution of residuals about zero (i.e. describe the standard deviation of the plotted histogram of deviations). Therefore, for data having only statistical deviations, the expectation value of VAR is unity, and the 2σ level of confidence (i.e. value where an identical measurement has 97.73% chance of having a smaller VAR) is approximately $(1 + 3/\sqrt{DF})$.

In most experiments, the variance was found to lie around unity.

Chi-square (X^2) is similar to VAR except that the sum of the weighted squares of residuals is not divided by DF, and the weighting factors include only uncertainty in the calculated count rates (not observed count-rates). In our experiments, background (i.e. constant amount to be subtracted from the initial data) was taken equal to zero, since it was to be directly determined, and uncertainty in dead time and

counting interval was set equal to zero. Therefore, one should expect to find VAR x DF $\simeq X^2$, which was the case.

. How well does the calculated curve compare with the data?

At first, one may look at the printed histogram of the residuals which should be Gaussian with standard deviation equal to VAR. This gives an over all picture of how the deviations between the data and the calculated curve are statistically distributed.

However, it is the detailed study of the residuals as they appear in the time sequence which indicates how well the calculated curve fits the data. There should be statistical variations in the signs of the residuals, i.e., alternate positive and negative values with no long series of residuals having the same sign. In our experiments, it was clear that if we made a one decaying component + background analysis of data too early after the end of the burst, some higher decaying components were present, and the residuals would show a long sequence of - signs followed by + signs.

Ultimately, one can make a statistical analysis of the residuals versus time, and derive a randomness estimate of this distribution.

There have been numerous codes based on this iterative scheme. For reference, we mention:

. A Fortran II Program for Analysis of radioactive decay curves. John L. Need and T. E. Fessler, NASA TN D-1453 (1962).

. Frenic code. Los Alamos Scientific Laboratory.

G. R. Keepin, T. F. Winnett, and R. K. Zeigler, J. Nuclear Energy 6, 1 (1957).

APPENDIX A2. DERIVATION OF THE DEAD-TIME CORRECTION FORMULA FOR THE CN110 ANALYZER AND MODEL 211 LOGIC UNIT

1. Description of operation:

The CN 110 Analyzer equipped with the Model 211 Logic Unit is a 256 channels analyzer with channel widths varying between 0.25 μ sec and 64 μsec (0.25 - 0.5 - 1 - 2 - 4 - 8 - 16 - 32 - 64 micro-seconds).

The analyzer has a basic dead-time of 16 μsec for recording of a count in the memory cells - While most analyzers can store a count in the proper channel right after the end of their inoperative period, the Model 211 operates in a quite different way: The channels are adjacent, and gated. To be able to record counts, a given channel must have its gate open (GATE = 1).

A gate is open if the address system activated it. In general, the advance (increment) of the address is a number of channels equal to 16 μsec divided by the channel length. This gives advances from 1 to 64 channels and allows more than one event per address cycle to be stored (if the channel length is larger than 16 μsec). In case of a channel length less or equal to 16 μsec, and after one count has been recorded, the address of the next open channel ready to record a count is changed and defined as the closest one after elapse of the basic dead-time (16 μsec).

Hence, it is the recording of a count which triggers the change of address. A typical sequence goes as follows:

- Channel length - $l \leq 16$ μsec.
- A count is recorded at Δt after the beginning of a channel. It is stored in the proper channel.
- The address of the next activated channel is changed to $16 + 1 - \Delta t =$ beginning of the next channel able to record a count.

It appears that the unit has a variable dead-time $= 16 + 1 - \Delta t$ which depends on the time Δt of apparition of the address triggering count. Since the appearance of a count changes the address to the next available channel, it follows that the analyzer can record a maximum of ONE count only per channel and per cycle in the case where $l \leq 16$ μsec. If a basic cycle (i.e. a burst and decay for a pulsed neutron experiment) is repeated N times, and the recorded counts of a given channel added at each time, the maximum total number of recorded counts is N (ONE per cycle). It must be realized that the output of a given channel is a non-linear process: It is a 0 or 1 event.

2. Statistical analysis:

2.1. Statistical distribution of incoming counts.

It is assumed, at first, that the incoming count-rate does not vary appreciably during a length of time equal to the channel length l. Therefore, it is a reasonable assumption to assume, because of the physical process involved, a Poisson distribution for incoming counts associated with a given channel i. We define

N = Number of experiments

C_i = Total expected number of incoming counts associated with channel i for N experiments

C'_i = Total number of recorded counts in channel i.

A general Poisson distribution describing of probability of arrival of k counts in a length of time t is

$$P(k, t) = e^{-\lambda t} \frac{(\lambda t)^k}{k!}$$

It the experiment is repeated a large number of times, the expected value of the Poisson variable is $\lambda_i t$.

For our particular case, t = 1 = channel length. Since the counts are equally distributed over the N trials, we can set the average to

$$\frac{C_i}{N} = \lambda_i t$$

Therefore, we have

$$P_i(k, 1) = e^{-\frac{C_i}{N}} \frac{\left(\frac{C_i}{N}\right)^k}{k!}$$

= Probability of having k incoming counts in channel i

$$P_i(o, 1) = e^{-\frac{C_i}{N}}$$

= Probability of NO incoming count in channel i.

$$1 - P_i(o,1) = 1 - e^{-\frac{C_i}{N}}$$

= Probability of one or more incoming counts appearing in channel i.

2.2. Statistical distribution of recorded counts.

The probability of RECORDING ONE count (and one only) in channel i is governed by two <u>independent</u> events:

. The gate of channel i is OPEN ($G_i = 1$)

. One or more counts appear in channel i.

Therefore

P'_i = Probability of recording 1 count in channel i

= p_i (G_i = 1. Gate is open) x (Probability that 1 or more counts appear in channel i)

$$= p_i (G_i = 1). \left\{1 - p_i (o, 1)\right\}$$

$$P'_i = p_i (G_i = 1) (1 - e^{-\frac{C_i}{N}})$$

If the experiment is repeated N times, the expected value of the total number of recorded counts is

$$C'_i = NP'_i = N\, p_i(G_i = 1)\, (1 - e^{-\frac{C_i}{N}})$$

The gate G_i will be open if, and only if no count has been RECORDED in the preceding channels which span a length of time of 16 μsec before beginning of channel i. Two situations arise:

2.2.1. Channel length less or equal to the basic dead-time.

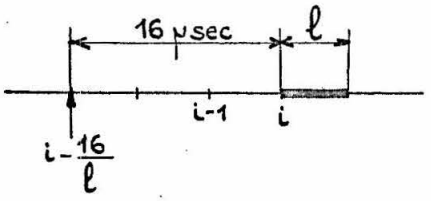

$1 \leq 16$ μsec

The nature of the channel lengths makes them a rational fraction of the dead time.

A number $n = \frac{16}{l}$ channels span the 16 μ sec basic dead time.

A total number $\sum_{j=i-n}^{j=i-1} C'_j$ of counts has been recorded during N experiments.

Since the total time spanning of these channels is 16 μsec, the total possible number of counts they could have recorded is N (1 at a time). Each time they recorded a count, the gate for channel i was closed.

$\sum_{i-n}^{i-1} C'_j$ = Number of times the gate of i was closed

N = Total number of experiments

$N - \sum_{i-n}^{i-1} C'_j$ = Number of times the gate of i was open

$\frac{N - \sum_{i-n}^{i-1} C'_j}{N}$ = Probability that the gate of i is open

$$P_i\ (G_i = 1) = \frac{N - \sum_{i-n}^{i-1} C'_j}{N}$$

Therefore, we have

$$C'_i = N\left(\frac{N - \sum_{i-n}^{i-1} C'_j}{N}\right)\left(1 - e^{-\frac{C_i}{N}}\right)$$

$$= \left(N - \sum_{i-n}^{i-1} C'_j\right)\left(1 - e^{-\frac{C_i}{N}}\right) \qquad (2.2.1.1)$$

Solving for C_i, we get

$$C_i = -N \operatorname{Log}\left[1 - \frac{C'_i}{N - \sum_{i-n}^{i-1} C'_j}\right]$$

This formula is identical with the one derived by W. R. Mills, Jr., L. S. Allen, F. Selig and R. L. Cadwell (29).

If $\frac{C_i}{N}$ is small, we have

$$1 - e^{-\frac{C_i}{N}} \simeq \frac{C_i}{N}\left(1 - \frac{C_i}{2N}\right)$$

with $C_i \simeq C'_i$, we get $(1-e^{-\frac{C_i}{N}}) \simeq \frac{C_i}{N}\left(1 - \frac{C'_i}{2N}\right)$

$$C'_i \simeq \frac{C_i}{N}\left(1 - \frac{C'_i}{2N}\right)\left(N - \sum_{i-n}^{i-1} C'_j\right) = C_i\left(1 - \frac{C'_i}{2N}\right)\left(1 - \frac{\sum_{i-n}^{i-1} C'_j}{N}\right)$$

$$\simeq C_i\left[1 - \frac{1}{N}\left(\frac{C'_i}{2} + \sum_{i-n}^{i-1} C'_j\right) + \frac{C'_i \cdot \sum C'_j}{2N^2}\right]$$

$\frac{C'_i \cdot \sum C'_j}{2N^2}$ is of higher order, and is not taken into account.

$$C'_i \simeq C_i\left[1 - \frac{1}{N}\left(\frac{C'_i}{2} + \sum_{i-n}^{i-1} C'_j\right)\right]$$

$$C_i \simeq C'_i\left[1 - \frac{1}{N}\left(\frac{C'_i}{2} + \sum_{i-n}^{i-1} C'_j\right)\right]^{-1}$$

Thus, the correction formula is identical with the standard dead time correction formula, provided that the dead time is taken equal to $(16 + \frac{1}{2}1)\ \mu$sec.

---

(29) Mills, Allen, Selig, Cadwell - Neutron and Gamma-Ray die-away in an heterogeneous system - Nuclear *Applications Vol. 1, 4* (August 65)

2.2.2. Channel length $\ell > 16$ μsec.

In this case, the unit acts as if the channel were divided into an integer number n of "subchannels" of length $\ell' = 16$ μsec

$$n = \frac{\ell}{16}$$

The process is the same: If a count is recorded at Δt ($\Delta t < 16$) in the first subchannel, then the next available subchannel for recording begins at $16 + \ell' - \Delta t = 32 - \Delta t$ μsec.

The indetermination arises as the distribution of the recorded counts in each subchannel is unknown. Only the total number of counts is known. In first approximation, we will assume that the recorded counts are equally distributed over the channel length, i.e. in each subchannel.

If we have n subchannels in channel i, and C'_i is the total number of recorded counts in channel i, we define the fraction

$C'_{i,j} = \frac{C'_i}{n}$ = Assumed number of recorded counts in the j^{th} subchannel of channel i.

The poisson distribution associated with a subchannel has $\lambda_i \ell = \frac{C_i}{N}$ changed into $\lambda_i \frac{\ell}{n} = \frac{1}{n}\frac{C_i}{N}$.

Then, $C'_{i,j}$ = number of recorded counts in j^{th} fraction of channel i is given according to (2.2.1.1)

$$C'_{i,j} = \left(1 - e^{-\frac{C_i}{nN}}\right)(N - C_{i,j-1})$$

For all subchannels

$$C'_i = \sum_{j=1}^{n} C'_{i,j} \qquad \text{with} \qquad C'_{i,j} = \frac{C'_i}{n} \quad j = 1, n$$

$$C'_{i,o} = C'_{i-1,n} = \frac{C'_{i-1}}{n}$$ (last fraction of previous channel)

$$= (1 - e^{-\frac{C_i}{nN}}) \sum_{j=1}^{n} (N - C'_{i,j-1})$$

$$C'_i = (1 - e^{-\frac{C_i}{nN}}) \left(nN - \frac{C'_{i-1}}{n} - \frac{n-1}{n} C'_i\right)$$

$$C_i = -nN \operatorname{Log} \left[1 - \frac{C'_i}{nN - \frac{C'_{i-1}}{n} - \frac{n-1}{n} C'_i}\right] \qquad (2.2.2.1)$$

Example:

$\ell = 32\ \mu\text{sec}$

$n = 2$

$$C_i = -2N \operatorname{Log} \left[1 - \frac{C'_i}{2N - \frac{1}{2}(C'_{i-1} + C'_i)}\right]$$

Check for $n = 1$

$$C_i = -N \operatorname{Log} \left[1 - \frac{C'_i}{N - C'_{i-1}}\right]$$ identical with (2.2.1.1)

APPENDIX A3. SOME REMARKS ON THE DISTRIBUTION OF COUNTS IN DECAY PHENOMENA

These notes survey briefly some of the conclusions reached by A. Ruark and L. Devol (30) and their implications.

$W_n(t_1, t_2)$ = probability that n counts will appear in the interval (t_1, t_2).

$f_r(t)\,dt$ = Probability that a count will appear in dt around t after r counts have appeared in (o, t).

By analogy with a disintegration process, we call N the initial strength of the source at t = 0.

1) Constant source:

If the diminution of the source during the experiment can be neglected, we have a Poisson distribution (known as Bateman formula).

$$W_n = e^{-ft}\,\frac{(ft)^n}{n!} \qquad (1.1)$$

where f is the average number of counts(or disintegrations) per unit time.

2) Decaying source:

Bortkiewicz gave the formula for a decaying source. However, one may derive a general scheme leading to both formulas.

Suppose we know a priori ft(t). We derive a differential equation for $W_n(o, t)$

---

(30) A. Ruark and L. Devol - General theory of Fluctuations in Radioactive Disintegrations - Phys. Review 49 (1936).

$$\begin{cases} W_n(0,\ t+dt) = W_{n-1}(0,t)\, f_{n-1}\, dt + W_n(0,\ t)\,(1 - f_n dt) & (2.1) \\ \dfrac{dW_n}{dt} = f_{n-1} W_{n-1} - f_n W_n \qquad n = 1,\ 2 \ldots & (2.2) \end{cases}$$

which gives:

$$W_n = \exp\left[-\int f_n\, dt\right] \cdot \int_o^t f_{n-1} W_{n-1} \exp\left[\int f_n dt\right] dt \quad (2.3)$$

If f is a known function f(t) of t only

$$W_n(0,t) = e^{-x}\,\frac{x^n}{n!} \quad \text{with } x = \int_o^t f(t)\, dt$$

In the case of a decaying source

$f_n(t)dt = (N - n)\,\lambda\, dt$

and we get

$$W_n(0,\ t) = C_n^N\,(e^{\lambda t}-1)^n\, e^{-N\lambda t} \quad (2.4)$$

$$C_n^N = \frac{N!}{n!\,(N-n)!}$$

$$W_n(t_1, t_1+t_2) = C_n^N\,(e^{\lambda t_2} - 1)^n\, e^{-N\lambda(t_1+t_2)}\left[1 + e^{\lambda t_2}(e^{\lambda t_1}-1)\right]^{N-n} \quad (2.5)$$

We may apply this result to a pulsed neutron experiment, where the time scale is divided into intervals $(0, t), (t, 2t), \ldots$ t being the channel length.

In the j^{th} channel, the probability of counting n particles is $W_n\left[(j-1)\ t,\ jt\right]$. For fixed values of n and t, these probabilities depend only on the channel index j.

It should be pointed out that these calculations assume that $f_n(t)$, i.e. the decay constant λ is known. In the analysis of

experimental data, λ is unknown but can be approximated locally, or over the entire range of data.

For the case of a constant source, we make $N \to \infty$, $\lambda \to 0$ while $N\lambda = f$ remains finite (constant "average"). Then, (2.4) leads to the Poisson distribution (1.1).

3) Effect of detector efficiency with a detector of negligible recovery time.

Assuming there is no detector-source space dependence, and that the detector has efficiency g, Ruark and Devol showed that the probability of recording n counts in the interval (t_1, t_1+t_2) is:

$$P_n(t_1, t_1+t_2) = C_n^N e^{-N\lambda(t_1+t_2)}(e^{\lambda t_2} - 1)^n g^n \cdot$$

$$\left[1 + e^{\lambda t_2}(e^{\lambda t_1} - 1) + (1 - g)(e^{\lambda t_2} - 1)\right]^{N-n}$$

The mean number of counts in the interval T_2 is

$$\bar{n} = Ne^{-\lambda t_1}(1 - e^{-\lambda t_2})\, g$$

The mean square deviation is

$$\overline{n^2} - (\bar{n})^2 = Ne^{-\lambda t_1}(1-e^{-\lambda t_2})\, g \left[1-e^{-\lambda t_1}(1-e^{-\lambda t_2})\, g\right]$$

The interesting fact about the distribution of recorded counts from such a detector is that when $N \to \infty$ with $N\lambda$ remaining finite, we find a Poisson distribution

$$P_n(T_2) = (N\lambda g\, t_2)^n \frac{e^{-N\lambda g\, t_2}}{n!}$$

which means that the limit Poisson approximation is unaffected by the efficiency of the detector.

4) Effect of finite recovery time of the detector.

Ruark and Devol treated the case of a detector with idealized recovery time τ and a constant source such that the counter receives f counts per second on the average.

Let $P_n(0, t)$ the probability that n counts occur in the interval (0, t).

(4.1). Counter not clogged at t = 0.

$$P_n(0,t) = F_n(t) - F_{n-1}(t) \qquad (4.1.1)$$

$$F_n(t) = e^{-f(t-n\tau)} \left\{ 1 + f(t-n\tau) + \ldots + \frac{[f(t-n\tau)]^n}{n!} \right\} \qquad (4.1.2)$$

for $t \geq n\tau$

Choosing a value of t between $(s-1)\tau$ and $s\tau$ gives

$$\bar{n} = sF_s - \sum_{j=0}^{s-1} Fj \qquad (4.1.3)$$

We check that, if $\tau = 0$

$P_n(0, t) = e^{-ft} \frac{(ft)^n}{n!}$ Initial Poisson distribution.

The question arises now in computing the first order effect of the dead-time τ over the distribution function $P_n(0, t)$ and comparing the average $\bar{n}$ with respect to the average ft of the incoming Poisson distribution.

. If $t \gg n\tau$, one may expect to find an average

$\bar{n} \simeq ft\,(1 - \bar{n}\tau)$ standard dead-time correction.

. If $t \simeq \tau$, i.e. the measuring time is not very large with respect to the dead time, we just have to apply formula (4.1.3).

For instance, assume:

$t = 8\ \mu$ sec.

$\tau = 5\ \mu$ sec.

i.e. $\tau < t < 2\tau$

gives

$$\bar{n} = 2F_2 - F_1 - F_0$$

We can record a maximum of 2 counts. The individual probabilities for recording 0, 1 or 2 counts are:

$$P_o = e^{-ft}$$

$$P_1 = e^{-f(t-\tau)} \left[1+f(t-\tau)\right] - e^{-ft}$$

$$P_2 = e^{-f(t-2\tau)} \left[1+f(t-2\tau)+\frac{f^2(t-2\tau)}{2!}\right] - e^{-f(t-\tau)} \left\{1 + f(t-\tau)\right\}$$

$$= F_2 - (P_1+P_o)$$

We want to compare this finite distribution with the incoming Poisson distribution

$$W_n = e^{-ft} \frac{(ft)^n}{n!}$$

$$W_o = e^{-ft}$$

$$W_1 = e^{-ft}(ft)$$

$$W_2 = e^{-ft} \frac{(ft)^2}{2}$$

We see that, when $\tau \simeq t$, there may be significant differences.

4.2. Count occurs at t = 0.

A similar analysis can be made of the probability $P'_n(0, t)$ of n counts in (0, t) after an initial count at t = 0.

At time τ, conditions are the same as at t = 0

$t \leq n\tau$ $\qquad P'_n = 0$

$n\tau \leq t \leq (n+1)\tau$ $\qquad P'_n = 1 - (P'_1 + \ldots + P'_{n-1})$

$t \geq (n+1)\tau$ $\qquad \begin{cases} P'_n = G_{n+1} - G_n & n \neq 0 \\ P'_o = e^{-f(t-\tau)} \end{cases}$

$$G_n = e^{-f(t-n\tau)} \left\{ 1 - f(t-n\tau) + \ldots + \frac{[f(t-n\tau)]^{n-1}}{(n-1)!} \right\}$$

The average $\bar{n}$ for $s\tau < t < (s+1)\tau$ is:

$$\bar{n} = s - \sum_{1}^{s} G_n$$

The last possible case takes place when a count appears in the interval of time $(-\tau, 0)$ before t = 0. A similar treatment may be made by making a translation of the time scale.

5) Application to our experiment.

So far, we described the following cases

- Decaying source - Effect of the efficiency of a detector with zero recovery time.
- Constant source: Effect of the recovery time of a perfectly efficient detector.

We want to find the probability distribution function of counts as they are fed within the CN 110 Analyzer. We may describe it over the channel length in two ways:

5.1) Decaying source - Detector with zero dead-time.

Let $P_n(k)$ the probability that n counts will appear in channel k of length l.

$$P_n(k) = P_n \left[(k-1)l,\ kl\right]$$

$$= C_n^N e^{N\lambda kl} (e^{\lambda l}-1)^n g^n \cdot$$

$$\left[1+ e^{\lambda l} (e^{\lambda (k-1)\ell}-1) + (1-g) (e^{\lambda l}-1)\right]^{N-n}$$

$$\bar{n} = Ne^{-\lambda(k-1)\ell}(1-e^{-\lambda l})\, g$$

By identifying $\bar{n}$ with $\frac{C'_k}{\text{Number of pulses}}$ (C'_k = unknown average per pulse incoming into channel k of the CN 110 Analyzer. See Ch. V. 1) one may express N as a function of C'_k. (g is assumed known.)

Then, one has to feed this distribution function into the scheme described in Appendix A2.

A problem arises as N enters into C_n^N. In addition, one must have an estimate of the decay constant. Finally, the dead-time of the detector is not taken into account.

5.2) Constant source over the channel length. Dead time of the detector is included.

This analysis is also equally complicated, for the question arises whether or not the detector is clogged at the opening of the channel. Therefore, one has to make a similar dependent event analysis as in Appendix A2.

6. Conclusion.

We hope that this brief treatment has pointed out the kind of problems which arise in a rational treatment of dead-time losses. The ideal situation would be to examine the case of a decaying source with a detector of finite recovery time. We believe that this analysis is quite difficult to apply practically, thus it has not been done. However, we believe that care and circumspection should be used every time one attempts to describe count-losses for fast varying sources and channel lengths of comparable size with the recovery time of the detector.

IX BIBLIOGRAPHY

(1) Noel Corngold: Theoretical Interpretation of Pulsed Neutron Phenomena - IAEA Sympsoium - Karlsruhe, Germany, May 1965.

(2) Meghreblian and Holmes: Reactor Analysis - McGraw Hill (1960).

(3) B. Davison: Neutron Transport Theory - Oxford Press (1957).

(4) Reactor Physics Constants. ANL 5800 (1963).

(5) K. H. Beckurts and K. Wirtz: Neutron Physics (1964).

(6) K. H. Beckurts and K. Wirtz: Neutron Physics (1964).

(7) Antonov and al: Vol. V, P/661, USSR.

(8) Von Dardel and Sjostrand: Phys. Rev. 94, 1272, (1954).

(9) Beckurts and Wirtz: Neutron Physics (1964).

(10) Honeck, H.: BNL719, 1186 (1962).

(11) Reactor Physics Handbook - ANL 5800.

(12) R. C. Erdmann: Time dependent monoenergetic neutron transport in two adjacent semi-infinite media. Thesis - California Institute of Technology (1966).

(13) M. R. Williams: Space energy separability in pulsed neutron systems. Brookhaven Conference on Neutron Thermalization (1962) - Reactor Science and Technology 1963, Vol. 17, pp. 55-66.

(14) Gelbard and Davis: NSE 13, 237 (1962).

(15) Kiefhaber, E.: NSE 18, 404 (1964).

(16) Beckurts: Neutron Physics, Page 374.

(17) W. H. Dio and E. Schoffer: Nuclear Phys. 6: 175-176 (1958).

(18) Kuchle: NSE 8, No. 1, 88, (1960).

(19) Beckurts and Wirtz: Neutron Physics, Page 408 (1964).

(20) Meghreblian and Holmes: Nuclear reactory theory
Reactor Physic Constants: ANL 5800, Page 30 (1963).

(21) Prasdocimi and Deruytter: The absorption cross section of Boron. J. Nucl. Energy A & B, 17, 83 (1963).

(22) W. J. Price: Nuclear Radiation Detection, Page 298 (1958).

(23) W. J. Price: Nuclear Radiation Detection (1958).

(24) D. J. Behrens: The fitting of exponential decay curves to the results of counting experiments. AERE T/R.629.

(25) Mills, Allen, Selig, Cadwell: Neutron and gamma ray die-away in an heterogeneous system. Nuclear Applications Vol. 1, 4 (August 65).

(26) D. J. Behrens: Notes on the nature of experiments, the statistics of counting experiments. A.E.R.E. T/R.629 (1951).

(27) R. Peierls: Statistical Error in Counting Experiments, Proc. Roy. Society (London) A149 (1935).

(28) A. Ruark and L. Devol: General theory of fluctuations in Radioactive Disintegrations. Phy. Review 49 (1936).